

**A Study of Some Supramolecular Assemblies Mediated by  
N-H $\cdots$ O, N-H $\cdots$ N and N-H $\cdots$ S Hydrogen Bonds**

A Thesis  
Submitted for the Degree of  
**Doctor of Philosophy**  
**(in Chemistry)**

To  
**University of Pune**

By  
**Mr. V. Nagarajan**

**Division of Organic Chemistry**  
**National Chemical Laboratory**  
**Dr. Homi Bhabha Road**  
**Pune-411 008**

**August-2012**

*Dedicated to My*  
*Amma-Appa*



**Smt. V. Janaki**  
**Shri. R. Veeraputhiran**





## राष्ट्रीय रासायनिक प्रयोगशाला

(वैज्ञानिक तथा औद्योगिक अनुसंधान परिषद)

डॉ. होमी भाभा रोड, पुणे - 411 008. भारत

**NATIONAL CHEMICAL LABORATORY**

(Council of Scientific & Industrial Research)

Dr. Homi Bhabha Road, Pune - 411008. India



### CERTIFICATE

This is to certify that the work presented in this thesis entitled “**A Study of Some Supramolecular Assemblies Mediated by N-H $\cdots$ O, N-H $\cdots$ N and N-H $\cdots$ S Hydrogen Bonds** ” submitted by **Mr. V. Nagarajan**, has been carried out by the candidate at National Chemical Laboratory, Pune, India, under my supervision. Such materials as obtained from other sources have been duly acknowledged in the thesis. This work is original and has not been submitted for any other degree or diploma of this or any other university.

**August 2012**

**Pune**

**Dr. V. R. Pedireddi**

## **CANDIDATE'S DECLARATION**

I hereby declare that the research work presented in the thesis entitled **“A Study of Some Supramolecular Assemblies Mediated by N-H···O, N-H···N and N-H···S Hydrogen Bonds”** was carried out by me at the National Chemical Laboratory, Pune, India, under the supervision of **Dr. V. R. Pedireddi**, Scientist, Division of Organic Chemistry, National Chemical Laboratory, Pune, India and submitted for the degree of Doctor of Philosophy in Chemistry to the University of Pune. This work is original and has not been submitted in part or full by me for any other degree or diploma of this or any other university.

**August 2012**

**Pune**

**V. Nagarajan**

## Acknowledgements

*It is great pleasure to express my sincere thanks to people who have assisted me in many ways to reach this stage.*

*It gives me an immense pleasure to express my deep sense of gratitude and profound thanks to my research guide Prof. V. R. Pedireddi for all the guidance, support and encouragement during this research carrier.*

*It is my privilege to thank Dr. Ganesh Pandey Head of the Division of Organic Chemistry, NCL and Dr. C. V. Ramana for their constant support and encouragement during the progress of this work.*

*I thank Dr. Sourav Pal, present Director NCL, and Dr. S. Sivaram, former Director NCL, for their support as for giving infrastructure facilities, and CSIR, New Delhi for financial support.*

*My heartfelt thanks to Dr. P. A. Joy, Dr. C. V. V. Sathyanarayana, Dr. Srinivas Hotha and Dr. Avinash Kumbhar for their support in many aspects.*

*I am grateful to Dr. Mrs. Vedavathi Puranik and Dr. Rajesh Gonnade, NCL Pune and Dr A. Srinivasan, NISER for their assistance in the single crystal X-ray diffraction.*

*I wish to thank my friendly and cooperative labmates, Prakash, Kapil, Sunil, Seetha, Marivel, Sathya, Amit, Manish, Yogesh, Manish, Prince, Ketaki, Mayura, Sharmita, Amrita, Purnendu for their help in various capacities and providing me with an excellent working ambience.*

*I am thankful to all the teachers and lecturers, who taught me throughout my career. Special thanks to Mrs. Janaki, Mr. Palsamy, Mr. Ramakrishnan, Mr. Murugaperuman, Mrs. Padma, Mr. Amalraj, Mr. Olivu Mr. Hari, Mr. Karthikeyan, Mrs. Helen Kiruba, Mr. Parvathy Nathan, Mrs. Parvathy, Mr. Ponraj, Prof. Sivansankaran Nair, Prof. Subramanian for their dedication.*

*I thank my brothers and sister especially Ponmani and Vanitha who always inspired in every stage of my career. Also I my grant parents Ramasamy and Valli*

*I thank all my friends especially Malli anna, Ramanujam, Pradap, Suresh, Sridhar, Khaja, Selva, Lenin, Edwin, Ramsundar, Palani, Avinash, Sandeep, Venkat, Senthil, Prakash, for giving great ambience at NCL, Pune.*

*The blessings and best wishes of my parents keep me active throughout my life. They made me what I am and I owe everything to them. Dedicating this thesis to them is a minor recognition for their invaluable support and encouragement.*

*I thank all of you once again for your kind support and cooperation*

V. Nagarajan

# CONTENTS

---

---

---

## Chapter I

### Introduction to Supramolecular Chemistry

---

1.1	Introduction	1
1.2	Earlier Developments in Supramolecular Chemistry	4
1.3	Recent Developments in Supramolecular Chemistry	8
1.4	Hydrogen Bonding	9
1.5	Supramolecular Patterns	11
1.6	Polymorphism	19
1.7	Co-crystals	20
1.8	Applications of Co-crystals	21
1.9	Low Molecular Weight Gelators	26
1.10	Preparation and Characterization of LMWGs	28
1.11	References	33

---

## Chapter II

### Synthesis and Structural Studies of Some 1,3,5-Benzenetricarboxamide Based Gelators

---

2.1	Introduction	41
2.2	Amide Based Gelators	42
2.3	Effect of peripheral substituents in the formation of supramolecular assemblies of gel	51
2.4	Preparation of the 1,3,5-Benzenetricarboxamide Derivatives	53
2.5	Preparation of Gels	53
2.6	SEM Analysis of Xerogel	55
2.7	Single Crystal X-ray Diffraction Analysis	56
2.8	Powder X-ray Diffraction Analysis	66
2.9	Thermo Gravimetric Analysis	68
2.10	Conclusions	72
2.11	Experimental Section	72
2.12	References	75

---

---

**Chapter III****Co-crystals of Trithiocyanuric acid with some N-donor compounds**

---

3.1 Introduction	78
3.2 Structure of molecular complex of trithiocyanuric acid and 4,4'-bipyridine obtained from DMSO	82
3.3 Structure of molecular complex of trithiocyanuric acid and 4,4'-bipyridine obtained from DMSO/MeOH	85
3.4 Structure of molecular complex of trithiocyanuric acid and 1,2- <i>bis</i> (4-pyridyl)ethane	88
3.5 Structure of the molecular complex of trithiocyanuric acid and 1,2- <i>bis</i> (4-pyridyl)ethane obtained under solvothermal conditions	90
3.6 Packing analysis in the molecular complex of trithiocyanuric acid and 1,2- <i>bis</i> (4-pyridyl)ethane	93
3.7 Structure of the molecular complex of trithiocyanuric acid with 1,3- <i>bis</i> (4-pyridyl)propane	95
3.8 Molecular complex of TCA and dipyridylsulfide	99
3.9 Structure of trithiocyanuric acid with 1,2- <i>bis</i> (2-pyridyl)ethane	101
3.10 Structure of the molecular complex of trithiocyanuric acid with phenazine	104
3.11 Structure of the molecular complex of trithiocyanuric acid with 1,7-phenanthroline	107
3.12 Structure of the molecular complex of trithiocyanuric acid with 1,7-phenanthroline obtained from DMSO	109
3.13 Structure of molecular complex of trithiocyanuric acid with piperazine	112
3.14 Conclusions	114
3.15 Experimental Section	115
3.16 References	121

---

**Chapter IV****Rational Analysis of Supramolecular Assemblies of Cyanuric acid**

---

4.1 Introduction	124
4.2 Structural analysis of co-crystals of cyanuric acid and aldrithiol-4	135
4.3 Co-crystals of cyanuric acid with diazabicyclo[2.2.2]octane	137
4.4 Self assembly of molecules in co-crystals of cyanuric acid with piperazine	139
4.5 Molecular complex of cyanuric acid with 3-aminopyridine	141
4.6 Packing analysis in the co-crystals of cyanuric acid with 2,4,6-triaminopyrimidine	143
4.7 Conclusions	146
4.8 Experimental Section	146
4.9 References	150

---

Publications

Symposia/Poster presentation

---





The aggregational behaviour of organic molecular entities has been exploited in recent decades to understand the pivotal role of intermolecular interactions such as hydrogen bonds in the self assembly process of small molecules towards the formation of supramolecular assemblies.<sup>1,2</sup> This Ph. D thesis, entitled, “**A Study of Some Supramolecular Assemblies Mediated by N-H $\cdots$ O, N-H $\cdots$ N and N-H $\cdots$ S Hydrogen Bonds**” is the compilation of a study of aggregation features of selective amides, imides and thioimides as described in four chapters. In Chapter 1, the importance of non-covalent interactions with an emphasis on the hydrogen bonds, towards the formation of supramolecular assemblies of organic molecules is reviewed, through illustrative examples, highlighting the significant and notable contribution of various research groups in the development of supramolecular chemistry as a frontier area of research. In Chapter 2, preparation of gels by self assembly process and some solid state structures of the gelators, exclusively formed by 1,3,5-benzenetricarboxamide derivatives are documented. Chapter 3 is an account of supramolecular assemblies formed by trithiocyanuric acid with some aza-donor compounds at variable temperature as well as in different reaction media. Finally, in Chapter 4, some exotic supramolecular assemblies of co-crystals of cyanuric acid with topologically different bases are discussed.

### Chapter 1

Formation of supramolecular ensembles in the solid state are generally being influenced by non-covalent interactions such as electrostatic, dipole-dipole,

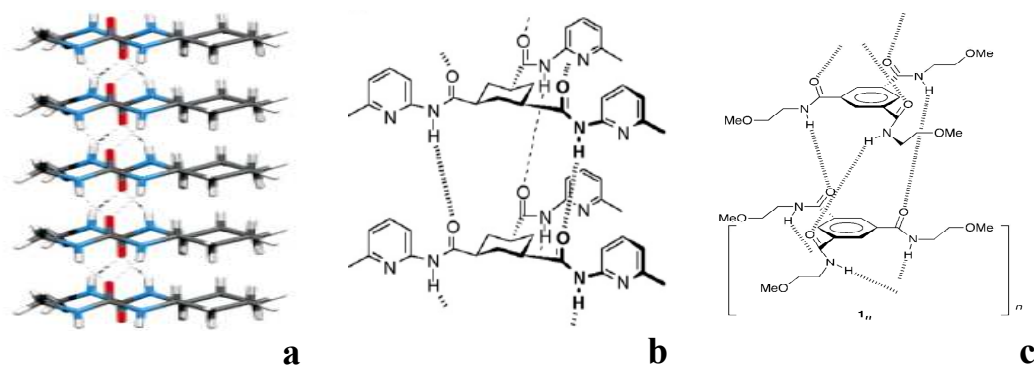
hydrogen bonds, hydrophobic, van der Waals etc.<sup>3</sup> The self assembly of different molecules through non-covalent interactions depends upon the information encoded within a molecule. For example, while self assembly of simple aliphatic hydrocarbons are mostly governed by the van der Waals interactions, topologically similar molecules but with functional groups like –COOH group, the aggregation is predominantly, by the highly directional hydrogen bonds.

A thorough understanding of various intermolecular interactions, in particular, hydrogen bonds in supramolecular assemblies, thus, is utmost important for successful and directed synthesis of supramolecular assemblies. In general the knowledge of intermolecular interaction can be enriched by deriving information from the structural features of a large number of compounds, which are generally deduced by high precision instrumentation methods, such as X-ray diffraction. Thus, analysis of the patterns of intermolecular interaction between the molecules within the solids is one of the aims of supramolecular chemistry to understand the properties of the material in bulk. In this regard, the molecular patterns, particularly, in the crystals are been classified into different types such as, tapes, ribbons, rosettes, diamondoids etc. Understanding such a structure-property relationship gives various strategical approaches to prepare the designed structural entities. Thus, supramolecular assemblies reported by various research groups, in the recent years, for the evaluation of the recognition patterns in supramolecular synthesis, would be discussed in this chapter with the aid of selective and

representative examples to account for the objective of the research work compiled in the remaining chapters.

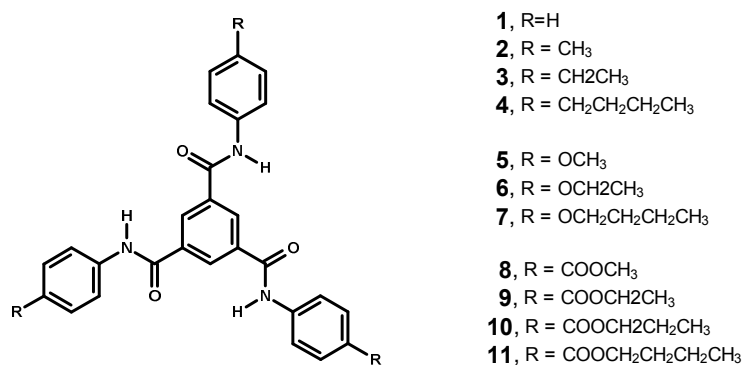
## Chapter 2

Molecular gels are due to the aggregation of molecules of gelators into fibrils, by self assembly process, often, through intermolecular interactions, followed by entanglement of the fibrils. Such a process, in general, creates a large void space, which is generally being occupied by large quantity of the solvent.<sup>4</sup> Study of hydrogen bonds mediated gels are of special importance due to facile formation of one-dimensional self-assembled fibrils, because of the directional features of the hydrogen bonds. In this regard urea based gelators,<sup>5</sup> as shown in Figure 1a, wherein the N-H $\cdots$ O hydrogen bonds direct the self assembly of molecules, are one of the well explored substrates in the recent literature. Among others, 1,3,5-cyclohexane\benzene trisamide derivatives<sup>5</sup> are also equally been thoroughly explored for the gelation studies, as one dimensional aggregation through N-H $\cdots$ O hydrogen bonds yielding



**Figure 1** One dimensional array of a) 1,2-cyclohexylbisurea derivative b) 1,3,5-cyclohexanetrissamide derivative c) 1,3,5-benzenetrissamide derivative.

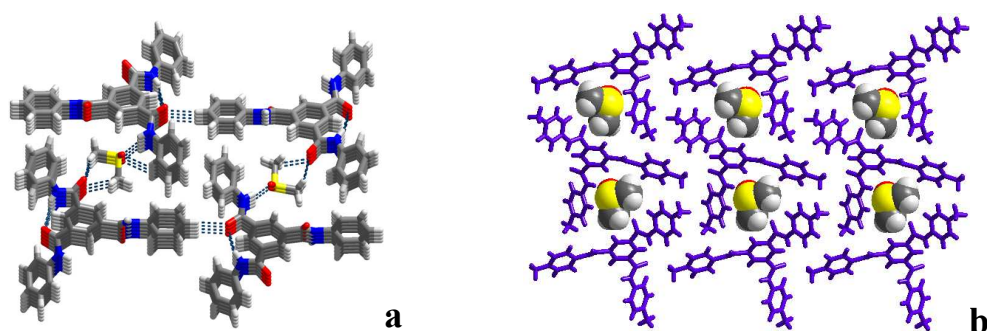
columnar structures is propensity of such compounds (Figure 1(b) & 1(c)). In many of the examples known in the literature, towards gelation ability, several studies are carried out on hydrogen bonded gelators with long alkyl chains<sup>6</sup> or functional groups that too yield hydrogen bonds present on the periphery of the gelators. Hence gelation studies of substrates without long alkyl group as well as hydrogen bonding groups on the periphery, as shown in Scheme 1, may add value to expand the horizon of spectrum of gels. Thus, the derivatives of 1,3,5-benzenetricarboxamide have been prepared to explore and evaluate the structural features for gelation properties. It is pertinent to report that, amides **1-4** are insoluble in most of the organic solvents except DMSO, DMF and sparingly soluble in methanol. Interestingly, compounds **1-3** gave gels from highly polar solvents like DMSO or DMSO-water.



**Scheme 1.** Molecular structure of the 1,3,5-benzene trisamide derivatives.

The structures of the gelators **1** and **2** have been established by single crystal X-ray diffraction method, on the crystals obtained from the solution of DMSO and methanol mixture to account for the gel formation. The packing diagrams are shown in Figure 2. It has been noted that the simulated powder X-ray diffractogram

match very well with the similar patterns recorded on the xerogels (without solvent), which shows the fibre structures of the xerogels of **2** and **3** is same as that of the structures obtained for **2** and **3** respectively from crystallization. The salient features of these gels and other gelators as shown in Scheme 1 are discussed in this Chapter in detail.

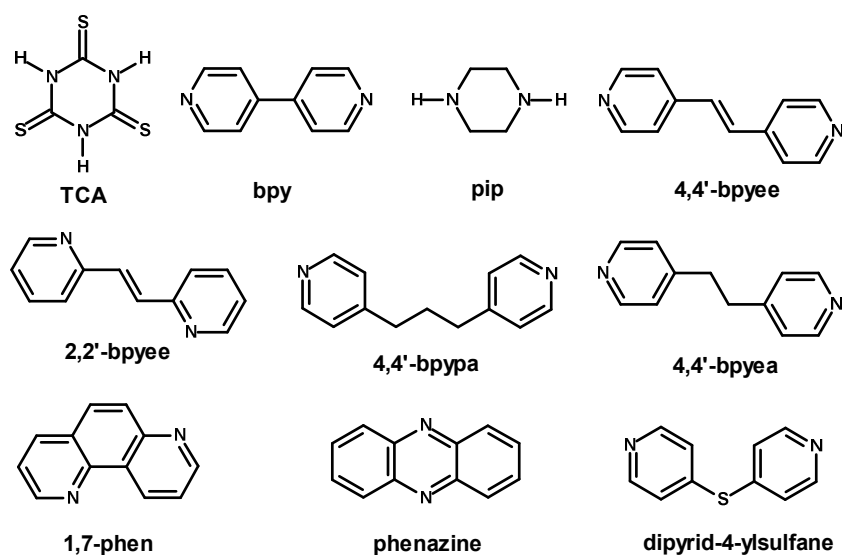


**Figure 2.** (a) Columnar structure obtained in **1.DMSO** highlighting the interaction of DMSO molecule through N-H $\cdots$ O and C-H $\cdots$ O hydrogen bonds. (b) three dimensional packing of **2.DMSO**

### Chapter 3

Molecular recognition between the complementary acceptors and donor moieties plays a major role in the self assembly process, towards the generation of supramolecular assemblies. Although, such ensembles are generally being prepared from solutions by slow evaporation method, the effect of solvents, temperature pressure, etc., are not well addressed in the supramolecular synthesis. Further, in the multiple component ensembles, if one of the components is associated with various donor or acceptor sites, a wide range of supramolecular assemblies could be realized with systematic variation of the cofomer or solvents, etc. In this regard, trithiocyanuric acid (**TCA**) molecule which possesses three hydrogen bond

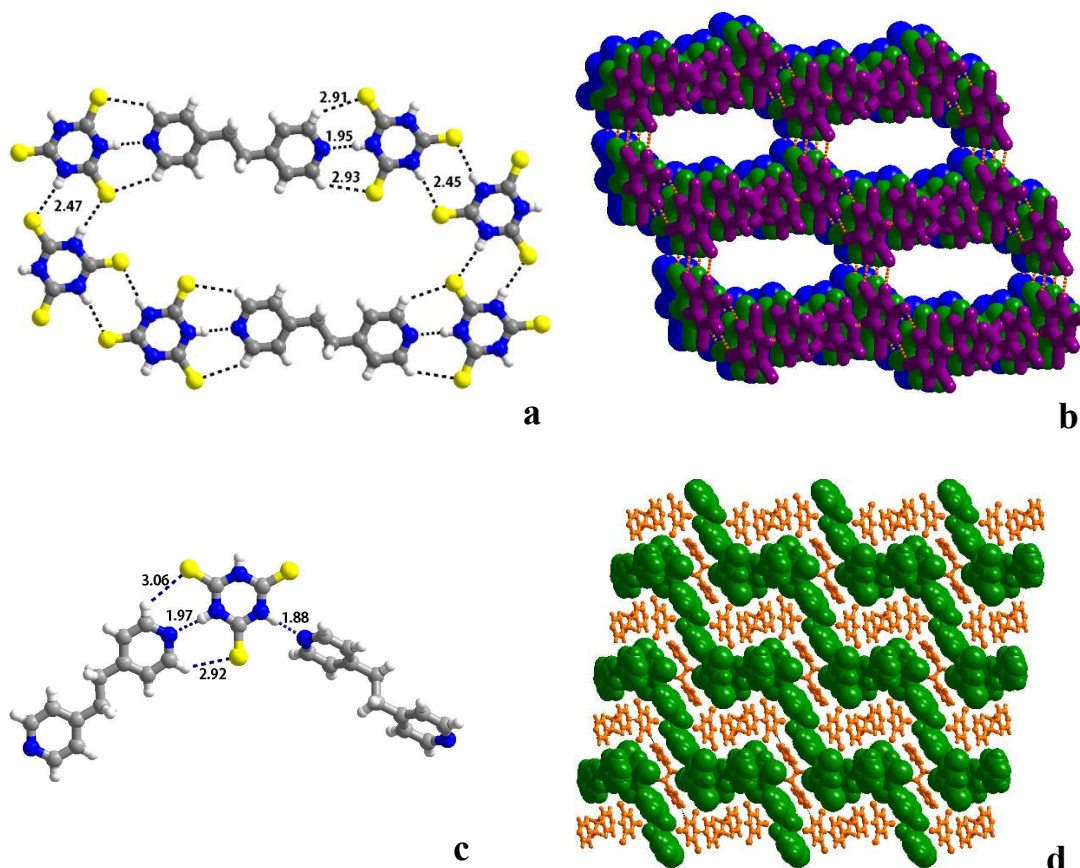
acceptors and three hydrogen bond donors, is one of exotic supramolecular reagent for the synthesis of myriad of assemblies. For example, due to the acidic nature of **TCA** molecule, it could form easily co-crystals with pyridine based ligands (aza-donor) as a co-former. Thus, to expand the horizon of **TCA** assemblies, co-crystallization of **TCA** with numerous nitrogen based ligands, as listed in Scheme 2, have been carried out.



**Scheme 2.** Molecular structure of **TCA** and aza-donor compounds.

In a typical example, **TCA** and 1,2-*bis*(4-pyridyl)ethylene (**bpypa**), in methanol at room temperature, gave a host-guest assembly, wherein the host network, composed of **TCA** and **bpypa** molecules, occludes solvent of crystallization, methanol molecules, as guests. The assembly is shown in Figure 3(b). However, under solvothermal conditions (high temperature and pressure) methanol as a solvent, gave entirely a different assembly, as shown in Figure 3(d). A thorough illustration of various other features of these assemblies along with the

salient features of structures of other complexes is discussed in detail in this chapter, in different sections.

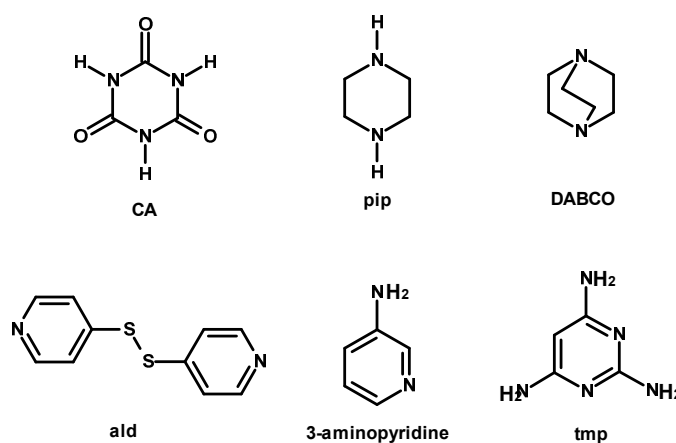


**Figure 3.** (a) Molecular recognition of TCA with **bpyea** in a eight membered cyclic network obtained at ambient conditions and its (b) three dimensional host network structure. (c) Molecular recognition of TCA with **bpyea** for complex obtained by solvothermal method and its (d) three dimensional arrangement.

## Chapter 4

Cyanuric acid (CA), an analogue of trithiocyanuric acid, with the replacement of ‘S’ by ‘O’ atoms is one of the other supramolecular reagent, that has been well explored in the supramolecular synthesis. However, taken into

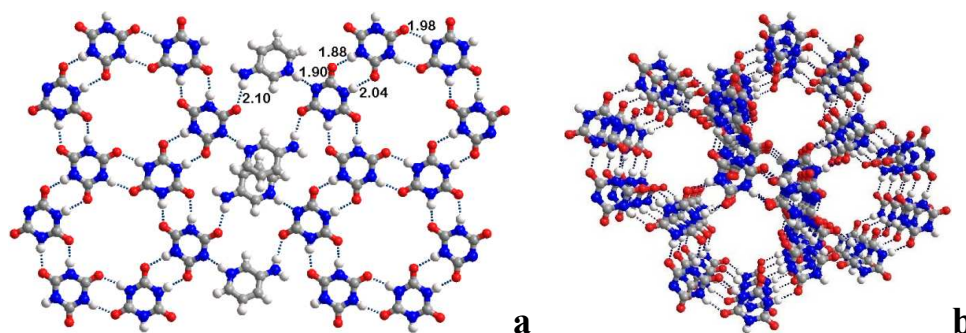
account the implication of **CA** in various solid state based structural studies in the frontier areas of co-crystal chemistry,<sup>7</sup> nanochemistry,<sup>8</sup> etc., the reported examples in the literature are not suffice to evaluate **CA** towards preparation of target driven structural studies. Thus, different co-crystals of **CA** have been prepared with different aza-donor molecules as listed in Scheme 3, to establish a rationale for the unusual and diversified assemblies being found by **CA**.



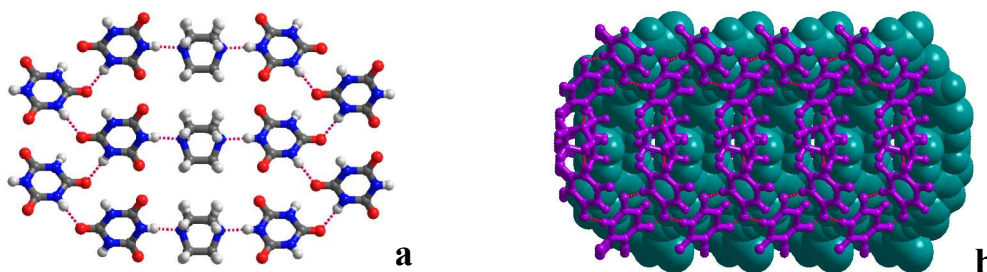
**Scheme 3.** Molecular structure of **CA** and aza donor compounds.

In a representative example, **CA** and 3-aminopyridine gave co-crystals in a 2:1 ratio, from a methanol, at room temperature. The structure consists of planar  $\alpha$ -networks of hexagons formed by six molecules of **CA** with the hexagonal units are hydrogen bonded to 3-aminopyridine molecules, as shown in Figure 4(a). In each hexagon, adjacent molecules of **CA** are held together by different types of N-H $\cdots$ O hydrogen bonds. In three dimensional structure of the co-crystal, the adjacent layers overlap such that channels are present along a crystallographic axis (Figure 4(b)).





**Figure 4.** (a) Arrangement of of CA molecules as hexagonal network, connected through 3-aminopyridine molecule by N-H $\cdots$ O hydrogen bonds. (b) Channels structure constituted by CA.



**Figure 5.** (a) Eight membered ring formed between CA and DABCO (b) Three dimensional arrangement of CA.DABCO adduct.

In contrast, co-crystallization of CA with DABCO, an aliphatic bicyclic base, gave a supramolecular assembly, wherein the CA and DABCO constitute an eight membered ensemble as shown in Figure 5(a). CA recognizes DABCO through N-H $\cdots$ O hydrogen bond, while the adjacent CA molecules are held together by catemeric single N-H $\cdots$ O hydrogen bonds (Figure 5(a)). In two dimensional arrangement, such arrays are extended to form a sheet structure, which are in turn stacked in three dimension. Packing of molecule in the crystal lattice is shown in Figure 5(b). The other structures obtained in this endeavour will be discussed in this chapter.

### References

1. (a) Lehn, J.-M. *Supramolecular Chemistry: Concepts and Perspectives*. VCH:Weinheim, 1995. (b) Pelesko, J.A. *Self Assembly: the science of things that put themselves together*, CRC, 2007.
2. (a) Jeffery, G. A. *An introduction to Hydrogen Bonding*; Oxford University Press: New York, 1997. (b) Desiraju, G. R. *Crystal Engineering: The Design of Organic Solids*. Elsevier: Amsterdam, 1989.
3. Atwood, J. L.; Steed, J. W. *Encyclopedia of supramolecular chemistry Vol.2*, Dekker, New York, 2004.
4. (a) Weiss, R.G.; Terech, P. *Molecular gels: materials with self assembled fibrillar network*, Springer, 2006. (b) van Esch, J.; Schoonbeek, F.; de Loos, M.; Kooijman, H.; Spek, A. L.; Kellogg, R. M.; Feringa, B. L. *Chem. Eur. J.* **1999**, *5*, 937-950 (c) Hanabusa, K.; Shimura, K.; Hirose, K.; Kimura, M.; Shirai, H. *Chem. Lett.* **1996**, 885 (d) van Esch, J.; Stokroos, I.; Kellogg, R. M.; Feringa, B. L. *J. Am. Chem. Soc.* **1997**, *119*, 12675.
5. (a) Fan, E.; Yang, J.; Geib, S. J.; Stoner, T. C.; Hopkins, M. D.; Hamilton, A. D. *J. Chem. Soc. Chem. Commun.* **1995**, 1251 (b) Lightfoot, M. P.; Mair, F. S.; Pritchard, G. R.; Warren, J. E. *Chem. Comm.* **1999**, 1945.
6. Hanabusa, K.; Kawakami, M. Kimura, A.; Shirai, H. *Chem.Lett.* **1997**, 191.

7. (a) Ranganathan, A.; Pedireddi, V. R.; Rao, C. N. R. *J. Am. Chem. Soc.* **1999**, *121*, 1752. (b) Arora, K. K.; Talwelkar, M. S.; Pedireddi, V. R. *New J. Chem.* **2009**, *33*, 57.
8. Whitesides, G. M.; John, E. E. S.; Mathias, J. P.; Seto, C. T.; Chin, D. N.; Mammen, M.; Grodon, D. M. *Acc. Chem. Res.* **1995**, *28*, 37.

## CHAPTER ONE

### Introduction to Supramolecular Chemistry

## 1.1 Introduction

Molecules are made up of atoms, through interatomic forces, like ionic, covalent and co-ordinate covalent bonds<sup>1</sup> depending upon the nature of electron transfer process takes place, indeed, further aggregate through intermolecular interactions,<sup>2</sup> which are largely classified as ion-dipole, dipole-dipole, dipole-quadruple interaction etc., particularly, in covalent compounds. Thus, the intermolecular interactions may be considered as force between species of opposite charges. Such intermolecular interactions are collectively represented, in general, as non-covalent interactions.<sup>3</sup> Aggregation of molecules through such non-covalent interactions into a bulk entity is a self driven process<sup>4</sup> (self assembly), because the attraction between the species with opposite charges is a spontaneous process. However, the ease of molecular aggregation depends upon the density of the charges present in each molecular species as mentioned earlier. In general, the strength and number of intermolecular interactions attribute the physical properties to the matter in bulk including its state. For example, long chain aliphatic hydrocarbons with relatively strong hydrophobic interactions exist in either liquid or solid state, while their

**Table 1.1.** Physical properties of some aliphatic hydrocarbons.

compound	m.p (°C)	b.p (°C)	state at 25°C
hexane (C <sub>6</sub> H <sub>14</sub> )	-95	69	liquid
decane (C <sub>10</sub> H <sub>22</sub> )	-30	80	liquid
tetradecane (C <sub>14</sub> H <sub>30</sub> )	6	253	liquid
icosane (C <sub>20</sub> H <sub>42</sub> )	37	343	solid

**Table 1.2.** Physical properties of representative aromatic hydrocarbons.

compound	m.p (°C)	b.p (°C)	state at 25°C
benzene (C <sub>6</sub> H <sub>6</sub> )	6	80	liquid
naphthalene (C <sub>10</sub> H <sub>8</sub> )	80	218	Solid
anthracene (C <sub>14</sub> H <sub>10</sub> )	218	342	Solid

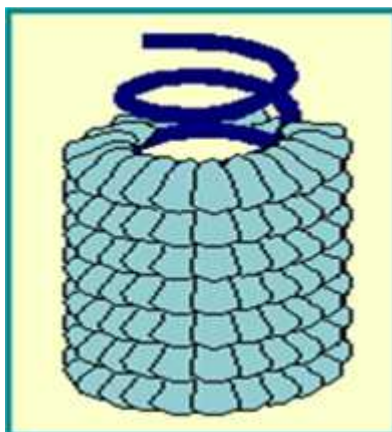
short chain analogues with weak hydrophobic interaction prevail either in liquid or in the gaseous state (Table 1.1). However, aromatic hydrocarbons, predominantly exist in solid state, in which self assembly is dominated by  $\pi$ - $\pi$  as well as C-H $\cdots$  $\pi$  interactions, which are relatively stronger than the hydrophobic interactions (Table 1.2).

Understanding of the aggregation of molecules in materials, through the knowledge of intermolecular interactions is one of the aims of supramolecular chemistry.<sup>5</sup> In this regard, it is noteworthy to mention that although studies related to theoretical aspects of the intermolecular forces are well documented in terms of nature, energy, directionality etc., with respect to the chemical bond concepts, utilization of such intermolecular interactions to tailor the properties of the functional materials is not well explored until recently.<sup>6</sup> This is partly due to the lack of sophisticated instrumentation techniques to visualize molecules, which is a kind of prerequisite for the understanding of the intermolecular interactions that are primarily responsible for the formation of bulk material. However, in recent times, X-ray diffraction techniques, which give the electron density maps, in the form of repeating units (unit cell), help to analyse the non-covalent interactions in the

solids, have emerged as a backbone in the current growth and developments in supramolecular chemistry.

X-ray crystallography studies for a long time focused, in general, more towards establishing the structures of minerals and simple inorganic salts.<sup>7</sup> However, realization of X-ray diffraction potentiality, especially addressing the complex structures of biologically important molecules to understand complicated bio-processes, expanded the horizons of the techniques. One of the notable examples unrevealed the understanding of biology of living beings, by X-ray diffraction studies, is the double helical structure of DNA.<sup>8</sup>

Similarly, determination of three dimensional structure of Tobacco Mosaic Virus (TMV) as shown in Figure 1.1, and analysis of its self assembly, one of the land mark contributions that enriched the knowledge of intermolecular interactions, could be attributed to the advancements in X-ray crystallography.<sup>9</sup> The TMV



**Figure 1.1.** Self assembly in TMV virus.

is composed of a single strand RNA encased in a protein sheath, comprising of 2130 identical protein monomers. Frankel-Conrat and Williams showed that TMV

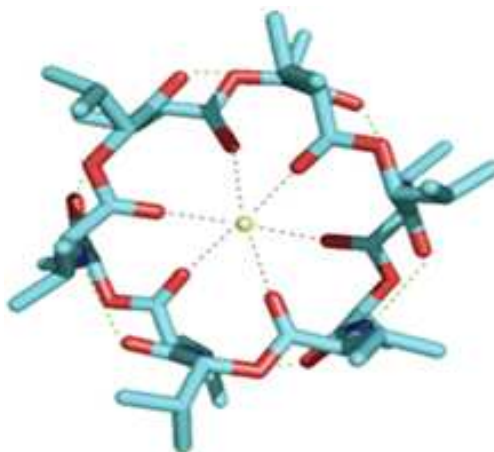
would dissociate into its component parts<sup>10</sup> and the isolated components then could be reconstituted *in vitro*, reforming the intact virus.

## 1.2 Earlier Development in Supramolecular Chemistry

Selective binding of substrates to the receptors through complementary sites, which is well known as molecular recognition is a very important phenomenon in many biological processes as demonstrated by Emil Fisher, as early as in 1894, through the lock and key model,<sup>11</sup> for several enzymatic transformations. Hence, understanding the structure activity relationship of biomolecules with respect to its confirmation in three dimensional space, using X-ray diffraction analysis, helps the structural chemists, for example, to identify a correct substrate, as a drug from the library, for the active sites of the biomolecules through docking process.<sup>12</sup> Binding of the substrate to the appropriate biomolecule at receptor sites is not just simple physical contact, but it depends on the strength of the non-covalent interactions between the complementary groups (opposite charges) and also with the size of the substrate. In the same way, transportation of small molecule across the membrane is a very important biological process, wherein the specific recognition of the substrate to the biomolecule is only through the complementary functionality. In case of transport of ions across the membranes, the process of wrapping of the ion(s) for the smooth transport across lipid bilayer membrane demonstrates the intellectuality of the nature to utilize self assembly mechanism. One of such examples, well known in biology, is the Na<sup>+</sup>/K<sup>+</sup> ion pump,<sup>13</sup> which helps to transport the signals from the nerve cells to the brain.



Similarly, another notable example is Valinomycin dodecadepsipeptide that transport  $K^+$  ions across the membrane of



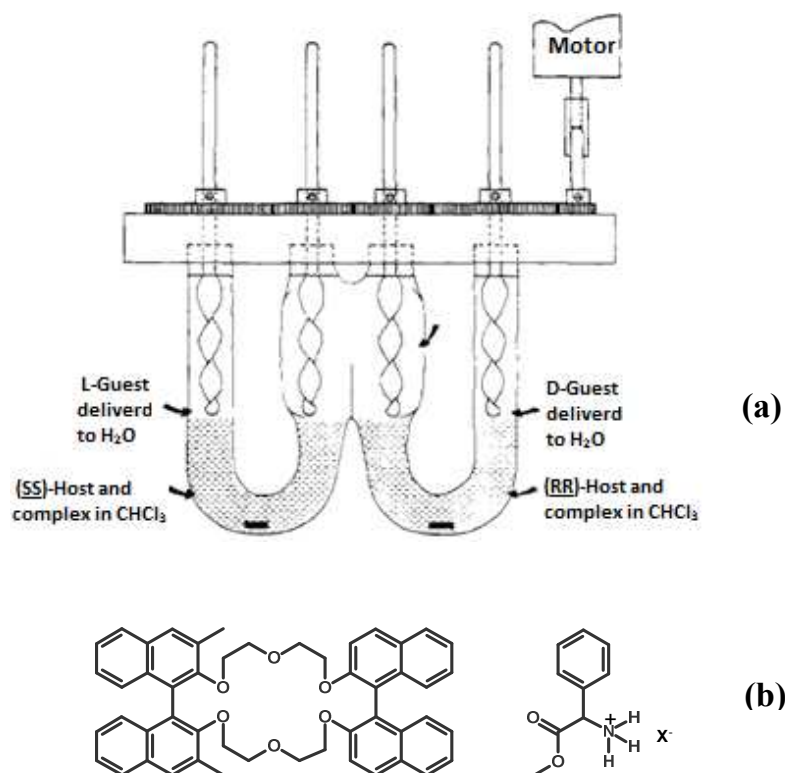
**Figure 1.2.** Structure of valinomycin.

mitochondria.<sup>14</sup> The depsipeptide contains ester and amide linkages, with all the carbonyl oxygen atoms projecting inside the cavity and capture the  $K^+$  ions. At the same time the isopropyl group, which resides at the periphery of the molecule, helps to wrap the ions completely during the transportation process. In addition, this system also highlights following significant features, which are resultant of the self assembly.

- (i) valinomycin binds only to  $K^+$  as the size of the cavity matches exactly for the  $K^+$  ion.
- (ii)  $K^+$  ions remain intact in the cavities due to their interaction with carbonyl oxygens, which signifies the binding features over physical fit.
- (iii) presence of hydrophobic exterior in valinomycin wraps the system towards the exchange of other ions which helps to transport the  $K^+$  ion into the interior of the mitochondria.

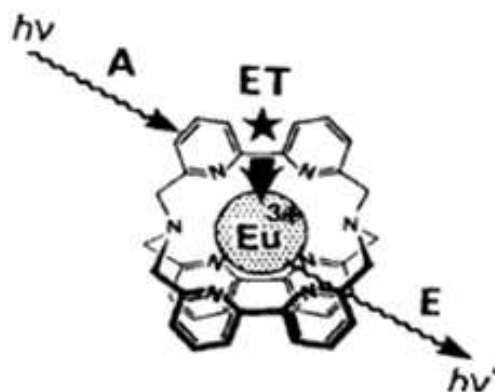
The chemical processes within the biosystems like transportation, separation, catalytic activity, etc., are highly selective that inspire the chemists to mimic such processes within the laboratory environment. In this regard, the serendipitous observation of crown ethers by Pederson<sup>15</sup> for the selective complexation with the alkali metal ions, is a kind of mimic of biological process, which lead to the preparation of many derivatives of crown ethers such as cryptands by J.-M. Lehn,<sup>16</sup> spherands by Cram,<sup>17</sup> etc., that created a new branch, host-guest chemistry, within the realm of research in chemical sciences. Taking the advantage of the knowledge of well established synthetic routes, a variety of host moieties have been developed for specific guest inclusion, to explore different applications in the areas of catalysis, separation, etc.<sup>18</sup> Some selected and representative examples are discussed in following sections.

Cram and co-workers<sup>19</sup> demonstrated the chiral separation of enantiomers of the salts of amino acids, using chiral crown ethers. In this experiment, in a W-shaped tube, the left and right arms are filled with chloroform solution of the optically pure (R,R) and (S,S) forms of crown ether derivative shown in Figure 1.3, while middle chamber is filled with racemic mixture of amino acid salt and LiPF<sub>6</sub> in water, such that it floats over the chloroform pool. Diluted HCl is been introduced in both right and left arms over the chloroform pools. Each pool contains a small stirrer for homogeneous mixing for good separation. By this process, chiral separation of 70-90% has been achieved for the halide salt of methyl ester of phenylalanine. The experimental process and set up is shown in Figure 1.3



**Figure 1.3.** a) Schematic representation of the apparatus used for the chiral separation of amino acids. b) molecular structure of chiral crown ether and the amino acid.

In another notable experiment,<sup>20</sup> enhanced luminescent property was demonstrated for the lanthanide ions when it is complexed with cryptand possessing the linker, 2,2'-bipyridine unit, that has binding sites to form a complex, and also act as light absorbing agent as well as serve as antenna to transfer the absorbed energy for the excitation of lanthanide ions (see Figure 1.4). Enhanced luminescent property with high quantum yield is observed for the lanthanide ions, because the ions wrapped tightly by the cryptate, thus precluding solvation, as compared to the aqueous ions, wherein luminescent property is mostly suffered by the solvation of water molecules.



**Figure 1.4.** Structure of europium cryptate

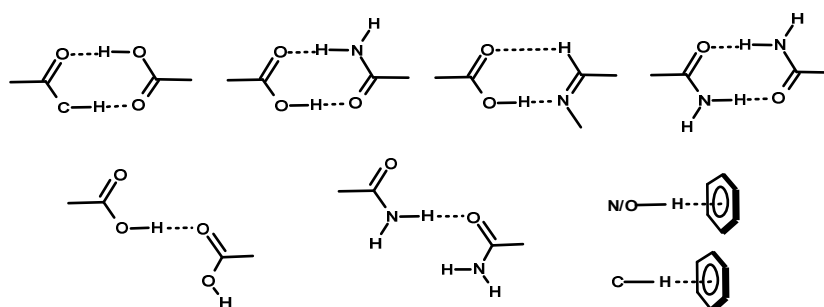
In fact, numerous exotic compounds like cyclodextrins,<sup>21</sup> calixarenes<sup>22</sup> etc., are well studied, emphasizing exotic host-guest properties through molecular recognition, by various research groups, which has led to the development of novel concepts and further developments in the studies of supramolecular chemistry.

### 1.3 Recent Development in Supramolecular Chemistry

Supramolecular chemistry originated with studies of inclusion of the specific guest species within the voids of host moieties, with a primary focus on binding of host and guest species by non-covalent interactions, as illustrated in the above sections. But, in recent times, realization and understanding of self assembly of a large number of molecules in the constrained media, like the solid state, through intermolecular interactions, indeed opened up novel avenues for the exploration of host-guest chemistry,<sup>23</sup> at large supramolecular chemistry, completely dominated by intermolecular interactions, which are quite flexible to tune with an ease. In this process, the synchronized growth in the advancement of X-ray diffraction techniques with high speed computers, and elegant computational

softwares used for the visualization of molecules boosted further the exponential growth of supramolecular chemistry.

Among the intermolecular interactions known in the literature, hydrogen bonds play a major role in the self assembly of organic molecules as most of the functional groups on organic molecules are able to form hydrogen bonds. Some of the functional groups that are well explored in the studies of molecular recognition and the corresponding intermolecular interactions, in the form of recognition patterns, formed by the specific functional groups, as well as observed between those functional groups, in organic molecular crystals, are shown in Scheme 1.1. It will be appropriate here to account some features about hydrogen bonds and its utility.



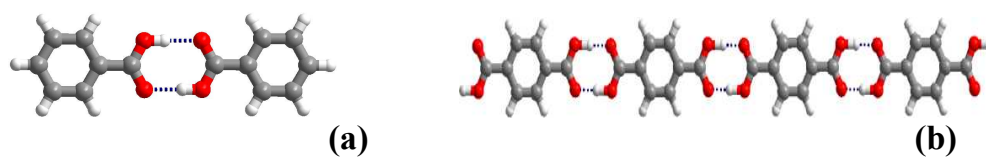
**Scheme 1.1.** Representation of hydrogen bonding patterns for different specific functional groups as well as between the functional groups.

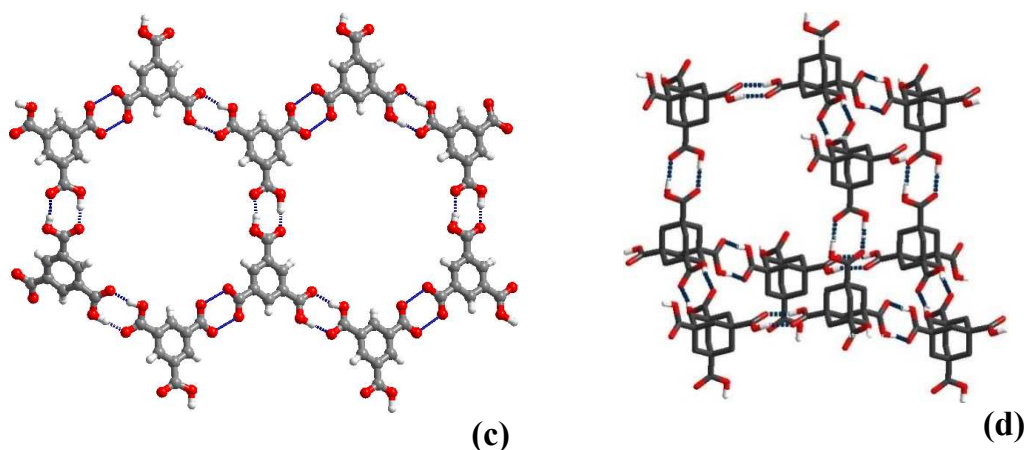
#### 1.4 Hydrogen Bonding

Hydrogen bond is a three centred interaction, where the hydrogen is bridged between two electronegative atoms; while the hydrogen is covalently bonded to one atom (donor), simultaneously it is also connected non-covalently to the other atom (acceptor). Hydrogen bond can be represented as shown below.

## D-H $\cdots$ A

Hydrogen bonds (2-40 kcal/mol) are weak as compared to covalent bonds ( $\sim 80$  kcal/mol) but much stronger than van der Waals interaction ( $< 2$  kcal/mol). In general the hydrogen bonds are classified based on their strength, due to the density of the charge associated with donors and acceptors into three categories; strong, moderate and weak. Excellent reviews<sup>24</sup> and monographs<sup>25</sup> are available describing different types of hydrogen bonds and their role in the formation of organic supramolecular assemblies. An important feature that can be deduced, even from the point of self assembly phenomenon is that hydrogen bond is highly directional, as it is an electrostatic attraction. This important feature of anisotropic nature of hydrogen bond directs the formation of supramolecular assemblies with ensembles of different dimensionality and topology, for example zero, one, two and three dimensional networks. For example benzoic acid<sup>26</sup> forms a zero dimensional dimer unit, as shown in Figure 1.5a, while terephthalic acid<sup>27</sup> forms one dimensional aggregation (Figure 1.5b). But, trimesic acid<sup>28</sup> forms two dimensional network (Figure 1.5c), whereas and adamantanetetracarboxylic acid<sup>29</sup> forms a diamondoid network structure, as shown in Figure 1.5d. Such distinct arrangements attribute varied properties to the materials.



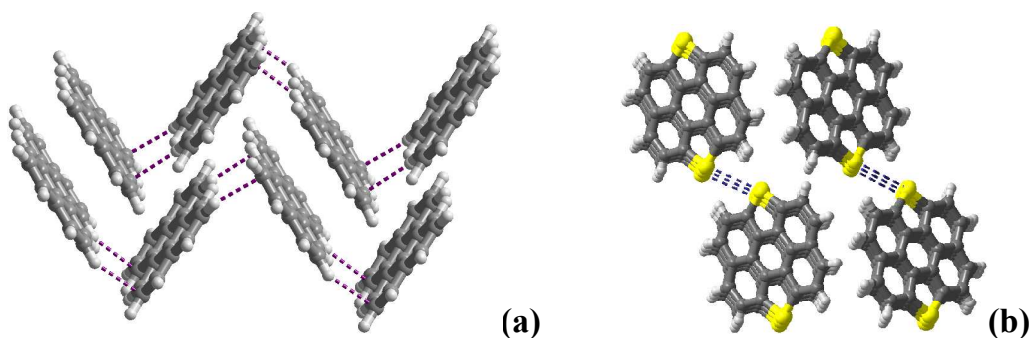


**Figure 1.5.** a) benzoic acid dimer. b) chain of terephthalic acid. c) trimesic acid in the form of hexagons in sheets. d) Diamondoid network structure formed by adamantanetetracarboxylic acid.

## 1.5 Supramolecular Patterns

### 1.5.1 Herringbones

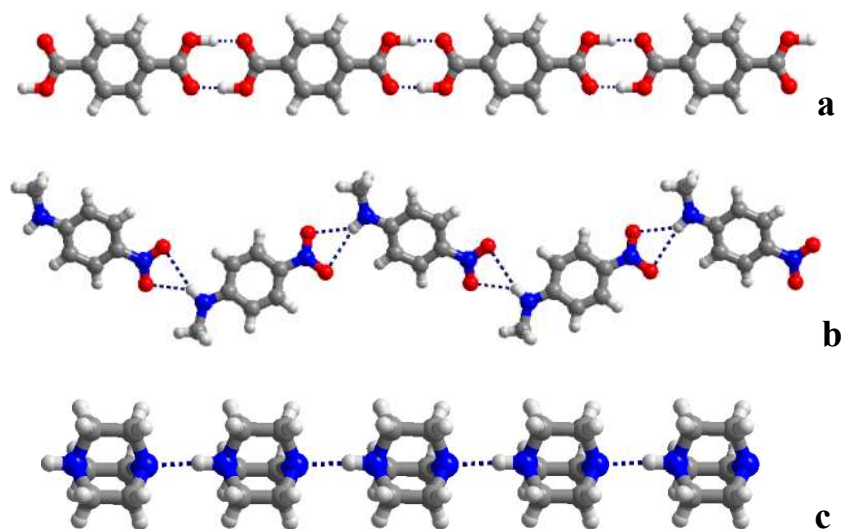
Zero dimensional molecular ensembles form, herringbone topological arrangement, in general, which shows poor charge mobility for molecular electronics. Such feature is so pronounced in the class of aromatic hydrocarbons, in which the arrangement is observed through C-H $\cdots\pi$  interactions.<sup>30</sup> However, recent studies demonstrate that co-facial arrangement stabilized by  $\pi\cdots\pi$  interactions enhances the electronic properties over herringbone patterns. For example perylene<sup>31</sup> forms a herringbone pattern (see Figure 1.6a) with charge mobility of  $0.27 \text{ cm}^2 \text{ V s}^{-1}$ . However, co-facial molecular pattern in dithioperylene<sup>32</sup> (see Figure 1.6b), through S $\cdots$ S interaction, show charge mobility of  $2.3 \text{ cm}^2 \text{ V s}^{-1}$ , which is approximately ten fold higher than the simple perylene derivative.



**Figure 1.6.** a) herringbone pattern obtained for perylene b) stacked arrangement of dithiopyrene through S...S interactions.

### 1.5.2 Tapes

The one-dimensional units, however, yield molecular tapes, in general, infinite in dimension. Some of the illustrative examples are given in Figure 1.7. Such molecular networks are indeed responsible for the attributed properties of the materials, like non-linear optics (NLO), dielectrics, etc.



**Figure 1.7.** Tape structures of formed by a) terephthalic acid. b) N-methylnitroaniline. c) monoprotonated DABCO molecular cation.

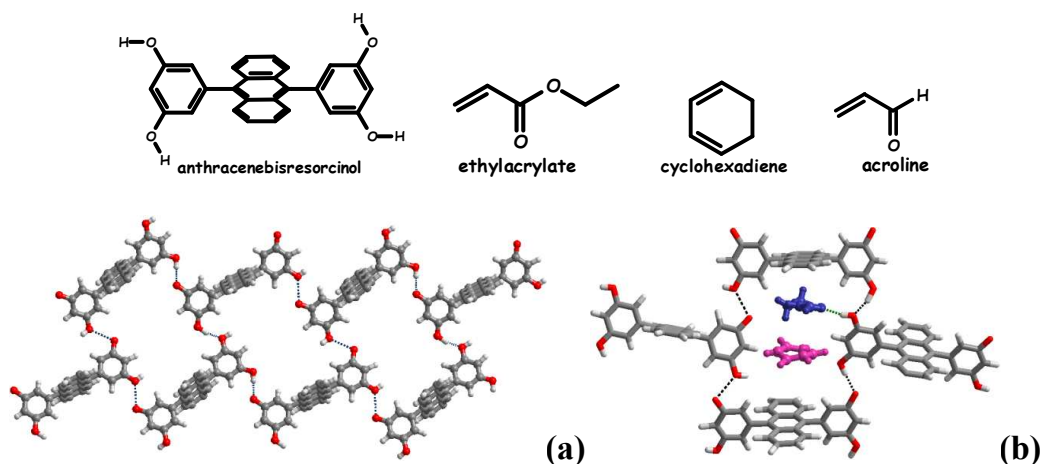


For example, *p*-*N*-methylnitroaniline<sup>33</sup> shows NLO properties due to the ability of propagation of large dipole moment of the molecule, as the adjacent molecules are held together in the form of tapes through bifurcated hydrogen bonds formed between amino and nitro groups, as shown in Figure 1.7b. Similarly, the monoprotonated DABCO molecular ion<sup>34</sup> which has giant dielectric constant, forms molecular tapes through N-H $\cdots$ N<sup>+</sup> hydrogen bonds (Figure 1.7c), which facilitates the transfer of charge along the direction of the tapes attributing dielectric properties for DABCO(HI) molecular ion.

### 1.5.3 Sheets

Two dimensional aggregation of molecules, in general, constitute sheets, especially in the case of planar molecules with substituents located at the appropriate positions that facilitate the desired aggregation. Among different sheet structures, the ones embedded with void space are of special important as such empty space could be used for selective absorption and desorption of guest species, which find exotic applications in catalysis, separation etc. Such cavity structures are due to the aggregation of molecules through intermolecular interactions, such as hydrogen bonds, as compared to the simple close packing forces like van der Waals. However, the cavity structures are not thermodynamically stable, thus, in the absence of appropriate guest species, the voids are being stabilized by interpenetration, self filling etc., in the three dimensional packing. For example, trimesic acid forms a sheet structure with 14 Å<sup>2</sup> cavities, but the void space is being filled by three fold interpenetration to form a close-packed solid. Although the stability of hydrogen bonded apo-hosts are scarcely stable, some exotic reports are

known in the literature, wherein the organic assemblies with sheet structures possessing cavities are quite effective as catalysts for selective reaction studies.



**Figure 1.8.** a) Sheet structure of anthracenebisresorcinol with cavities. b) cyclohexene and ethylacrylate included as guests in the apo-host formed by anthracenebisresorcinol.

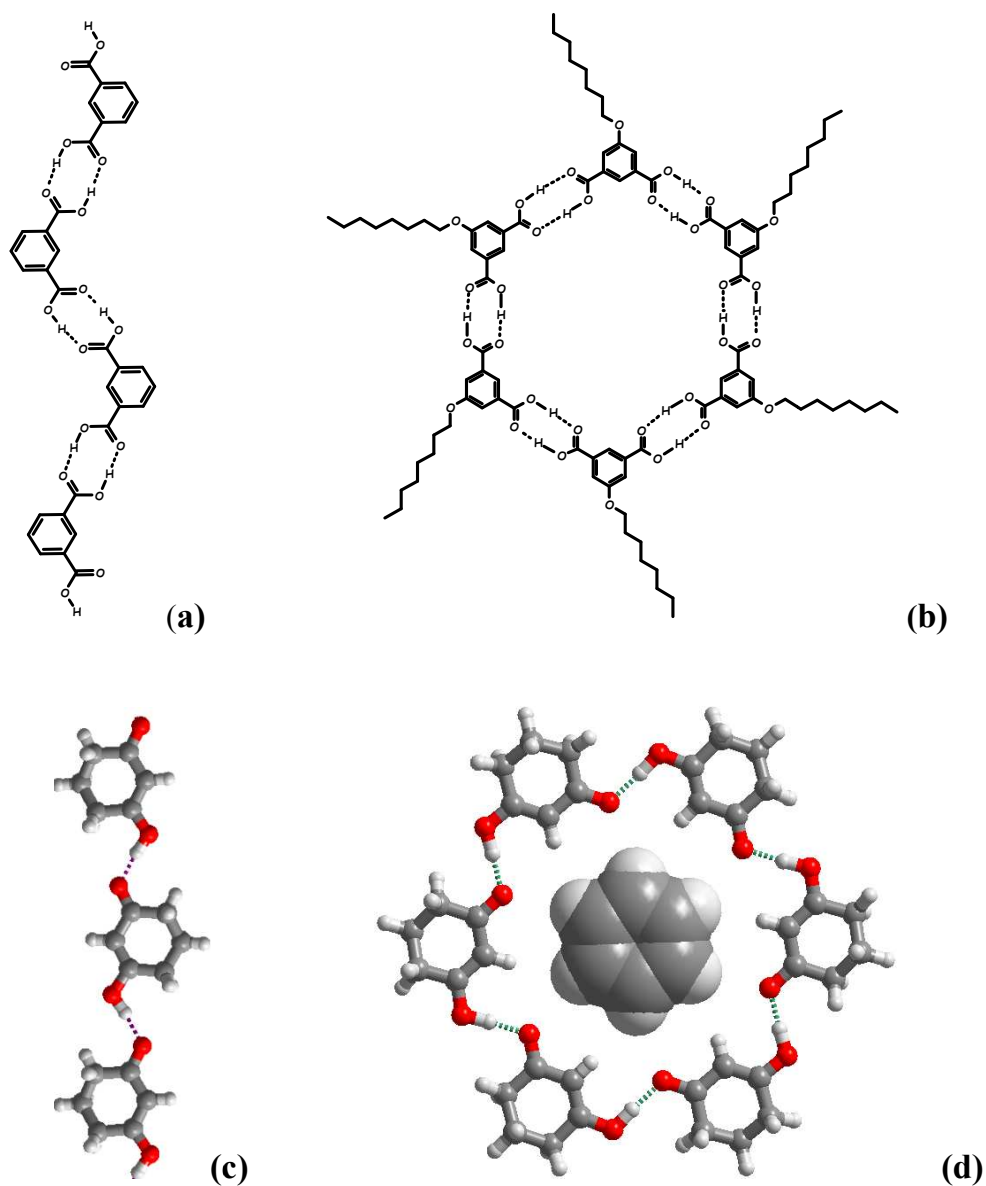
For example, anthracenebisresorcinol<sup>35</sup> forms an apohost (see Figure 1.8) after the removal of the guest species, which is stable and indeed catalyses a Diels-Alder reaction between acroline and cyclohexadiene by adsorbing within the cavities, thereby making the reaction more enantioselective and also reducing reaction time by many folds. However, a reaction with ethylacrylate, or any other higher analogous of acrylates, the catalyst showed poor reactivity as compared to acroline, but with increased enantioselectivity is observed. Such anomalous observations were attributed to the following aspects as reported in the literature.

- (i) the flexible nature of hydrogen bonding host undergoes changes to accommodate the guest, known as induce fit binding, which affects the removal/exchange of the guest species from the host.

- (ii) if the product has less hydrogen bonding ability to the host as compared to the reactant then the reaction will be facilitated.
- (iii) enhanced rate can be obtained for dissociative reaction with more entropy as compared to the associative reaction.
- (iv) if the solvent is used in the reaction contains more hydrogen bonding ability than the guest (product) then the reaction may be facilitated with the solvent which can replace the guest easily.

#### **1.5.4 Interplay Between Tapes and Cyclic Hexamers**

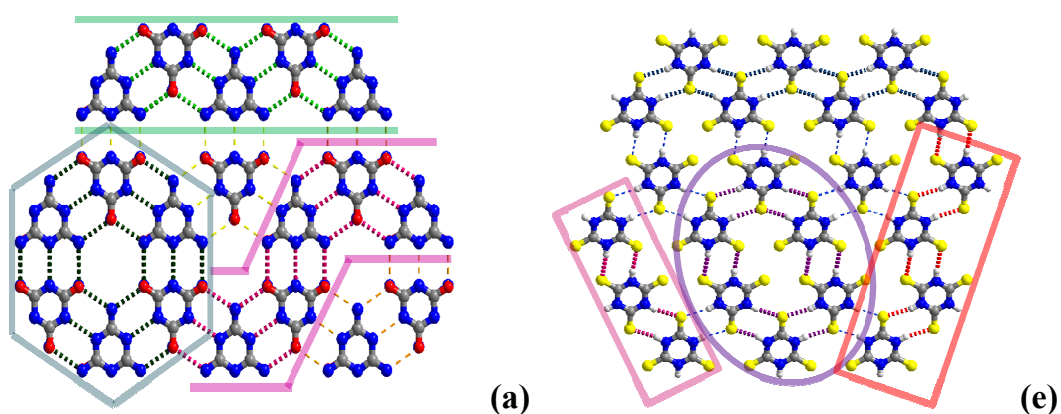
As the intermolecular interactions are tunable, within the ambient energy limits, interplay of topological arrangement is quite facile, thus, enhancing the number of supramolecular assemblies of a specific molecular entity. Such novel assemblies may be realized by different factors such as modifying the peripheral group, guest species etc. Isophthalic acid<sup>36</sup> forms a linear tapes structure or cyclic hexamers, depending upon the presence or absence of alkyl/alkoxy chains, as illustrated in Figures 1.9a and b, serves as a representative example. Further, Etter and co-workers<sup>37</sup> had shown that guest induced transformation of tapes to cyclic hexamer through 1,3-cyclohexanedione. Crystallization of 1,3-cyclohexanedione in the absence of benzene forms tapes, but in the presence of benzene it forms a cyclic hexamer as host with the cavities being filled by the benzene molecules (Figures 1.9c and d).

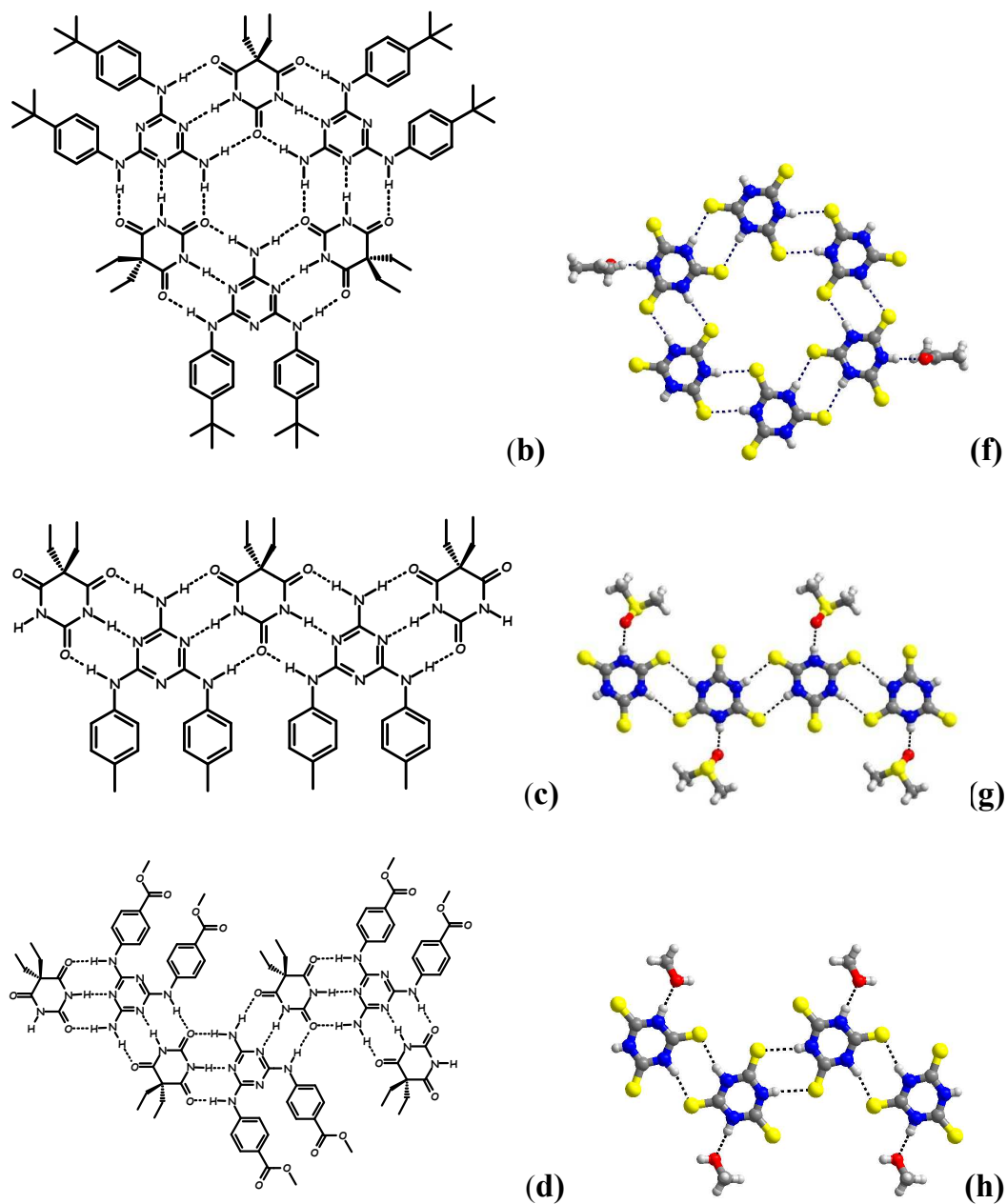


**Figure 1.9.** Tapes and cyclic hexamer observed in a) isophthalic acid b) 5-octyloxyisophthalic acid c) 1,3-cyclohexanedione. d) benzene included 1,3-cyclohexanedione.

However, it is noteworthy to highlight that retrosynthetic analysis of the two dimensional sheet within the supramolecular assembly of melamine and cyanuric acid complex, as shown in Figure 1.10a, identifies three different patterns

such as tapes, ribbons and cyclic hexamers. Whitesides and co-workers<sup>38</sup> have shown successfully, the formation of tapes, ribbons and cyclic hexamers, independently, by the substituted melamines with barbituric acid derivatives (see Figure 1.10 b-d). Such transformations were achieved by varying the bulkiness of the substituent present on the periphery of the molecules. It was noted that increased bulkiness shift the patterns in the order of tapes  $\rightarrow$  ribbons  $\rightarrow$  cyclic hexamers. Interestingly, symmetrically substituted cyclic imide, trithiocyanuric acid (TCA), which forms stacked sheets<sup>39</sup> in its crystal lattice, also contains different tapes as well as cyclic ensembles within the sheets, as shown in Figure 1.10e. It is observed that crystallization of TCA from various solvents, always gives crystals with the corresponding solvent of crystallization. A noteworthy feature from the analysis of those structures<sup>40</sup> is that TCA molecules form either tapes or cyclic hexamers, as shown in the representative examples in Figure 1.10 (f-h). Solvents such as acetone and 2-butanone direct the formation of an assembly with cyclic hexamer, whereas tapes are obtained with solvents like DMSO, DMF, etc.





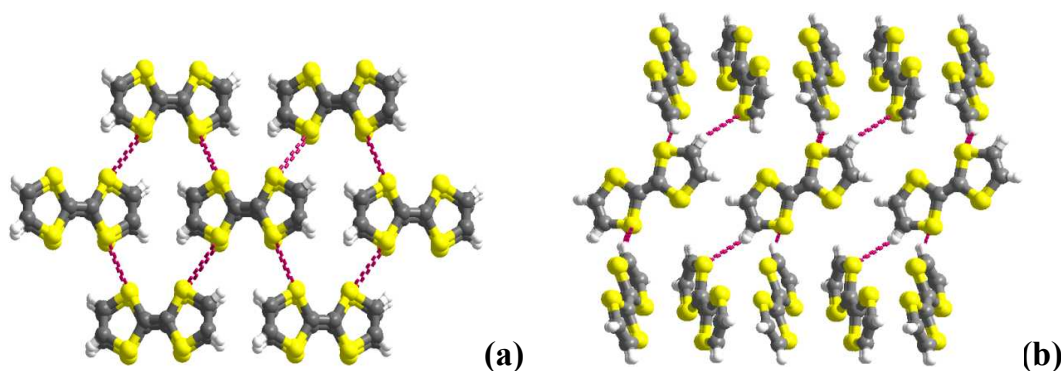
**Figure 1.10.** Tapes, ribbons and hexamers molecular ensembles observed in a) adduct of melamine and cyanuric acid. b-d) substituted melamine and barbituric acid derivatives. e) Trithiocyanuric acid f) TCA with butanone, g) TCA with DMF and h) TCA with methanol.

One of the salient features evolved through the study of intermolecular interactions and topology of molecular ensembles, is ability of a specific molecule to form different ensembles. However, if such a feature is observed without change of molecular contents, those assemblies are well described in the literature as polymorphism,<sup>41</sup> as discussed in following section.

## 1.6 Polymorphism

In general, different forms of a given compound are obtained by crystallization from different solvents, though in recent times such forms are being prepared directly within the solid state, following processes at non-ambient conditions. Such forms are called polymorphs, which show distinctly different physical properties. Thus, polymorphism is a phenomenon wherein a molecule exists at least in two different structures in the solid state. Different physical properties are arrived from the polymorphic crystals is due to the variations in the arrangement of the molecules.<sup>42</sup> Therefore, polymorphism can be identified as a new methodology to prepare materials of different properties, without undergoing complex procedures of synthesis to obtain the new materials. Numerous examples are known in the literature that are known to be polymorphs and search of new forms is always a continuous process. Tetrathiofulvalene (**TTF**) with two forms serves as a representative example.<sup>43</sup> Of the two forms,  $\alpha$ -**TTF** crystallizes in a monoclinic system, with space group  $P2_1/c$ , another one is  $\beta$ -**TTF**, which crystallizes in a triclinic system, with  $P1$  space group. The two different forms are obtained upon crystallization of **TTF** from *n*-heptane and chlorobenzene. Packing of molecules in the two forms are given in Figure 1.11. The two forms show

considerable differences in the packing, with  $\alpha$ -TTF exhibiting strong  $\pi$ - $\pi$  stacking and S $\cdots$ S interactions while  $\beta$ -TTF preferentially pack by C-H $\cdots$ S hydrogen bonds. Thus, transistors based on  $\alpha$ -TTF show field-effect mobility of high value of 1.20 cm<sup>2</sup>/(V s), whereas  $\beta$ -TTF with the value 0.23 cm<sup>2</sup>/(V s).



**Figure 1.11.** a) structure of  $\alpha$ -TTF formed through  $\pi$ - $\pi$  and S $\cdots$ S interaction b) structure of  $\beta$ -TTF formed through C-H $\cdots$ S interaction.

It is noteworthy to mention that while crystallizing a compound from the solvents, often solvent of crystallization also get incorporated in the crystal lattices.<sup>44</sup> As a result, the structural differences arise between the anhydrous and solvated crystals. In fact, the study of Etter and co-workers shown in Figure 1.9(a) and (b) illustrates the large difference that could be realized in the structural features.

### 1.7 Co-crystals

Considering the incorporation of solvents by chance, in the crystal lattice, and thereby changing the topological arrangement of the molecules leading to the materials of different property, deliberate inclusion of appropriate complimentary molecules, which are able to form corresponding patterns with the primary



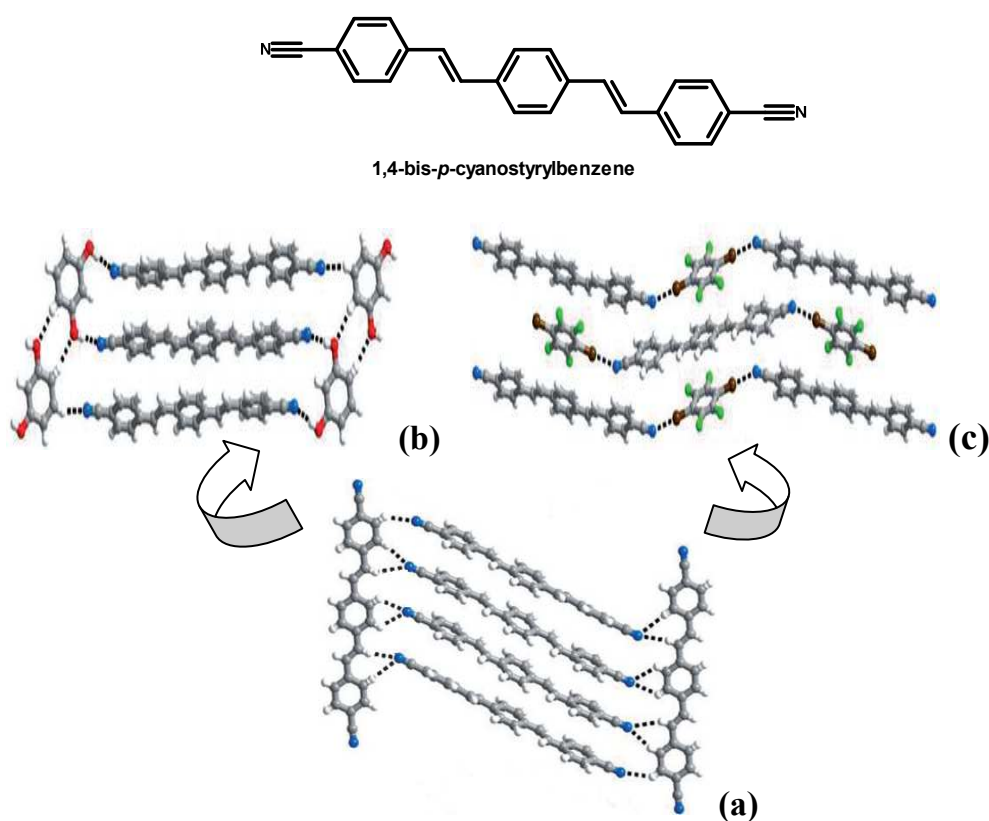
component may also yield materials of different properties than either of the components. Such materials are complemented as co-crystals in the literature, which revolutionized study of supramolecular chemistry in recent times. Taking the nature of interaction between the specific functional groups, simultaneous crystallization of different chemical constituents (co-crystallization) into a single phase, either at ambient or non-ambient conditions is the thrust area of research in the contemporary supramolecular chemistry. In fact, numerous reports available in literature reflects the impact of such processes in various applications,<sup>45</sup> and some of such examples are discussed in following sections, highlighting the significance of the co-crystals.

## **1.8 Applications of Co-crystals**

### **1.8.1 Variation in Luminescent Property**

Several research groups have demonstrated that co-crystallization as a means to prepare materials to fine tune the properties like luminescent, sensitivity of explosives, etc. In this regard, a recent study by Jones and co-workers<sup>46</sup> highlights the tuning of luminescent properties of stilbene derivatives through co-crystallization process. For example, 1,4-*bis-p*-cyanostyrylbenzene, co-crystallized with complimentary ligands resorcinol and dibromotetrachlorobenzene that can form desired intermolecular interactions, like hydrogen and halogen bonds. It was noted that co-crystals of 1,4-*bis-p*-cyanostyrylbenzene with resorcinol did not show any change in luminescent property. It appears that the observed differences are due to the similar stacking arrangement in the co-crystals (Figure 1.12b) and in

parental crystals of styrylbenzene (Figure 1.12a) compared to the change in packing noted in the co-crystals with the dibromotetrachlorobenzene (Figure 1.12c).

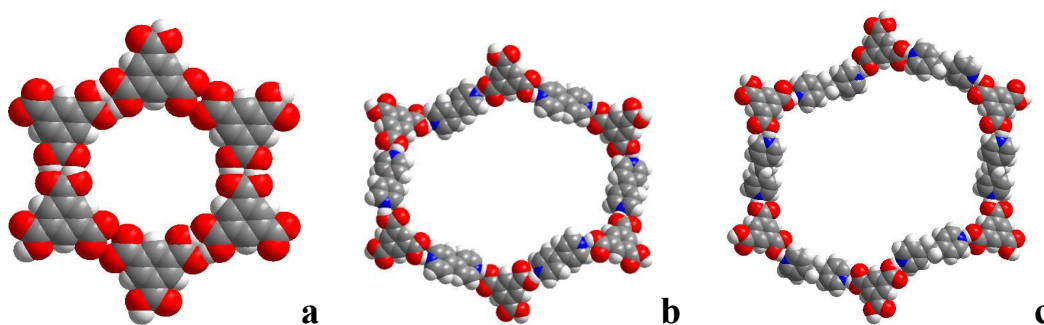


**Figure 1.12.** Stacking arrangement in the crystals of a) 1,4-bis-p-cyanostyrylbenzene and in its co-crystals with b) resorcinol and c) dibromotetrachlorobenzene.

### 1.8.2 Preparation of Cavity Structures

A major boost of co-crystal studies in the supramolecular chemistry is mainly due to the success achieved through the preparation of assemblies that mimic natural materials, particularly like zeolites which possesses large void space and find a lot of applications in the areas of catalysis, separation, storage, etc. For

example, trimesic acid<sup>28</sup> (**TMA**) which forms a cavity structure (honeycomb network), as shown in Figure 1.13a, within its sheet structure, is an effective host for the incorporation of guests of appropriate dimension. Also the cavity dimension is easily variable by co-crystallization process as per the demand. For example, Zaworotko and co-workers<sup>47</sup> have demonstrated that co-crystals of trimesic acid (**TMA**) with 4,4'-bipyridine (**bpy**) gives enhanced cavity size of  $35 \times 26 \text{ \AA}^2$  compared to  $14 \times 14 \text{ \AA}^2$  cavity dimension observed in pure **TMA**.



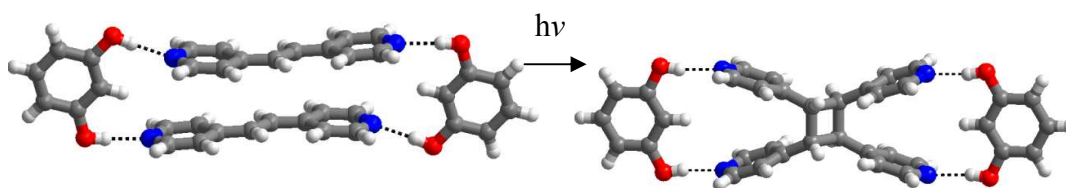
**Figure 1.13.** a) Structure of **TMA** with a cavity,  $14 \times 14 \text{ \AA}^2$  b) co-crystal of **TMA** with **bpy**, and a cavity,  $35 \times 26 \text{ \AA}^2$  c) co-crystal of **TMA** and **bpyea**, with a cavity  $41 \times 35 \text{ \AA}^2$ .

Further enhancement in the cavity size is been realized by increasing the length of co-former, 1,2-*bis*-(4-pyridyl)ethane (**bpyea**), even to the extent of  $41 \times 35 \text{ \AA}^2$ . The different cavity structures are shown in Figure 1.13.

### 1.8.3 [2+2] Cycloaddition

One of the facets of co-crystallization studies that has shown its thrust is the simplification of complicated synthetic processes of macromolecules. [2+2] cycloaddition reactions are well known in organic solid state chemistry since the

variable reactivity was demonstrated by Schimdt and co-workers<sup>48</sup> in the experiments of solid state reactions of *trans*-cinnamic acid. In recent times, such feature in combination with molecular recognition was used by MacGillivray and co-workers to demonstrate preparation of exotic macromolecules like ladderanes<sup>49</sup> which found to be cost and time effective means as well as by simple processes. For example, in the initial study,<sup>49</sup> resorcinol and 1,2-*bis*-(4-pyridyl) ethene (**bpjee**) were co-crystallized and the obtained material was used as template, in which **bpjee** molecule lie within the reactive distance to yield the corresponding dimeric product. The reaction path is shown in Figure 1.14. Such reaction was extended for the synthesis of ladderanes by replacing the aza-donor with an appropriate aza-donor that possesses polyolefins.



**Figure 1.14.** [2+2] cycloaddition reaction of co-crystals of resorcinol and **bpjee**

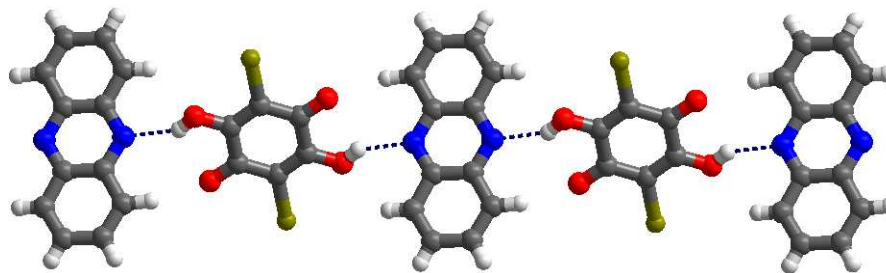
#### 1.8.4 Pharmaceutical Co-crystals

As co-crystals show different properties than the parental compounds, although do not undergo any chemical transformation, such feature is very well being explored in pharma industry to alter the properties of drug molecules without changing the actual API(Active Pharmaceutical Ingredients). In this regard, the basic problems encountered with some drug molecules like solubility, stability, bioavailability etc.<sup>50</sup> are able to be altered by co-crystallization process. Modification in these properties of a drug can be sought along by preparing

appropriate derivatives of API, which is generally complex procedure and also activity of such new entity may not be definite. However, in recent times, co-crystallizing the API with the co-formers, which are mostly food additives, has been shown to alter the properties of the API's, providing route for direct utilization of the API for its bioactivity. For example, itraconazole<sup>51</sup> is an antifungal drug which is highly water insoluble. To attain the required bioavailability the drug is administered in the amorphous form coated on the surfaces of sucrose beads. To overcome the dissolution problems, series of co-crystals of itraconazole with some carboxylic acids is reported. All the co-crystals show higher dissolution profile as compared to the pure crystalline itraconazole. Among all co-crystals L-malic acid co-crystal shows high dissolution profile.

### **1.8.5 Ferroelectrics**

Solids with resultant dipole moment are effective candidates in electronics, NLO etc. Usually molecules tend to aggregate in such a way to cancel the dipole moment present in individual molecule. Recently co-crystals are identified as ferroelectric material through displacive mechanism. For example, Horiuchi and co-workers<sup>45c</sup> showed that bromoanilic acid and phenazine co-crystals act as a room temperature ferroelectrics through such a mechanism. The acidic proton present in bromoanilic acid forms hydrogen bond to phenazine (see Figure 1.15). At low temperature displacement of the proton causes movement of the moiety too, which attributes ferroelectric property for this material.



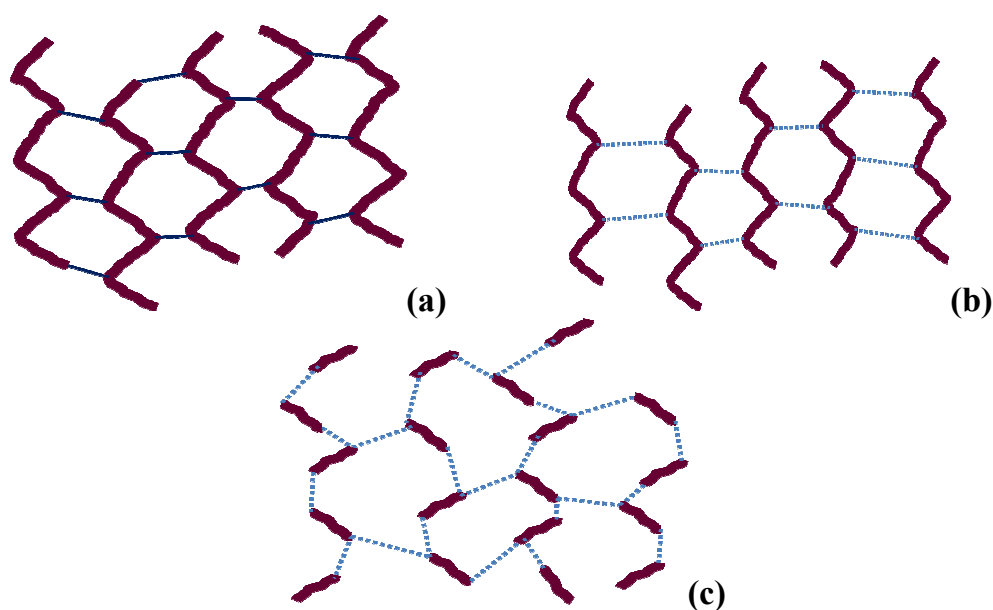
**Figure 1.15.** Molecular arrangement of bromoanilic acid and phenazine through O-H...N hydrogen bond.

In summary, supramolecular chemistry deals with design and synthesis of materials, invariably in solid state, based on the topology and self-assembly of molecules determined by intermolecular interactions in the form of distinct patterns, which is primarily characterized by X-ray diffraction techniques. In recent times, studies pertain to even semi solids, in nature, for example, gels have gained considerable interest expanding the realm of influence of intermolecular interactions.

### 1.9 Low Molecular Weight Molecular Gels (LMWGs)

The examples described in the earlier sections, explaining the efficacy of intermolecular interactions, topological patterns of the self assembled molecules, co-crystals applications etc., which ultimately deals with the materials in the solid state. However, the same concepts are also viable in semi-solid state, which are broadly classified as gels, which deals with inclusion of solvents in a specific host type environment. Since the encapsulation as well as formation of host structures are generally being governed by self-assembly and intermolecular interactions, gelation studies and thrust for preparation of novel gels evolved as a frontier area of research in the current advancements towards exotic applications.

Gels are biphasic systems, wherein the solid phase forms a fibrous network structure with a cavity, which is been filled by the liquid phase and it is immobile mostly due to surface tension.<sup>52</sup> Gels can be classified based on the entanglement of the fibres into two categories chemical and physical gels (see Figure 1.16). In chemical gels, the fibres are connected by covalent bond, whereas in physical gels the fibres are connected by non-covalent interactions. Further, physical gels can be classified into two categories as macromolecular gels and supramolecular gels. In macromolecular gels the fibres formed via covalent interactions, although they are entangled through non-covalent interaction.



**Figure 1.16.** Schematic representation of a) chemical gel b) macromolecular physical gel c) supramolecular gel. note: thin continuous lines indicates covalent bonds; dashed lines represent non-covalent interactions.

However, in supramolecular gels the formation of fibres as well as entanglement is entirely through non-covalent interactions. Formations of gels through specific non-covalent interactions depend upon the information present in the gelator molecule, as well as on the nature of the solvent in which the gel is been prepared. For example, gelation of a specific gelator in water proceed through the aggregation of the molecules by the hydrophobic interactions, while the gel formation in organic solvents is been promoted by other non-covalent interactions, including dipole interactions. Small molecular gels aggregation through relatively weak interaction (4-40 kcal/mol) can be exploited towards various applications due to its flexibility and reversibility. Many gelators with core unit such as fatty acids, cholesterol, saccharide, aromatic, amino acids, etc., in conjunction with long chain alkyl groups are some of the well explored gelators, known in from the literature.

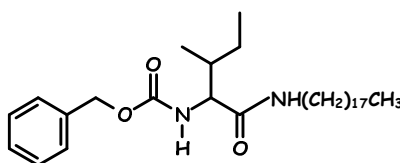
### **1.10 Preparation and Characterization of LMWGs**

In general, gels are prepared by heating the gelator in a solvent followed by slow cooling. In addition to this, gels also can be prepared by adding different solvents in succession. A simple test for the homogeneous gels is the inversion vial test, wherein the gel exhibits no gravitational flow. The strength of the gel can be further carried out by doing rheological measurements such as steady sheer, oscillation, stress relaxation, etc. Further melting of the gel ( $T_g$ ) can be identified by DSC techniques or dropping ball experiments,

Electron microscopy techniques are generally the best to understand physical network of interconnected fibres, morphology of the fibres and entanglement of fibres. Nevertheless, three dimensional structure of the aggregates



that form the fibres is more difficult to obtain, but still powder X-ray diffraction studies on dried gels provide information qualitatively on the organisation of the molecules within the aggregates. In a few cases, LMWGs are been found to form crystals, offering the possibility to use single crystal X-ray diffraction techniques to deduce the precise organisation of the molecules. Among the gels, organogels have attracted researchers as such gels are generally formed by self assembly processes, which are quite flexible to achieve the requisite modifications with an ease.

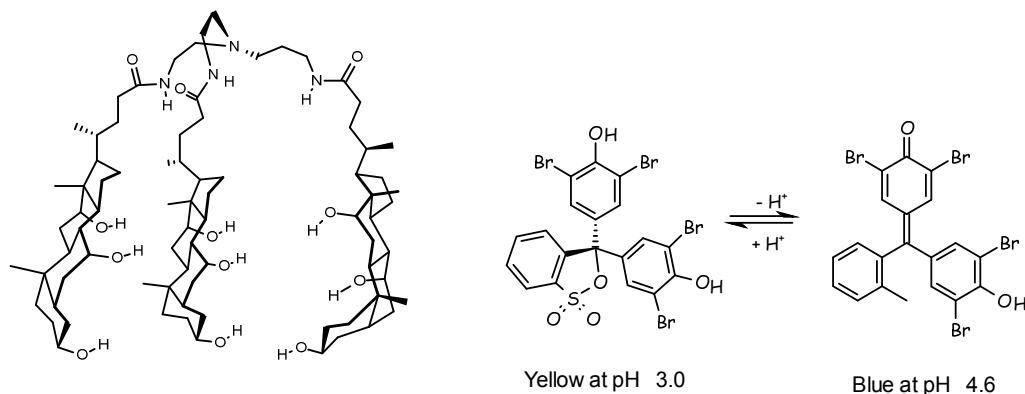


**Figure 1.17.** Molecular structure of an amino acid based gelator.

In recent times, replacement of liquid electrolytes with corresponding polymeric viscous electrolytes, in modern electrochemical energy devices, have been invoked to decrease electrolytic thickness, leakage problems etc. Since polymer electrolyte shows less conductivity as compared to the liquid electrolytes, organogels have been tested in the place of polymer, where the liquid electrolyte is been gelled in the presence of gelator. Interestingly, conductivity measurements on such systems are found to be quite comparable with respect to the liquid electrolyte. For example amino acid derivative,<sup>53</sup> as represented in Figure1.17, which shows gelating ability in various solvents, including different electrolytes, give conductance almost equal to that of the solution electrolyte.

The peculiar property of supramolecular gel is reversibility from gel to sol. This reversibility of gel attained due to the external stimuli such as temperature,

chemical, light, etc., that helps to identify supramolecular gels as a smart materials. For example, Maitra and co-workers<sup>54</sup> reported that the tripodal cholic acid gelator that acts as a host compound undergoes thermoreversible sol-gel conversion in

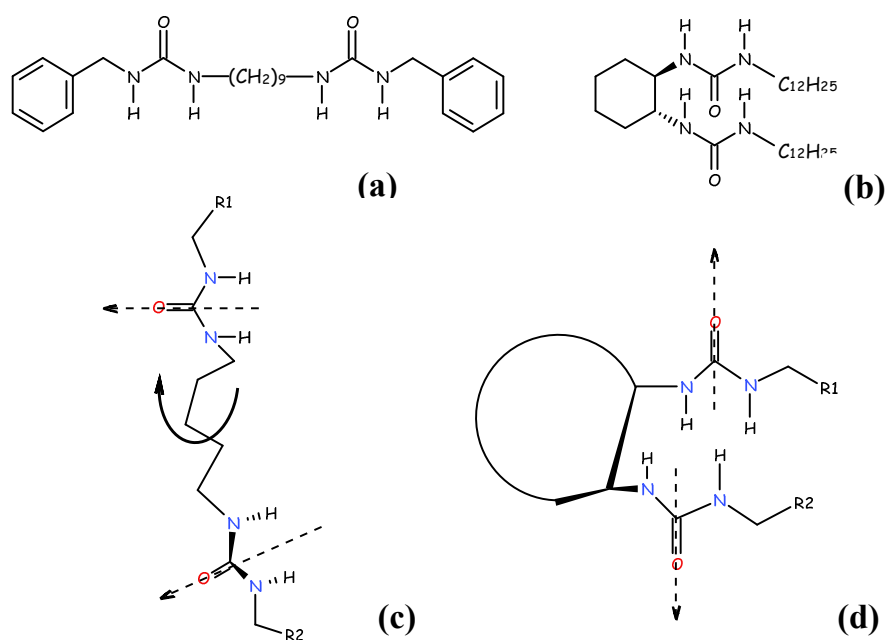


**Figure 1.18.** Structure of a tripodal cholic acid gelator.

aqueous acids at low concentration of 0.4 mg/ml. In the gel, hydrophobic pockets, most likely due to association of the lipophilic beta-faces of cholic acid groups, are able to recognise and entrap specifically ionized form of bromophenol blue, but not its neutral form. The binding of the guest was observed as a colour change upon gelation, from yellow to green (see Figure 1.18).

Most of the supramolecular gels are been identified serendipitously. However, systematic structural studies performed by different research groups gave the following postulation for modelling an effective gelator– (i) the presence of multiple self-complementary and unidirectional interactions to achieve anisotropic self assembly (ii) the control of fibre-solvent interfacial energy to tune solubility and prevent crystallization and (iii) the presence of fibre-fibre interactions to achieve cross-linking and subsequently network formation. Based on these

postulation, the gelator molecules should have the molecular confirmation for one dimensional aggregation supported by peripheral substituents for fibre-fibre interaction. One of the approaches towards the preparation of a targeted gel, with anisotropic self assembly is through invoking appropriate functional groups that recognize each other to undergo spontaneous self assembly. The self assembly of molecules with functional groups are mostly governed by the directional hydrogen bonds.



**Figure 1.19.** Molecular structure of bisurea derivatives in a) acyclic b) cyclic forms. c) and d) conformation of the form shown in (a) and (b) respectively.

In this regard, 1,2-cyclohexanebisamide, as reported by Hanabusa,<sup>55</sup> wherein the molecules gelate in many organic solvents and oils due to the aggregation in one dimension, through  $\text{N-H}\cdots\text{O}$  hydrogen bonds. Secondary amides are identified as better directing groups for the anisotropic self assembly of

molecule in one dimension. In addition, urea based gelators with well defined molecular geometry, are extensively studied for selective gelation studies, due to the placement and orientation of the functional moieties. For instance, bisurea derivatives with linear and cyclic backbones,<sup>56</sup> as shown in Figure 1.14, show that gelation with a variety of solvents is more pronounced in cyclic derivative. The reason for this behaviour is been proposed that the conformation flexibility with the linear derivative yields fibres in dissimilar direction, as compared to the conformationally rigid bisurea derivative, wherein the conformation is fixed, as shown in Figure 1.19.

Apart from the functional group that yield strong non-covalent interactions like hydrogen bonds, the peripheral substituents also play a major role in the formation of network structure, facilitating entanglement of the fibres, through the fibre-fibre interaction.

Taken into account the salient features described in the above sections, studies pertains to self assembly both in solid as well as semi-solids, like gels, need to be explored further to deduce definite conclusions as well as to direct towards target oriented synthesis and applications. Thus, it has been proposed to focus molecular self assembly studies on a class of amides, imides, etc., in the form of gels and co-crystals, and the observed findings are compiled in following Chapters.

**1.11 References**

- (1) (a) DeKock, R. L.; Gray, H. B. *Chemical Structure and Bonding*; University Science Books, 1989. (b) Burdett, J. K. *Chemical Bonding in Solids*; Oxford University Press, USA, 1995.
- (2) (a) Scheiner, S. *Molecular interactions: from van der Waals to strongly bound complexes*; Wiley, 1997. (b) Hobza, P.; Müller-Dethlefs, K.; Hirst, J.; Jordan, K. D.; Lim, C. *Non-Covalent Interactions: Theory and Experiment*; Royal Society of Chemistry, 2009.
- (3) (a) Gans, W.; Boeyens, J. C. A. *Intermolecular Interactions*; Plenum Press, 1998. (b) Hobza, P.; Müller-Dethlefs, K. *Non-Covalent Interactions: Theory and Experiment*; RSC Pub., 2009. (c) Kihara, T. *Intermolecular forces*; Wiley, 1978. (d) Rigby, M. *The Forces between molecules*; Clarendon Press, 1986. (e) Israelachvili, J. N. *Intermolecular And Surface Forces*; Academic Press, 2010.
- (4) (a) Robinson, B. H. *Self-Assembly*; IOS Press, 2003. (b) Lindoy, L.F.; Atkinson, I. M.; Chemistry, R. S. *Self-Assembly in Supramolecular Systems*; Royal Society of Chemistry, 2000. (c) Pelesko, J. A. *Self Assembly: The Science of Things That Put Themselves Together*; Chapman & Hall/CRC, 2007.
- (5) (a) Vögtle, F.; Alfter, F. *Supramolecular chemistry: an introduction*; Wiley, 1991. (b) Lehn, J. M. *Supramolecular Chemistry: Concepts and Perspectives : a Personal Account Built Upon the George Fisher Baker*

*Lectures in Chemistry at Cornell University [and The] Lezione Lincee, Accademia Nazionale Dei Lincei, Roma; VCH, 1995.*

- (6) (a) Diederich, F.; Stang, P. J.; Tykwinski, R. R. *Modern Supramolecular Chemistry: Strategies for Macrocyclic Synthesis*; Wiley-VCH, 2008. (b) Steed, J. W.; Atwood, J. L. *Supramolecular Chemistry*; Wiley, 2009.
- (7) Dana, E. S. *A Text-Book of Mineralogy. with an Extended Treatise on Crystallography and Physical Mineralogy*; Read Books Design, 2011.
- (8) Watson, J. D.; Crick, F. *The Structure of DNA*; Biological Laboratory, 1953.
- (9) (a) Klug, A. *Philos. Trans. R. Soc. London (Biol)* **1999**, 354, 531. (b) Smith, M. L.; Fitzmaurice, W. P.; Turpen, T. H.; Palmer, K. E. In *Plant-Produced Microbial Vaccines*; Karasev, A. V., Ed. 2009; Vol. 332, p 13. (c) Stubbs, G. *Philos. Trans. R. Soc. London (Biol)* **1999**, 354, 551.
- (10) (a) Fraenkelconrat, H. *Bioessays* **1990**, 12, 351. (b) Fraenkel-Conrat, H.; Singer, B. *Philos. Trans. R. Soc. London (Biol)* **1999**, 354, 583.
- (11) Fischer, E. *Ber. Dtsch. Chem. Ges.* **1894**, 27, 2985.
- (12) Comba, P. *Modeling of Molecular Properties*; John Wiley & Sons, 2011.
- (13) (a) Yu, H. B.; Ratheal, I.; Artigas, P.; Roux, B. *Aust. J. Chem.* **2012**, 65, 448. (b) Faller, L. D. *Arch. Biochem. Biophys.* **2008**, 476, 12. (c) Glynn, I. M. *Annual Review of Physiology* **2002**, 64, 1. (d) Glynn, I. M. *J. Physiol. (Lond.)* **1993**, 462, 1.
- (14) (a) Muraveva, T. I.; Ryabova, I. D.; Oreshnik.Na; Novikova, M. A. *Biokhim.* **1973**, 38, 845. (b) Guerin, B.; Bunoust, O.; Rouqueys, V.; Rigoulet, M. *J. Biol. Chem.* **1994**, 269, 25406.

- (15) Pedersen, C. J. *Angew. Chem. Int. Ed. Engl.* **1988**, 27, 1021.
- (16) Lehn, J. M. *Angew. Chem. Int. Ed. Engl.* **1988**, 27, 89.
- (17) Cram, D. J. *Angew. Chem. Int. Ed. Engl.* **1988**, 27, 1009.
- (18) (a) Llc, B. *Crown Ethers: Crown Ether, Metallocrown, 15-Crown-5, 18-Crown-6, 12-Crown-4, Dibenzo-18-Crown-6*; General Books LLC, 2010. (b) Q. Ashton Acton, P. D. *Cyclic Ethers: Advances in Research and Application: 2011 Edition, ScholarlyBrief*; ScholarlyEditions.
- (19) Newcomb, M.; Toner, J. L.; Helgeson, R. C.; Cram, D. J. *J. Am. Chem. Soc.* **1979**, 101, 4941.
- (20) (a) Lehn, J. M.; Pietraszkiewicz, M.; Karpiuk, J. *Helv. Chim. Acta* **1990**, 73, 106. (b) Blasse, G.; Dirksen, G. J.; Vandervoort, D.; Sabbatini, N.; Perathoner, S.; Lehn, J. M.; Alpha, B. *Chem. Phys. Lett.* **1988**, 146, 347. (c) Alpha, B.; Balzani, V.; Lehn, J. M.; Perathoner, S.; Sabbatini, N. *Angew. Chem. Int. Ed. Engl.* **1987**, 26, 1266. (d) Rodriguezubis, J. C.; Alpha, B.; Plancherel, D.; Lehn, J. M. *Helv. Chim. Acta* **1984**, 67, 2264.
- (21) Lock, J. *Cyclodextrins: Molecular Wheels for Supramolecular Chemistry*; University of Adelaide, School of Chemistry and Physics, Discipline of Chemistry, 2004.
- (22) Gutsche, C. D.; Chemistry, R. S. o. *Calixarenes: An Introduction*; RSC Publishing, 2008.
- (23) (a) Hart, H.; Lin, L. T. W.; Ward, D. L. *J. Am. Chem. Soc.* **1984**, 106, 4043. (b) Weber, E.; Hens, T.; Brehmer, T.; Csoregh, I. *J. Chem. Soc. Perk. T 2* **2000**, 235. (c) Wuest, J. D. *Chem. Commun.* **2005**, 5830. (d) Delori, A.;

- Suresh, E.; Pedireddi, V. R. *Chem. Eur. J.* **2008**, *14*, 6967. (e) Friscic, T.; Trask, A. V.; Jones, W.; Motherwell, W. D. S. *Angew. Chem. Int. Ed.* **2006**, *45*, 7546. (f) Harris, K. D. M. *Supramol. Chem.* **2007**, *19*, 47. (g) Moorthy, J. N.; Natarajan, R.; Venugopalan, P. *J. Org. Chem.* **2005**, *70*, 8568. (h) Ranganathan, A.; Pedireddi, V. R.; Chatterjee, S.; Rao, C. N. R. *J. Mater. Chem.* **1999**, *9*, 2407.
- (24) (a) Steiner, T. *Angew. Chem. Int. Ed.* **2002**, *41*, 48. (b) Fan, E.; Vicent, C.; Geib, S. J.; Hamilton, A. D. *Chem. Mater.* **1994**, *6*, 1113.
- (25) (a) Gilli, G.; Gilli, P. *The Nature of the Hydrogen Bond: Outline of a Comprehensive Hydrogen Bond Theory*; Oxford University Press, 2009. (b) Jeffrey, G. A. *An Introduction to Hydrogen Bonding*; Oxford University Press, 1997. (c) Desiraju, G. R.; Steiner, T. *The Weak Hydrogen Bond: In Structural Chemistry and Biology*; Oxford University Press, 2001.
- (26) Bruno, G.; Randaccio, L. *Acta Crystallogr. Sect. B: Struct. Sci.* **1980**, *36*, 1711.
- (27) Bailey, M.; Brown, C. J. *Acta Crystallogr.* **1967**, *22*, 387.
- (28) Duchamp, D. J.; Marsh, R. E. *Acta Crystallogr. Sect. B: Struct. Sci.* **1969**, *B* *25*, 5.
- (29) Ermer, O. *J. Am. Chem. Soc.* **1988**, *110*, 3747.
- (30) Nishio, M.; Hirota, M.; Umezawa, Y. *The CH-[pi] Interaction: Evidence, Nature, and Consequences*; Wiley, 1998.
- (31) Kotani, M.; Kakinuma, K.; Yoshimura, M.; Ishii, K.; Yamazaki, S.; Kobori, T.; Okuyama, H.; Kobayashi, H.; Tada, H. *Chem. Phys.* **2006**, *325*, 160.



- (32) Jiang, W.; Zhou, Y.; Geng, H.; Jiang, S. D.; Yan, S. K.; Hu, W. P.; Wang, Z. H.; Shuai, Z. G.; Pei, J. A. *J. Am. Chem. Soc.* **2011**, *133*, 1.
- (33) Panunto, T. W.; Urbanczykclipkowska, Z.; Johnson, R.; Etter, M. C. *J. Am. Chem. Soc.* **1987**, *109*, 7786.
- (34) (a) Szafranski, M.; Katrusiak, A. *J. Phys. Chem. B* **2008**, *112*, 6779. (b) Olejniczak, A.; Katrusiak, A.; Szafranski, M. *Cryst. Growth Des.* **2010**, *10*, 3537.
- (35) (a) Tanaka, T.; Tasaki, T.; Aoyama, Y. *J. Am. Chem. Soc.* **2002**, *124*, 12453. (b) Endo, K.; Koike, T.; Sawaki, T.; Hayashida, O.; Masuda, H.; Aoyama, Y. *J. Am. Chem. Soc.* **1997**, *119*, 4117.
- (36) Yang, J.; Marendaz, J. L.; Geib, S. J.; Hamilton, A. D. *Tetrahedron Lett.* **1994**, *35*, 3665.
- (37) Etter, M. C.; Urbanczykclipkowska, Z.; Jahn, D. A.; Frye, J. S. *J. Am. Chem. Soc.* **1986**, *108*, 5871.
- (38) (a) Zerkowski, J. A.; Seto, C. T.; Whitesides, G. M. *J. Am. Chem. Soc.* **1992**, *114*, 5473. (b) Zerkowski, J. A.; Seto, C. T.; Wierda, D. A.; Whitesides, G. M. *J. Am. Chem. Soc.* **1990**, *112*, 9025. (c) Zerkowski, J. A.; Macdonald, J. C.; Seto, C. T.; Wierda, D. A.; Whitesides, G. M. *J. Am. Chem. Soc.* **1994**, *116*, 2382.
- (39) Guo, F.; Cheung, E. Y.; Harris, K. D. M.; Pedireddi, V. R. *Cryst. Growth Des.* **2006**, *6*, 846.
- (40) Ahn, S.; PrakashaReddy, J.; Kariuki, B. M.; Chatterjee, S.; Ranganathan, A.; Pedireddi, V. R.; Rao, C. N. R.; Harris, K. D. M. *Chem. Eur. J.* **2005**, *11*, 2433.

- (41) Bernstein, J. *Polymorphism in Molecular Crystals*; Oxford University Press, USA, 2002.
- (42) (a) Mangin, D.; Puel, F.; Veessler, S. *Org. Process Res. Dev.* **2009**, *13*, 1241. (b) Nangia, A. *Acc. Chem. Res.* **2008**, *41*, 595. (c) Gavezzotti, A. *J. Pharm. Sci.* **2007**, *96*, 2232. (d) Bernstein, J.; Davey, R. J.; Henck, J. O. *Angew. Chem. Int. Ed.* **1999**, *38*, 3440. (e) Braga, D.; Grepioni, F.; Maini, L.; Polito, M. In *Molecular Networks*; Hosseini, M. W., Ed. 2009; Vol. 132, p 25.
- (43) Ellern, A.; Bernstein, J.; Becker, J. Y.; Zamir, S.; Shahal, L.; Cohen, S. *Chem. Mater.* **1994**, *6*, 1378.
- (44) Herbstein, F. H. *Cryst. Growth Des.* **2004**, *4*, 1419.
- (45) (a) Akpınar, H.; Mague, J. T.; Novak, M. A.; Friedman, J. R.; Lahti, P. M. *Crystengcomm* **2012**, *14*, 1515. (b) Ghosh, S.; Reddy, C. M. *Crystengcomm* **2012**, *14*, 2444. (c) Horiuchi, S.; Ishii, F.; Kumai, R.; Okimoto, Y.; Tachibana, H.; Nagaosa, N.; Tokura, Y. *Nature Mater.* **2005**, *4*, 163. (d) Perumalla, S. R.; Sun, C. C. *Crystengcomm* **2012**, *14*, 3851.
- (46) Yan, D. P.; Delori, A.; Lloyd, G. O.; Friscic, T.; Day, G. M.; Jones, W.; Lu, J.; Wei, M.; Evans, D. G.; Duan, X. *Angew. Chem. Int. Ed.* **2011**, *50*, 12483.
- (47) (a) Shattock, T. R.; Vishweshwar, P.; Wang, Z. Q.; Zaworotko, M. J. *Cryst. Growth Des.* **2005**, *5*, 2046. (b) Sharma, C. V. K.; Zaworotko, M. J. *Chem. Commun.* **1996**, 2655.
- (48) (a) Hung, J. D. L., M.; Luwisch, M.; Schmidt, G. M. *J. Isr. J. Chem.* **1972**, *10*, 585. (b) Cohen, M. D. C., R.; Lahav, M.; Nie, P. L. *J. Chem. Soc., Perkin Trans.* **1973**, *2*, 1095. (c) Green, B. S. H., L. *J. Org. Chem.* **1974**, *39*, 196.

- (49) Macgillivray, L. R.; Papaefstathiou, G. S.; Friscic, T.; Hamilton, T. D.; Bucar, D. K.; Chu, Q.; Varshney, D. B.; Georgiev, I. G. *Acc. Chem. Res.* **2008**, *41*, 280.
- (50) (a) Friscic, T.; Jones, W. *J. Pharm. Pharmacol.* **2010**, *62*, 1547. (b) Qiao, N.; Li, M. Z.; Schlindwein, W.; Malek, N.; Davies, A.; Trappitt, G. *Int. J. Pharm.* **2011**, *419*, 1. (c) Schultheiss, N.; Newman, A. *Cryst. Growth Des.* **2009**, *9*, 2950. (d) Blagden, N.; de Matas, M.; Gavan, P. T.; York, P. *Adv. Drug Deliv. Rev.* **2007**, *59*, 617. (e) Shan, N.; Zaworotko, M. J. *Drug Discov. Today* **2008**, *13*, 440. (f) Trask, A. V. *Mol. Pharm.* **2007**, *4*, 301. (g) Vishweshwar, P.; McMahon, J. A.; Bis, J. A.; Zaworotko, M. J. *J. Pharm. Sci.* **2006**, *95*, 499.
- (51) Remenar, J. F.; Morissette, S. L.; Peterson, M. L.; Moulton, B.; MacPhee, J. M.; Guzman, H. R.; Almarsson, O. *J. Am. Chem. Soc.* **2003**, *125*, 8456.
- (52) (a) Fages, F.; Araki, K. *Low Molecular Mass Gelators: Design, Self-Assembly, Function*; Springer, 2005. (b) Weiss, R. G.; Terech, P. *Molecular Gels: Materials With Self-assembled Fibrillar Networks*; Springer, 2006.
- (53) (a) Hanabusa, K.; Hiratsuka, K.; Kimura, M.; Shirai, H. *Chem. Mater.* **1999**, *11*, 649. (b) Placin, F.; Desvergne, J. P.; Lassegues, J. C. *Chem. Mater.* **2001**, *13*, 117.
- (54) Maitra, U.; Mukhopadhyay, S.; Sarkar, A.; Rao, P.; Indi, S. S. *Angew. Chem. Int. Ed.* **2001**, *40*, 2281.
- (55) Zweep, N.; Hopkinson, A.; Meetsma, A.; Browne, W. R.; Feringa, B. L.; van Esch, J. H. *Langmuir* **2009**, *25*, 8802.

- (56) van Esch, J.; Schoonbeek, F.; de Loos, M.; Kooijman, H.; Spek, A. L.; Kellogg, R. M.; Feringa, B. L. *Chem.Eur. J.* **1999**, *5*, 937.

## CHAPTER TWO

Synthesis and Structural Studies of Some 1,3,5-

Benzenetricarboxamide Based Gelators

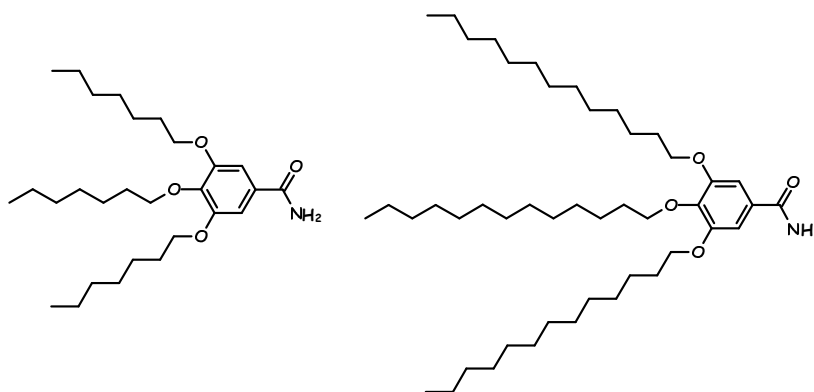
## 2.1 Introduction

Most of the molecular gels are observed serendipitously<sup>1</sup>. However, in recent times, preparation of functional gels based on design strategies has been successfully demonstrated with a high degree of precision and reproducibility.<sup>1d,2</sup> In this process, self assembly is a critical step, especially, towards preparation of gels of low molecular weight compounds, which proceed by two step mechanism- (i) formation of fibres and (ii) entanglement of the fibres to form network structure. In general, such processes are directly related to the nature of the intermolecular interactions which drive the molecules to orient in a specific direction. There are many intermolecular interactions which are found to be directional, but amongst hydrogen bonds<sup>3</sup> play a major role in the formation of gels, provided the functional groups present on a molecule are oriented in a required fashion. Gelators possessing the functional groups such as alcohol, acid, amide etc., are well known as hydrogen bonded gelators, as they self assemble primarily through hydrogen bonds. Among many functional groups which have been explored in the area of hydrogen bonded gels, amides are of special interest, because both primary and secondary amides possess potential hydrogen bond donor and acceptors. In following sections, important features of the amide groups in the formation of gel, are highlighted.

## 2.2 Amide Based gelators

### 2.2.1 Primary amide gelators

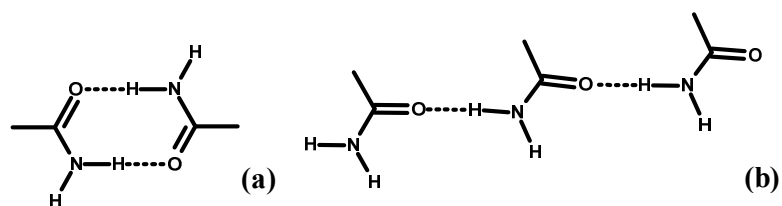
To start with, simple primary amides, for example, benzamide derivatives, as shown in Figure 2.1, Beginn and co-workers<sup>4</sup> have demonstrated the gelation features of 3,4,5-trialkoxymethylbenzamide derivatives, by preparing the gels in a cross linked polymer matrix. In a typical experiment, the monomer, cross-linker and photoinitiator along with the benzamide gelator heated in a vial and subjected to shock-freezing of the solution at  $-180^{\circ}\text{C}$  followed by polymerization at  $-50^{\circ}\text{C}$ . The surface of the resultant solid is analysed by tapping mode SFM microscopy, such analysis, indeed, reveals the morphology of the fibres in gels embedded in the polymer matrix.



**Figure 2.1.** Molecular structures of benzamide mediated gelators.

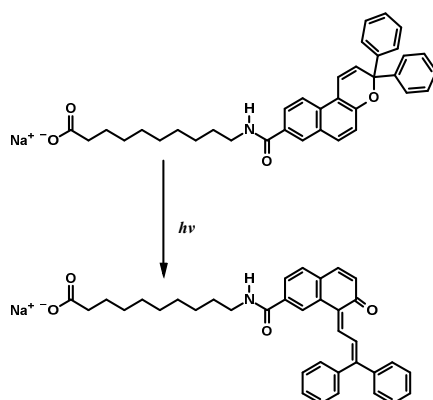
### 2.2.2. Secondary amide gelators

Amides form two types of hydrogen bonding patterns, as shown in following Figure 2.2, which are cyclic and acyclic patterns in nature.



**Figure 2.2.** Hydrogen bonding patterns in amides a) primary amide and b) secondary amide

The acyclic patterns, which are propensity of secondary amides, are of interest in the design and synthesis of gels as these interactions may facilitate the molecules to align in a specific direction at ease. In fact, several gels mediated by secondary amides are well known in the literature. For example, monoamide derivative of sodium salt of 11-aminoundecanoic acid, which shows an excellent gelation ability even with bulky substituents in the amide core, like naphthalene, adamantane, etc. Interestingly, in this series 2H-chromene substituted derivative<sup>5</sup> of sodium 11-aminoundecanoate was shown to undergo interconversion between gel and solution

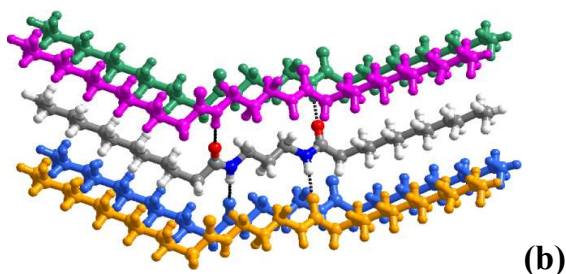
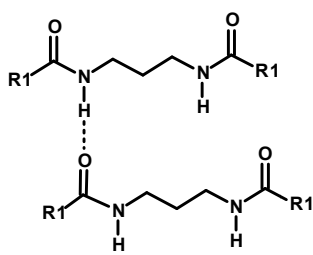


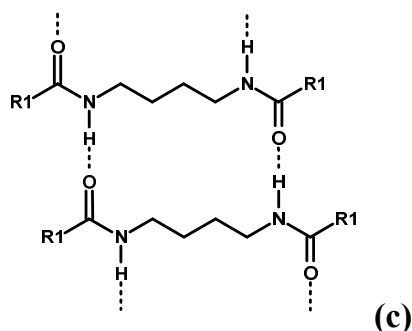
**Figure 2.3.** Photochemical conversion between the open and closed forms of 2H-chromene unit in sodium-11-aminoundecanoate.



state by distinct colour change upon photoirradiation, which is due to the interconversion of 2H-chromene unit between its open and closed forms, as shown in Figure 2.3. This type of gel could be utilized as a smart material.

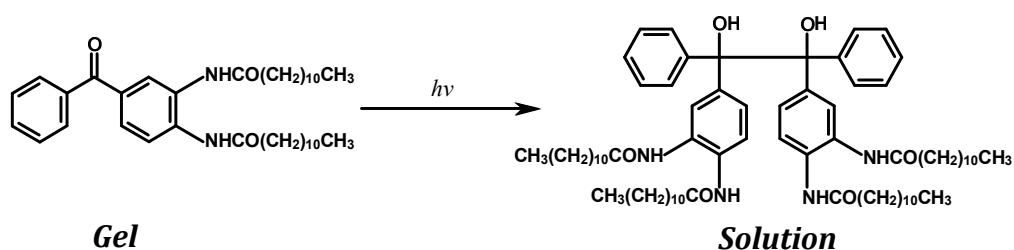
Similarly, polysubstituted gelators are designed and synthesized using substituents which enhance the ease of self assembly by forming multiple interactions and also ultimately strengthen the structural rigidity of the gels. In this process, secondary amide based *bis*, *tris* and *poly* amides mediated compounds have been demonstrated to be the excellent gelators with unique structural ensembles and tailor made properties. For example, secondary bisamides have been shown to form different fibrous structures differentiable by topological arrangement as demonstrated by Tomioka and co-workers<sup>6</sup> for the gelators which are analogous to each other, differentiated by carbon chain length between the amide groups, as shown in Figure 2.4. Thus, amides with odd number of carbons are found to be yielding interwoven structure through ensembles of pentameric units, while amides with even numbered carbons form dimeric units, yielding ribbon structure, through two single N-H...O hydrogen bonds due to the *anti* orientation of the two amide groups.





**Figure 2.4.** Representation of the hydrogen bonding pattern in bisamide derivatives. a) *syn* orientation of the amide groups yielding single hydrogen bond. b) ensemble of five bisamide molecules. c) hydrogen bonds in the amides with *anti* orientation.

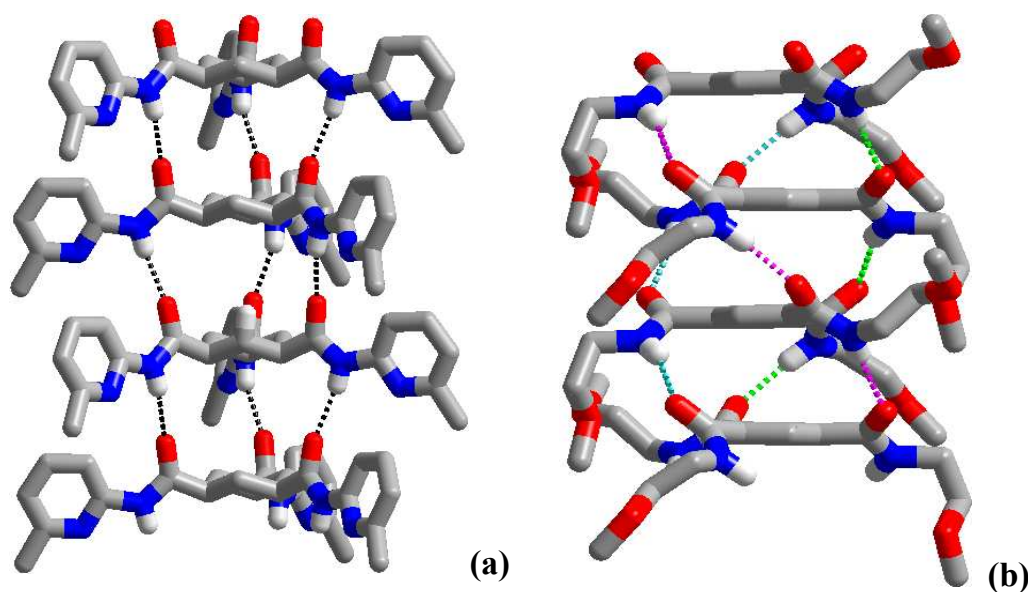
Also, a bisamide of benzophenone derivative has been shown to form a gel in the presence of propanol. Such gels, upon photoirradiation undergoes a chemical reaction by the conversion of benzophenone derivative into the corresponding pinacol (see Figure 2.5) as known in solution state also, suggesting similar chemical activity both in solution and gelation media. Such a conversion is easily could be monitored by the change of physical state from gel to solution<sup>7</sup>.



**Figure 2.5.** Reaction scheme showing the conversion of benzophenone based gelator into a pinacol.

In recent times, other higher analogues of secondary amides gained much attention and amongst  $C_3$  symmetry based gelators like 1,3,5-benzene/

cyclohexanetricarboxamide derivatives have been explored thoroughly. Varied substituents at the periphery of these tricarboxamide derivatives gave a variety of functional molecular gels, due to facile one dimensional molecular aggregation to yield the columnar assembly by utilizing the amide groups. In this process, Hamilton and group<sup>8</sup> exemplified the molecular self assembly in the gelator family of 1,3,5-cyclohexanetricarboxamide derivatives, through the formation of three single hydrogen bonds by the three amide groups with the corresponding moieties on the adjacent molecules, facilitating the stiff columnar packing. Such an assembly is shown in Figure 2.6a.

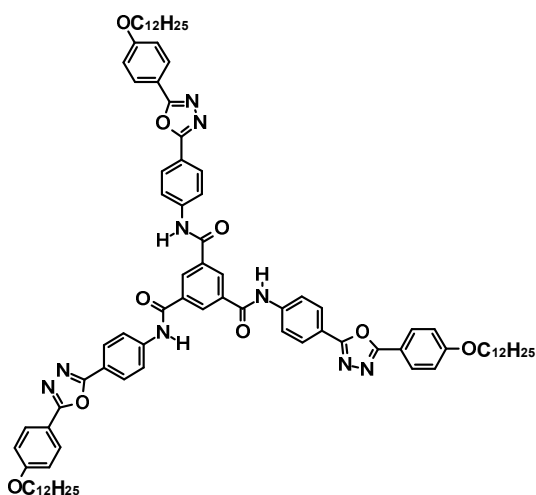


**Figure 2.6.** Different types of triple hydrogen bonding patterns observed in a typical 1,3,5-substituted tricarboxamide derivatives a) cyclohexane core b) benzene core.

Such columnar units further aggregate, eventually to yield fibres. However, in case of compounds of aromatic analogues, 1,3,5-benzenetrisamide derivatives,<sup>9</sup>

show a triple helical hydrogen bonding pattern between the amide groups of adjacent molecules and directs the columnar packing (see Figure 2.6b). Such columnar assembly, further, is stabilized by  $\pi\cdots\pi$  interaction between the core benzene units.

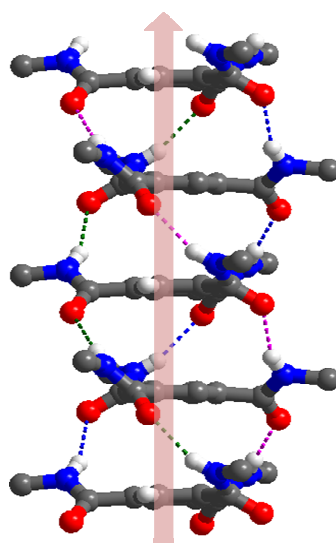
Recently, Park and co-workers<sup>10</sup> also have shown that fine tuning of interactions for the desired aggregation may be achieved by varying the polarity of the solvents employed in the gelation process. For example, one of the 1,3,5-benzenetricarboxamide derivatives, as shown in Figure 2.7, form a gel in  $\text{CHCl}_3$ , with intense blue luminescence as the apolar solvent promotes the aggregation to yield a gel, whereas the same amide from  $\text{CH}_3\text{OH}$ , failed to give a gel as the polar solvent always compete with the solute, for aggregation over self assembly of the solute and thereby achieving different optical properties between gel and solution states.



**Figure 2.7.** Molecular structure of a 1,3,5-benzenetricarboxamide derivative

The possible molecular aggregation for this gelator proposed by the authors is the columnar packing by utilizing the triple helical hydrogen bonds as discussed above. This was confirmed by recording powder X-ray diffractogram for the xerogel, by observing a characteristic peak (at  $2\theta \sim 2.2$ ) for one dimensional columnar aggregation.

In fact, triple helical hydrogen bonding patterns of 1,3,5-benzenetricarboxamide derivatives tender other applications in the solid, liquid crystalline state apart from gel. In this regard, 1,3,5-benzenetricarboxamide derivatives are shown as good candidates in the field of electronics. Such property is attributed due to the contribution of the dipole moment from each amide group in

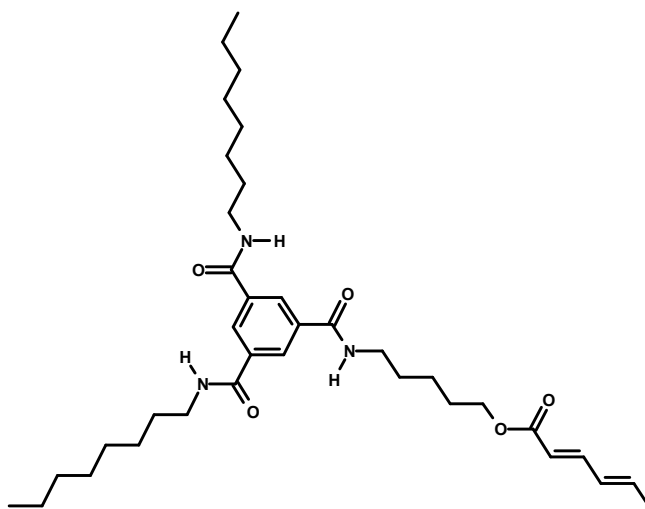


**Figure 2.8.** Orientation of the dipole moment in a 1,3,5-benzenetricarboxamide derivative.

the columnar aggregate, where the amide groups are arranged in a head to tail fashion results into unidirectional orientation with a macroscopic dipole<sup>11</sup> (Figure

2.8). Such resultant dipole from the molecular aggregates is one of the prerequisite for the properties like ferroelectric, pyroelectric, piezoelectric, etc.

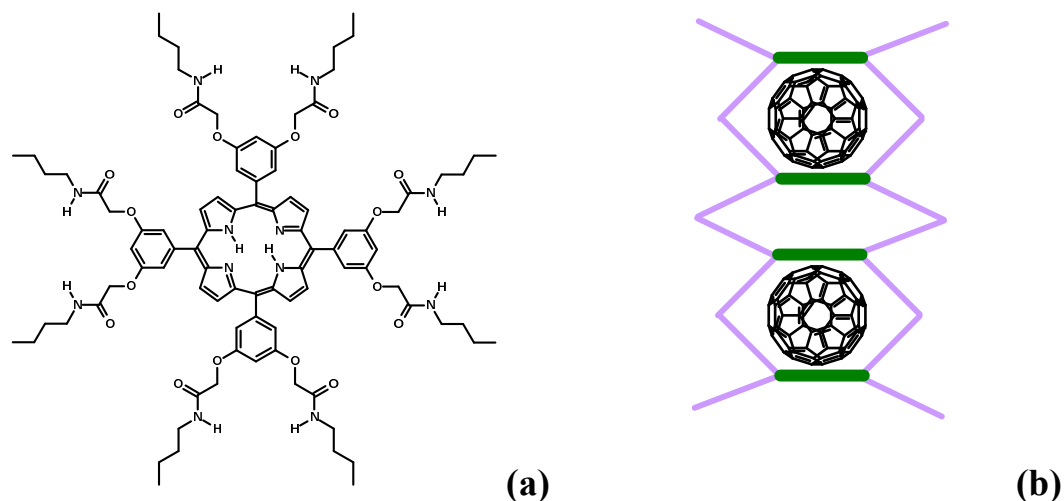
Further, 1,3,5-benzenetricarboxamide derivative which forms, in general, well defined molecular aggregates, a columnar structure, were also used for covalent fixation. For example Meijer and co-workers<sup>12</sup> have shown that a typical tricarboxamide, as shown in Figure 2.9, which possess a polymerizable sorbate



**Figure 2.9.** Molecular structure of a 1,3,5-benzenetricarboxamide derivative, with sorbate as one of the peripheral group.

group at the periphery of the molecule (see Figure 2.9), yield a polymer in cyclohexane solution through radical polymerization process by 1,4-addition, as characterized from FT-IR and NMR techniques. The fibres of the polymers with well defined structure are characterized by the AFM technique, which shows the successful covalent fixation of the columnar structure.

In addition, substantial studies with increased amide substitution, for example polyamides, are also reported in recent literature. Although, the polyamides as such may not be favorable for gelation as it increases the crowding, thereby preclude one dimensional aggregation, a prerequisite for gelation, successful polyamide gelators have been designed by increasing the dimension of the core moiety, thereby decreasing the crowding between the amide moieties.



**Figure 2.10.** a) Structure of a porphyrin based polyamide gelator. b) representation of the proposed structure of the fibres in the gel, formed by polyamide shown in (a).

For example, a large core based moiety, porphyrins, as shown in Figure 2.10, form gels with more mechanical strength. Gelation studies have been carried out in the presence of fullerene, as porphyrin/fullerene systems are well explored in the field of electronics. The computational modelling of the structure of the polyamide shows a capsule structure, wherein four of the eight amide groups are utilized to form dimeric capsule unit and the remaining amide groups are utilized to

connect the dimeric units, as shown in Figure 2.10b, leading to the formation of void space being occupied by fullerene units. It is also interesting to note that, in the presence of structure directing agent, like fullerene, the polyamide forms a gel with fibrous structure, otherwise a sheet structure is observed on its own as inferred from the TEM analysis<sup>13</sup>.

### **2.3 Effect of peripheral substituents in the formation of supramolecular assemblies of gel.**

The hydrogen bonding groups on the gelator molecules help to aggregate the molecules into fibres through hydrogen bonds, but at the same time peripheral substituents on the gelator molecule also play a major role in the formation of gel, controlling in the morphology of the resultant fibres, to enhancing the solubility of the gelator, entanglement of the fibres, etc.

For example, 1,3,5-cyclohexanetricarboxamide derivatives<sup>14</sup> with linear and branched alkyl chains show different gelation property. while straight chain analogue forms gels at lower concentrations, from a variety of solvents, as compared to the branched chain isomers, which form gels at higher concentrations and also only from a limited solvents.

Lu and co-workers have shown that, crowding of peripheral substituents slows down the aggregation process, and as a result, the time required for the gelation is longer for the highly crowded gelator as compared to the less crowded analogue which gives gel easily. Indeed, due to such slow aggregation, gelators possessing crowded substituents often yield thin fibers.<sup>15</sup>

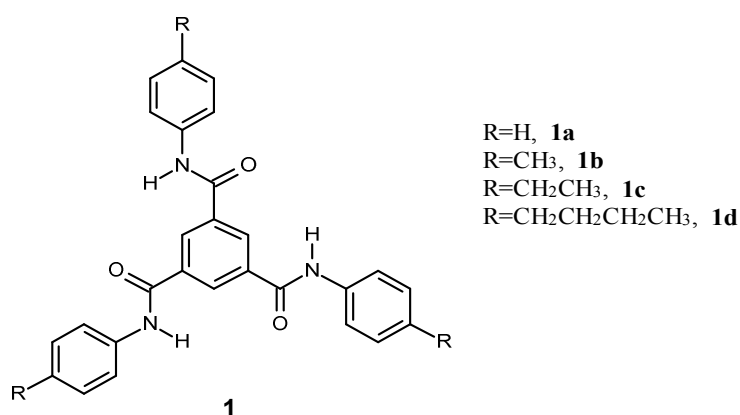


Similarly gelators with long chain alkyl substituents are more facile than the short chain analogues. This is attributed to the fact that contribution of each  $-\text{CH}_2-$  group, towards the transition enthalpy of sol-gel, in the form of van der Waals interactions, increases by 3.5-4.2 kJ/mol in polar solvents and 2.2 kJ/mol in apolar solvents.<sup>16</sup> However, some exceptions are known in the literature wherein, the shorter analogues also act as a good gelator.<sup>19</sup> One should note here that, as the chain length increases, the solubility varies from solvent to solvent and as a result the gelation also varies from polar to non-polar solvents.<sup>17</sup>

After reviewing the literature for various gelators, it is apparent that peripheral substituents play a significant role in the formation of a specific gel, because each type of gelator possesses different types of units that are quite diverse such as saccharides, cholesterol, aromatics, etc. In fact such functionalities affect even the solubility of the gelator in a particular solvent. However, the influence of the increased number of alkyl groups in the long chain peripheral functionality in the gelation of 1,3,5-benzenetrisamide derivatives is well documented in the literature<sup>18</sup> but not much studies are known about short chain alkyl groups.<sup>19</sup> Thus, herein, the gelation study of some 1,3,5-benzenetricarboxamide derivatives which possesses short chain alkyl group (methyl to butyl) on the periphery have been carried out, to establish the structure of the assemblies, unequivocally, and to compare with the reported similar assemblies, in particular with respect to the formation of triple helical hydrogen bonding patterns.

## 2.4. Preparation of the 1,3,5-benzenetricarboxamide derivatives

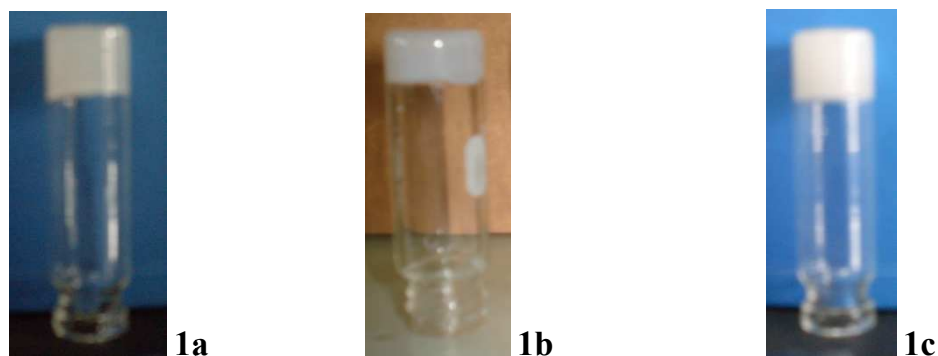
All 1,3,5-benzenetricarboxamide derivatives, as shown in the Scheme 1, are prepared by careful addition of the respective aniline derivatives, in excess, to trimesyl chloride in THF solution with constant stirring. All the derivatives are isolated as solids and characterized by NMR spectroscopy.



**Scheme 1.** Molecular structures of the 1,3,5-benzenetricarboxamide derivatives.

## 2.5. Preparation of gels

All the derivatives of tricarboxamide **1** are insoluble in most of the organic solvents and also in water. But they are highly soluble in DMSO, DMF and partially soluble in methanol. However, conventional slow evaporation method fails to yield gels for all the derivatives of **1** in DMF and methanol. Nevertheless, **1a**, **1b** and **1c** formed gels in DMSO at higher concentrations (~ 15mg/mL), within 3-4 days. It is noteworthy to mention that during the process of preparation of the gels, a serendipitous observation was noted that, addition of 2-3 drops of water into the DMSO solution of the gelator gave gels, instantaneously. The gel formation is confirmed by the inversion vial test as shown in Figure 2.11.



**Figure 2.11.** Images of gels of a) **1a** b) **1b** and c) **1c**

Interestingly, the gel formation was observed in DMSO/H<sub>2</sub>O even at much lower concentrations (~0.5mg/mL). Table 1 shows the concentration and time profile of gel formation in DMSO or DMSO/H<sub>2</sub>O. Considerable reduction in both the concentration (almost a difference of ~ 30 fold) and the time (96h to a few seconds) taken to form gels suggest that the self aggregation of the molecule is triggered by water to yield the gel with high rate of formation.

**Table 1:** Concentration and time required to form gel of **1**

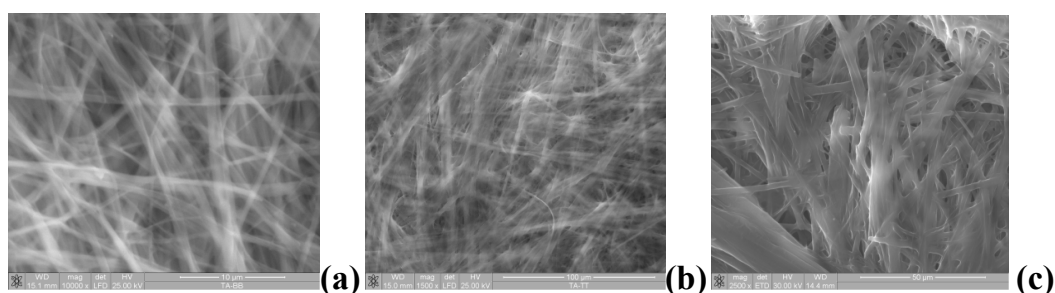
compounds	minimum concentration W/V %( mg/mL)		time required for gel formation	
	DMSO/water	DMSO	DMSO/water	DMSO
<b>1a</b>	0.5	15	2-3 sec	96 hrs
<b>1b</b>	0.7	15	2-3 sec	90 hrs
<b>1c</b>	0.5	15	2-3 sec	96 hrs

The possible reason for the instantaneous gel formation with DMSO/H<sub>2</sub>O could be (i) Breaking of the hydrogen bond between the DMSO and gelator by the water molecules followed by establishing the strong hydrogen bond with the DMSO

molecule which might have helped the instantaneous aggregation of the gelator molecules. (ii) insoluble nature of the gelator in water may also have triggered the self assembly with higher rate. However, in case of **1d**, neither DMSO nor DMSO/H<sub>2</sub>O media fail to give any sort of gel.

## 2.6 Scanning Electron Microscope (SEM) analysis of xerogel

To understand the morphology of the solid phase of the gel, they are dried in ambient conditions to get dried gels. Scanning Electron Microscope (SEM) images of the dried gels show the fibrous nature of the gels with thickness of the fibres in the micrometer range, indicates the wealth of the aggregation of molecules (see Figure 2.12).



**Figure 2.12.** SEM images shows the fibrous nature of the xerogel of a) **1a** b) **1b** and c) **1c**.

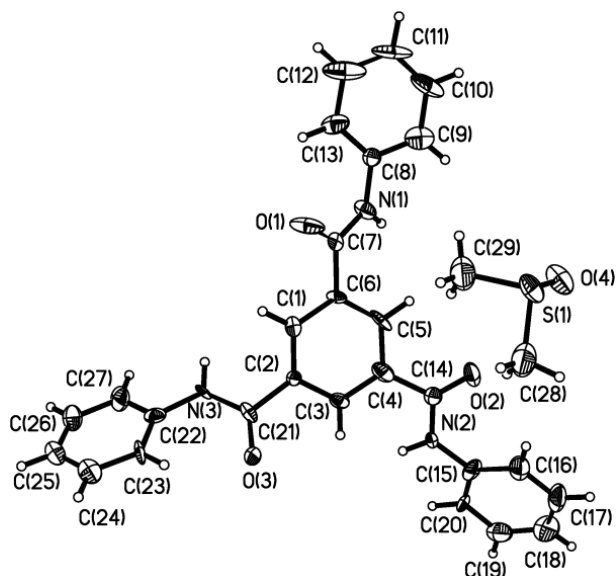
In fact, characterization of the fibrous structure is more challenging and exciting. But till to date no tools are available to establish the structures of fibres unequivocally. However, a serendipitous observation of formation of crystals in some cases, during gelation studies of **1a-1c**, provided an opportunity to analyse the self assembly in the gels on the basis of single crystal data as described below.

Interestingly, during the preparation of gel it was noticed that below certain concentrations the gelators yield crystalline fibres instead of gel. This could be explained based on the crystallographic mismatch branching (CMB) process by Liu and co-workers, which explains that at supersaturation, branching of fibres leads to network structure to yield gel. However, below saturation, the probability of such branching is less and it could give single crystals. Based on this model, attempts are made towards crystallization of the gelators **1a-1c** at much lower concentration in DMSO. Good quality crystals suitable for crystal structure determination by X-ray diffraction methods were obtained for **1a** and **1b** only, whereas **1c** did not give the requisite quality crystals. Although gelation was not successful with **1d**, single crystals were obtained easily from DMSO solvent by slow evaporation process. The structures of **1a**, **1b** and **1d** are discussed in following sections.

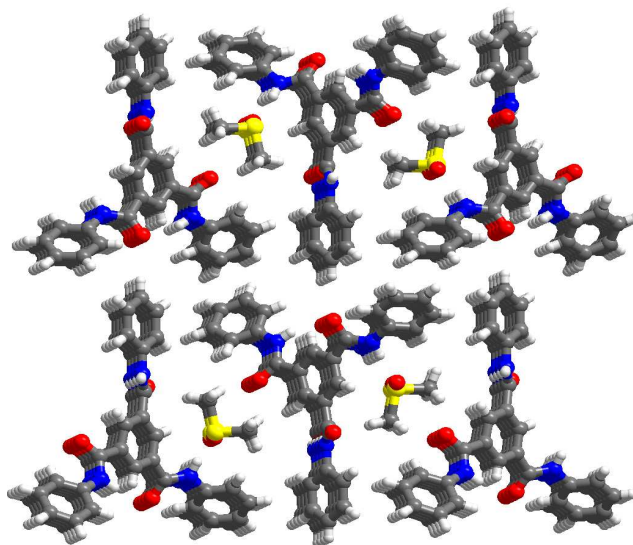
## 2.7 Single crystal X-ray diffraction analysis

### 2.7.1 Structure of the gelator *N,N'N''*-triphenyl-1,3,5-benzenetricarboxamide-DMSO adduct, **1a.DMSO**

Crystallization of **1a** in DMSO, at very low concentration, gives crystals of thin needles. Single crystal X-ray diffraction analysis reveals the composition of **1a** and DMSO in the asymmetric unit is in a 1:1 ratio. The contents are shown in Figure 2.13, in the form of ORTEP. Crystallographic details are listed in Table 2.8. Analysis of packing of molecules in the crystals of adduct of **1a.DMSO** reveals that, a channel structure is realized with the molecules of **1a** being host and the solvent of crystallization DMSO as guest molecules.

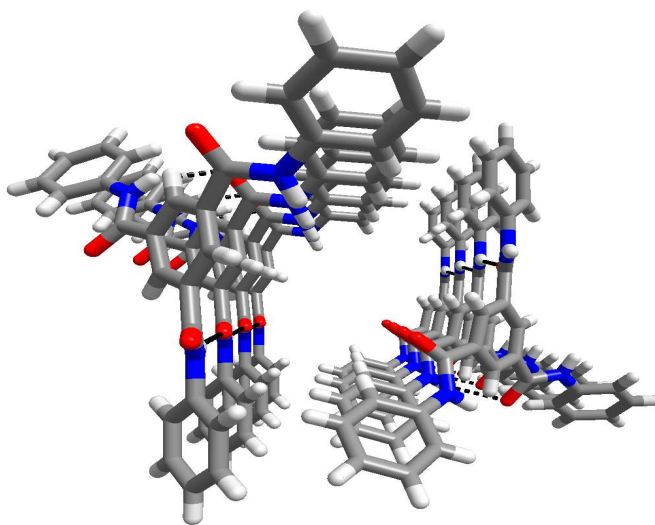


**Figure 2.13.** ORTEP of contents in the asymmetric unit of **1a**.DMSO

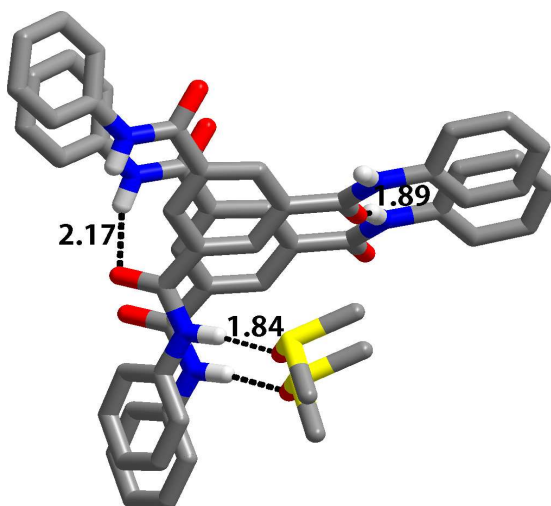


**Figure 2.14.** Three dimensional arrangement of **1a**.DMSO.

The dimension of the void in the channels observed is  $11 \times 7 \text{ \AA}^2$ . Such an arrangement is shown in Figure 2.14. A typical host structure as shown in Figure 2.15, is due to the columnar packing of molecules of **1a** being held together by hydrogen bonds formed by the amide moieties.



**Figure 2.15.** One dimensional channel structure formed by molecules of **1a**.



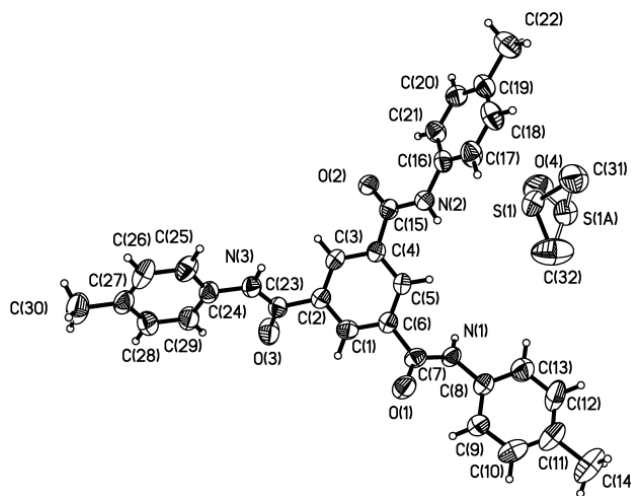
**Figure 2.16.** Intermolecular interactions between the moieties in the columnar arrangement.

A typical interaction is shown in Figure 2.16. The adjacent molecules in the columnar assembly stack by N-H $\cdots$ O hydrogen bonds, with H $\cdots$ O distance of 1.89 and 2.17 Å formed by two of the amide moieties present on each molecule of **1a**. The remaining one is glued to the DMSO molecules by N-H $\cdots$ O hydrogen bond

with H $\cdots$ O distance of 1.84 Å. Complete characteristics of hydrogen bonds are given in Table 2.9.

### 2.7.2 Structure of *N'N'*-tritoly-1,3,5-benzenetricarboxamide-DMSO adduct, **1b**.DMSO.

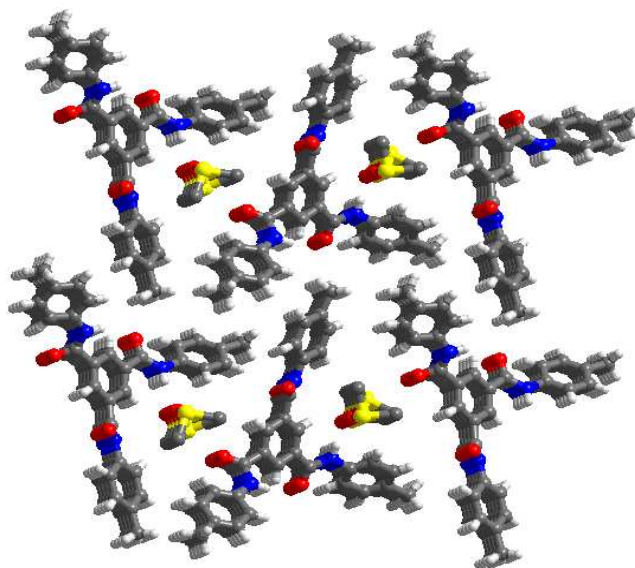
Good quality single crystals of **1b** obtained from DMSO solution by slow evaporation process. The structural analysis of **1b**.DMSO shows that the composition of asymmetric unit is a 1:1 ratio of **1b** and DMSO as observed in the case of **1a**.DMSO, except that DMSO molecules are in disordered orientations. ORTEP of the contents in the asymmetric unit is shown in Figure 2.17.



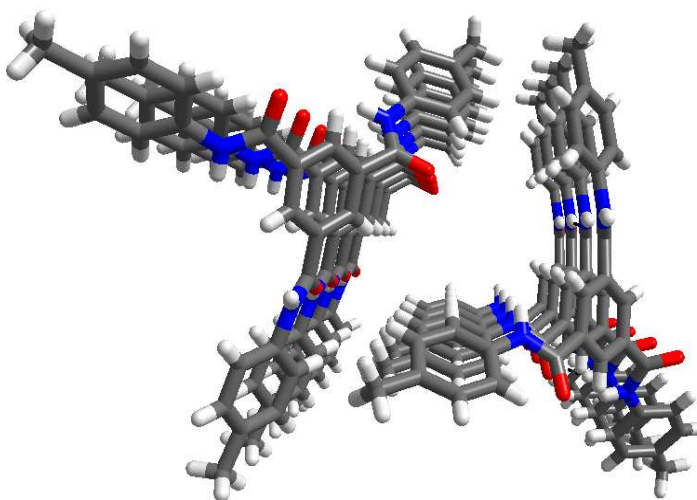
**Figure 2.17.** ORTEP of contents in the asymmetric unit in **1b**.DMSO

Pertinent details of the crystallographic details are given in Table 2.8. The arrangement of molecules in the crystal lattice is also very much similar to as observed in **1a**.DMSO





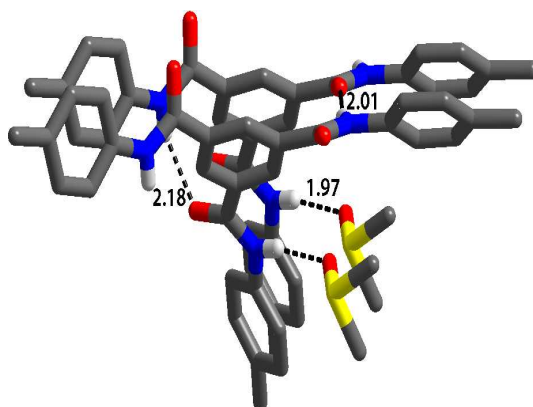
**Figure 2.18.** Three dimensional arrangement of **1b**.DMSO, depicting the host-guest assembly.



**Figure 2.19.** One dimensional columnar arrangement of **1b**.

In the structure of **1b**.DMSO also, channels of dimension  $12 \times 7 \text{ \AA}^2$  are being created by the molecules of **1b**, which are being occupied by DMSO molecules. The arrangement is shown in Figure 2.18. The DMSO molecules are in disordered orientation, perhaps due to the increased channel dimension in

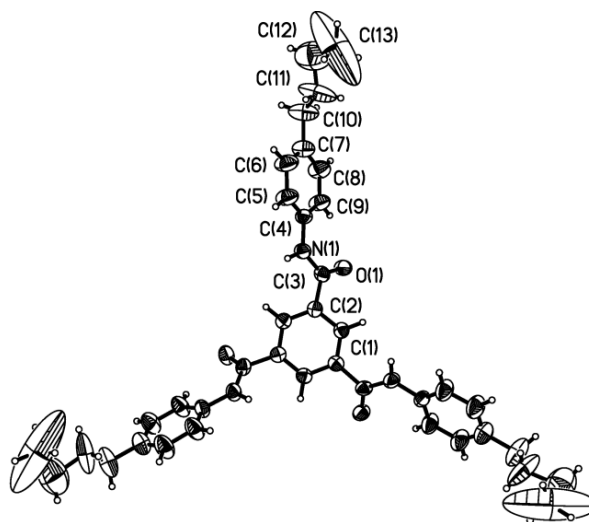
**1b**.DMSO compared to **1a**.DMSO. A typical host network in the form of columnar module is shown in Figure 2.19. Within each module, the adjacent molecules of **1b** are held together by N-H $\cdots$ O hydrogen bonds with corresponding H $\cdots$ O distances of 2.01 and 2.18 Å (Table 2.9), formed by two of the amides. The remaining unit is connected to the guest species by N-H $\cdots$ O (H $\cdots$ O, 1.97 Å, Table 2.9) hydrogen bonding (see Figure 2.20).



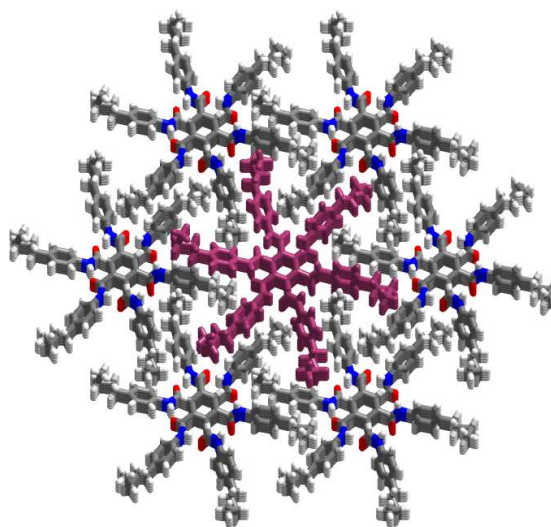
**Figure 2.20.** Molecular recognition between the corresponding sites in **1b**.DMSO within columnar unit.

### 2.7.3 Packing analysis in the crystals of *N,N,N''*-tri(4-butylphenyl)-1,3,5-benzenetricarboxamide, **1d**.

Single crystals of **1d** are obtained from DMSO by slow evaporation process within 48 hrs. The asymmetric unit, unlike in **1a** and **1b** does not contain solvent of crystallization. The contents of the asymmetric unit are shown in Figure 2.21, in the form of ORTEP.



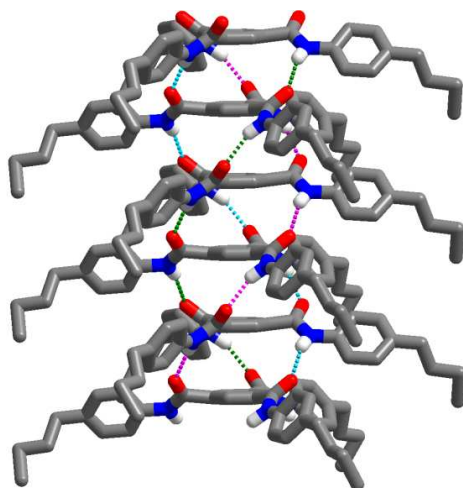
**Figure 2.21.** ORTEP of amide **1d** in its crystal structure.



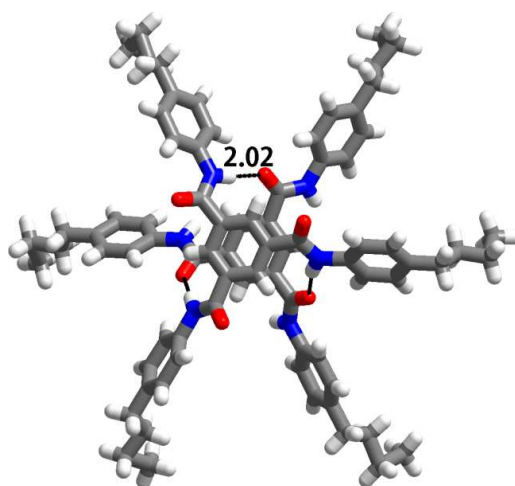
**Figure 2.22.** Three dimensional arrangement of molecules of **1d** in the form of hexagonal columnar packing.

In the crystal lattice, molecules are stacked to yield hexagonal columnar structure, as shown in Figure 2.22. Analysis of a discrete columnar unit shows a triple helical hydrogen bonding pattern, between the amide groups through N-H $\cdots$ O hydrogen bonds, as shown in Figure 2.23. Such hexagonal columnar packing is well known

in the literature.<sup>9</sup> A close look at the hydrogen bonding features, suggest that such helical pattern is made feasible as the adjacent molecules within hexagonal columns are rotated by 60° from each other, as shown in Figure 2.24.



**Figure 2.23.** One dimensional columnar aggregation with triple helical hydrogen bonding pattern in **1d**.



**Figure 2.24.** Molecular recognition between molecules of **1d**.

A comparison of structures **1a**, **1b** and **1d** reveals that while **1a** and **1b** are similar, the deviation observed in **1d** may be attributed to the change of substituents on the

periphery of the molecules. Quantification of such changes may be ascribed possibly to two factors. Firstly, the deviation of the amide groups with respect to the mean plane of the central phenyl ring. Such information compiled from the data obtained in the literature is shown in Table 2.3 and Table 2.4, while similar data is given in Table 2.5 for the structures in this study, **1a**, **1b** and **1d**. Table 2.3 shows the angles of deviations of the three amide groups from the plane of phenyl ring for some 1,3,5-benzenetricarboxamide derivatives, which forms a discrete columnar arrangement through triple helical hydrogen bonds. The range of deviation of the angles for the three amide groups is from 35-47°.

**Table 2.3.** Mean angle between the three amide groups and the core phenyl ring of some 1,3,5-benzenetricarboxamide derivatives which forms discrete columnar structure.<sup>9,20</sup>


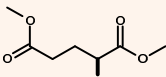
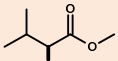
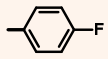
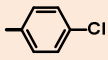
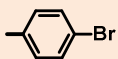
Side chain	Angle 1	Angle 2	Angle 3
	36.8	42.4	45.5
	46.5	46.5	46.5
	40.5	40.5	40.5
	39.5	40.5	45.6
	43.4	43.4	43.4
	42.1	42.1	42.1
	38.5	38.5	38.5
	39.9	39.9	39.9

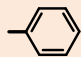
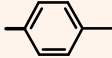
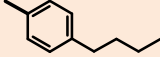
Table 2.4 shows the angles of deviations of the three amide groups from the mean plane of the phenyl ring for some derivatives of 1,3,5-benzenetricarboxamide derivatives, which forms sheet structures. The angle of deviation is very low in the range of 10-26° for at least two of the amide groups.

**Table 2.4.** Mean angle between the three amide groups and the core phenyl ring of some 1,3,5-benzenetricarboxamide derivatives which form sheet structure.<sup>21</sup>

Side chain	Angle 1	Angle 2	Angle 3
-CH <sub>3</sub>	10.5	15.4	48.4
-CH <sub>2</sub> CH <sub>3</sub>	10.1	12.9	46.8
-CH <sub>2</sub> CH <sub>2</sub> CH <sub>3</sub>	25.7	25.7	25.7

Thus, it is evident from Table 2.5 that the angle of deviation observed in **1a**, **1b** and **1d**, clearly indicates all the three angles fall within the range of columnar assembly, with the structure of **1d** establishing a close relation with the structures reported in the literature perhaps due to the presence of triple hydrogen bonding also. In addition, the loser twist observed in **1a** and **1b** appears to be cause for not able to establish triple helical hydrogen bonding pattern and at the same time did not show agreement even with the data corresponding to sheet structures (Table 2.4)

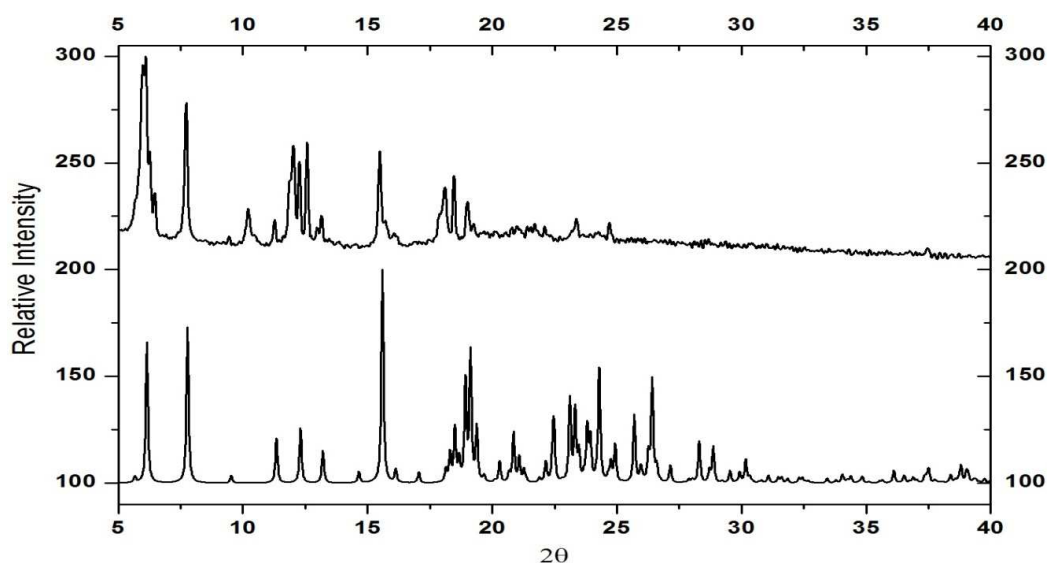
**Table 2.5.** Mean angle between the three amide groups and the core phenyl ring in **1a**, **1b** and **1d**.

Side chain	Angle 1	Angle 2	Angle 3
	25.1	34.7	39.4
	26.8	38.7	48.1
	41.3	41.3	41.3

Secondly, the substituent with longer chain in **1d** than in **1a** and **1b** perhaps did not permit enough void space, thus precluding solvate incorporation in **1d**.

## 2.8. Powder X-ray diffraction analysis

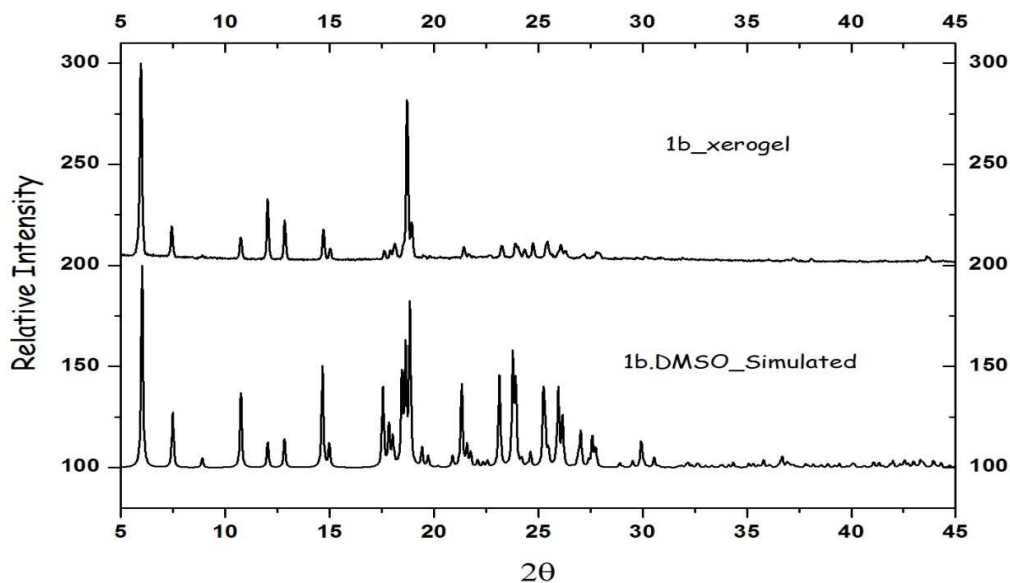
In general, fibres of the native gels are well organized entities of molecules, hence show crystalline nature. Thus, X-ray diffraction is one of the successful methods often being carried out for the characterization of the gels. For this purpose, sample preparation proceeds by the conversion of the gel into xerogel either by air or freeze dried, without compromising on the crystallinity. Thus, characterization of xerogels of adducts **1a** and **1b** has been carried out by powder X-ray diffraction methods.



**Figure 2.25.** Powder diffractogram of the xerogel of **1a** (top) experimental and (bottom) calculated.

It has been observed that simulated single crystal data of **1a** and **1b**, calculated powder diffraction patterns **1a** and **1b** (see Figure 2.25 and 2.26) simulated, match

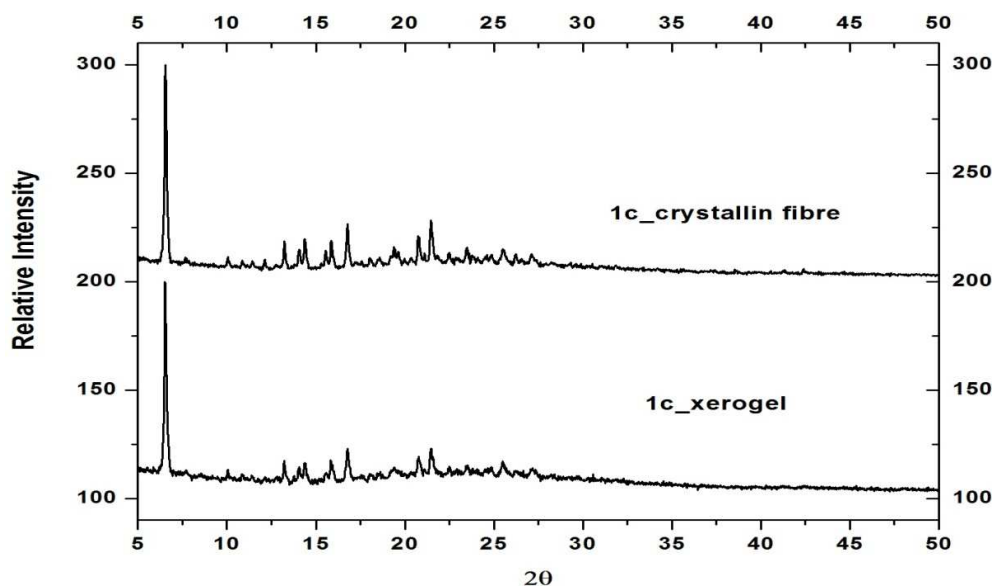
with the powder diffractogram of the xerogel of **1a** and **1b**, respectively, and indicate that the structure of the xerogel is same as that of the crystal structure obtained from the DMSO solution.



**Figure 2.26.** PXRD patterns for **1b.DMSO**.

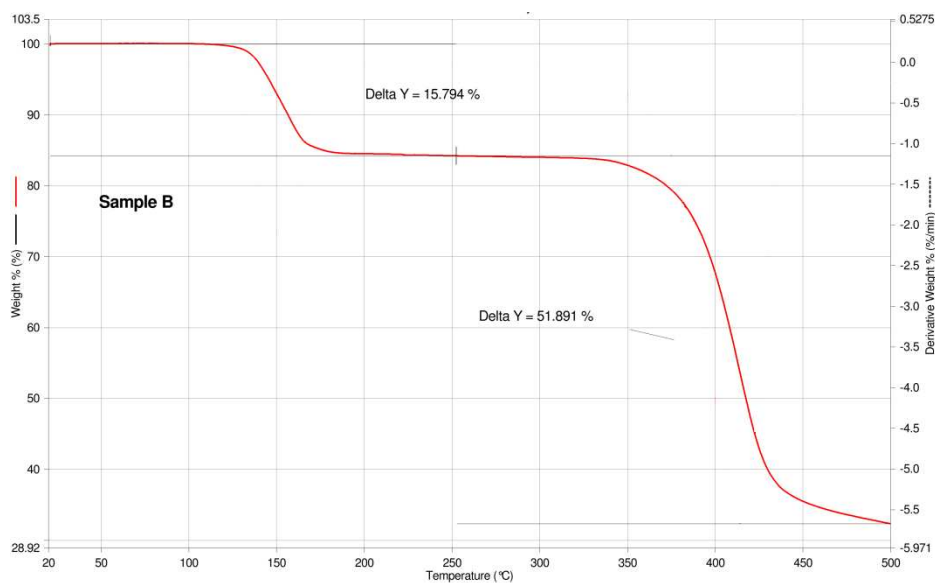
Further, an interesting feature evolved from powder X-ray diffraction studies is that, **1c** failed to yield good quality single crystals, but its experimental powder pattern of the sample obtained in microcrystalline form upon slow evaporation, match with that of xerogel powder pattern of **1c**. However, it has been observed from the powder patterns, that the crystallinity of **1c** is poor in both xerogel and the fibres obtained. The patterns are shown in Figure 2.27. Since the xerogel and simulated patterns match in **1a** and **1b**, suggesting similar crystalline environment, taken into account the similarity between xerogel of **1c** and experimental powder pattern of it, the packing of molecules in **1c** may also perhaps have similar arrangement as observed in the crystal structures of **1a** and **1b**.





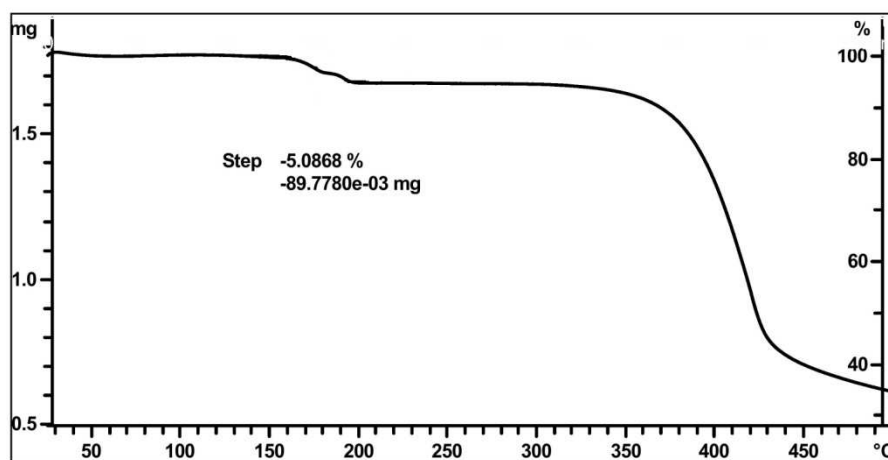
**Figure 2.27.** Comparison of PXRD pattern obtained for the xerogel of **1c** and the crystalline fibre obtained at lower concentration.

## 2.9. Thermogravimetric Analysis (TGA) Experiments



**Figure 2.28.** TGA plot of the xerogel of **1a.DMSO**

Analysis of xerogel of **1a** by TGA shows a weight loss of 15.7% (calculated 15%) in the temperature range of 150-180°C corresponding the mass of DMSO molecules present in the crystal lattice of the fibres of xerogel, as shown in Figure 2.28. Similarly, TGA experiment for the xerogel of **1c** also shows weight loss around 180°C but only 5% (Figure 2.29).

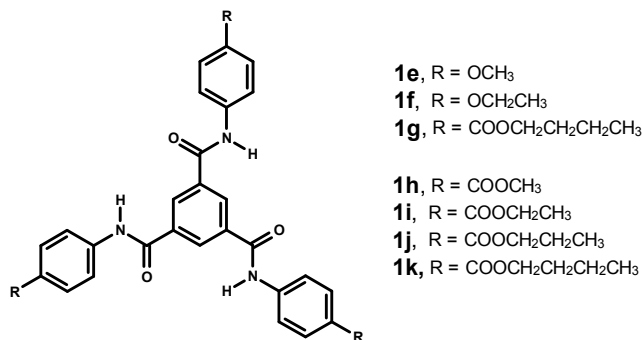


**Figure 2.29.** TGA plot of the xerogel of **1c**.DMSO

Such a weight loss indicates certainly presence of a solvent in the gel but effective quantification could not be made for the actual amount of solvent present in the crystal lattice. However, the thermal studies corroborate the information obtained from powder and single crystal data that the trisamide derivatives **1a-1c** form gels, through self-assembly process, by occluding solvents like DMSO in the channels created by amide moieties through columnar packing.

Based on the gelation studies of compounds **1a-1d**, the following 1,3,5-benzenetricarboxamide derivatives, as shown below are prepared to investigate the

gelation ability and evaluation of their properties. In this series, **1e-1g** are due to the alkoxy substituents, whereas **1h-1k** are due to the alkylester substituents.



Compounds **1e**, **1f**, **1h-1j** form gels with DMSO/H<sub>2</sub>O or DMSO. The statistics of gelation processes in terms of concentration and time are given in Tables 2.6 and 2.7 respectively. It appears that amides with higher alkyl groups, at the periphery fails to yield gel in DMSO, DMSO/H<sub>2</sub>O or any combination of solvent in both alkoxy and alkylester substituted systems (**1g** and **1k**). The trend of gel formation observed in **1a-1c** also followed in **1e**, **1f** and **1h-1j**.

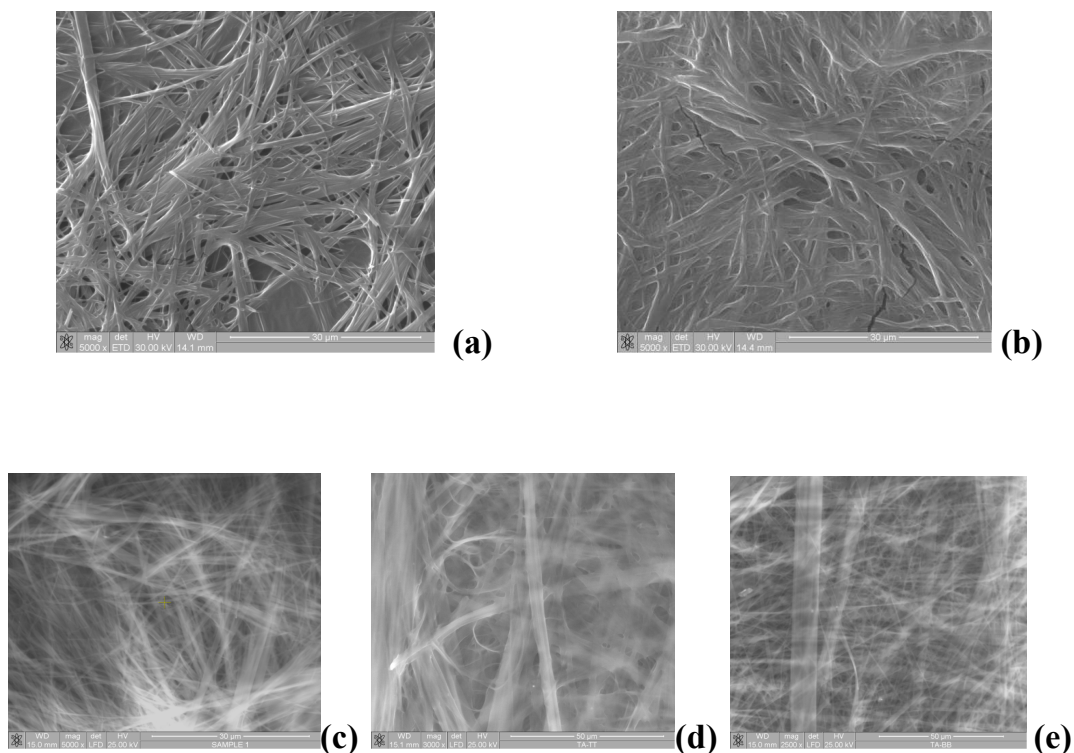
**Table 2.6.** Concentration and time required to form gel of **2**

compounds	minimum concentration W/V % ( mg/mL)		time required for gel formation	
	DMSO/water	DMSO	DMSO/water	DMSO
<b>1e</b>	0.5	15	2-3 sec	192 hrs
<b>1f</b>	0.5	15	2-3 sec	78 hrs

**Table 2.7.** Concentration and time required to form gel of **3**

compounds	minimum concentration W/V %( mg/mL)		time required for gel formation	
	DMSO/water	DMSO	DMSO/water	DMSO
<b>1h</b>	0.5	15	2-3 sec	75 hrs
<b>1i</b>	0.4	15	2-3 sec	82 hrs
<b>1j</b>	0.6	15	2-3 sec	96 hrs

The gels are characterized for their physical characteristics by SEM as shown in Figure 2.30. The SEM images shows the fibrous nature of the gelator **1e**, **1f** and **1h-1j**.

**Figure 2.30.** SEM images of gels formed by a) **1e**, b) **1f** c) **1h** d) **1i** and e) **1j**

## 2.10. Conclusion

1. Gelation ability of some 1,3,5-benzenetricarboxamide derivatives with various peripheral substituents, associated especially with short alkyl chains have been explored.
2. The gelation shows that gel formation is observed for the short chain analogues in DMSO or DMSO/H<sub>2</sub>O.
3. The structural analysis of compound **1a**, **1b** and **1d** gives an understanding of mechanistic path for the formation of one dimensional aggregation.
4. The SEM images of all the gelators show the fibrous nature of the gel.
5. The crystal grown at lower concentration is same as that of the xerogel indicates that the molecular aggregation is not affected by the concentration.

## 2.11 Experimental sections

### 2.11.1 Preparation of gel

All the gelators (~15mg) were dissolved in DMSO. Slow evaporation of the solution for 3-4 days gave gel. However approximately 0.5mg of the gelators dissolved in 1 mL of DMSO followed by the addition of 2-3 drops of water yield gel instantaneously.

### 2.11.2 X-ray Structure Determination

Good quality single crystals of **1a**, **1b** and **1d** were carefully selected using Leica microscope and glued to a glass fibre using an adhesive (cyanoacrylate). In all the cases, the crystals were smeared in the adhesive solution to prevent

decomposition of crystals. The intensity data were collected on a Bruker single-crystal X-ray diffractometer, equipped with an APEX detector. Subsequently, the data were processed using the Bruker suite of programs (SAINT), and the convergence was found to be satisfactory with good  $R_{\text{ini}}$  parameters. Absorption corrections were applied using SADABS package. The structure determination by direct methods and refinements by least-squares methods on  $F^2$  were performed using the SHELXTL-PLUS package. The processes were smooth without any complications. All non-hydrogen atoms were refined anisotropically, while hydrogen atoms are treated isotropically. All the intermolecular interactions were computed using PLATON. All packing diagrams are generated using Diamond software.

### **2.11.3 X-ray Powder diffraction Measurements**

X-ray Powder diffraction (XPRD) data were collected on a PANalytical diffractometer with Cu-K $\alpha$  radiation ( $\lambda = 1.5406$ ), operating at 40 kV and 30 mA with step size 0.017 ( $2\theta$ ) in a continuous scanning mode.

### **2.11.4 Thermogravimetric measurements**

Thermogravimetric analyses (TGA) were performed on a Mettler Toledo TGA/SDTA 851e module. The sample is placed in open alumina pans for TGA experiments. Sample size is in the range of 5-10mg. The samples were heated in the temperature range 25-500°C at a rate of 10°C/min. The samples were purged with flow of dry nitrogen at 150 ml/min.

**Table 2.8.** Crystallographic information for the structures of **1a**, **1b** and **1d**

	<b>1a</b>	<b>1b</b>	<b>1d</b>
formula	(C <sub>27</sub> H <sub>21</sub> N <sub>3</sub> O <sub>3</sub> ) (C <sub>2</sub> H <sub>6</sub> OS)	(C <sub>30</sub> H <sub>27</sub> N <sub>3</sub> O <sub>3</sub> ) (C <sub>2</sub> H <sub>6</sub> OS)	(C <sub>39</sub> H <sub>45</sub> N <sub>3</sub> O <sub>3</sub> )
<i>M<sub>r</sub></i>	513.60	555.63	603.78
crystal habit	needles	needles	needles
color	colorless	colorless	colorless
crystal system	orthorhombic	monoclinic	hexagonal
space group	<i>P</i> 212121	<i>P</i> c	<i>P</i> 63
<i>a</i> [Å]	4.909(2)	5.107(2)	16.763(2)
<i>b</i> [Å]	18.531(7)	14.694(4)	16.763(2)
<i>c</i> [Å]	28.733(1)	20.099(6)	7.372(1)
<i>α</i> [°]	90	90	90
<i>β</i> [°]	90	98.69(1)	90
<i>γ</i> [°]	90	90	120
<i>V</i> [Å <sup>3</sup> ]	2613.8(2)	1491.0(8)	1794.0(4)
<i>Z</i>	4	2	2
<i>ρ<sub>calc</sub></i> (g cm <sup>-3</sup> )	1.305	1.224	1.118
<i>T</i> [K]	298(2)	298(2)	298(2)
<i>λ</i> (MoK <sub>α</sub> )[Å]	0.71073	0.71073	0.71073
<i>μ</i> (mm <sup>-1</sup> )	0.164	0.148	0.071
2 <i>θ</i> range [°]	50.56	50.62	50.58
limiting indices	-5 ≤ <i>h</i> ≤ 5 -21 ≤ <i>k</i> ≤ 22 -34 ≤ <i>l</i> ≤ 34	-6 ≤ <i>h</i> ≤ 6 -17 ≤ <i>k</i> ≤ 17 -24 ≤ <i>l</i> ≤ 23	-20 ≤ <i>h</i> ≤ 19 -20 ≤ <i>k</i> ≤ 19 -8 ≤ <i>l</i> ≤ 8
<i>F</i> (000)	1080	576	648
obsd reflns	19384	10710	13257
unique reflns [ <i>R</i> (int)]	4721(0.2289)	5234(0.0535)	2155 (0.0544)
reflns used	2812	3272	1818
no. of parameters	321	373	136
GOF on <i>F</i> <sup>2</sup>	1.226	1.048	1.489
<i>R</i> <sub>1</sub> [ <i>I</i> > 2σ( <i>I</i> )]	0.1500	0.0658	0.0980
<i>wR</i> <sub>2</sub>	0.2957	0.1774	0.2336

**Table 2.9.** Characteristics of hydrogen bond distances (Å) and angles (°) observed for **1a**, **1b** and **1d**.<sup>§</sup>

H-bond	<b>1a</b>			<b>1b</b>			<b>1d</b>		
N-H <sup>⋯</sup> O	1.89	2.86	159	2.01	2.98	162	2.02	2.99	160
	2.17	2.99	138	2.18	2.99	136			
	1.84	2.83	166	1.97	2.96	167			
C-H <sup>⋯</sup> O									
	2.37	3.44	172	2.23	2.91	119	2.44	3.34	140
	2.31	2.89	112	2.36	2.94	112	2.25	2.88	115
	2.30	2.91	114	2.38	3.13	125			

§ In each row the three numbers for every structure represent H<sup>⋯</sup>A and D<sup>⋯</sup>A distances and <D-H<sup>⋯</sup>A.

## 2.12 References

- (1) (a) Wang, Y. J.; Tang, L. M.; Yu, J. *Prog. Chem.* **2009**, *21*, 1312. (b) Steed, J. W. *Chem. Soc. Rev.* **2010**, *39*, 3686. (c) Noro, A.; Hayashi, M.; Matsushita, Y. *Soft Matter* **2012**, *8*, 2416. (d) Fages, F.; Araki, K. *Low Molecular Mass Gelators: Design, Self-Assembly, Function*; Springer, 2005.
- (2) (a) Fages, F.; Vogtle, F.; Zinic, M. In *Low Molecular Mass Gelators: Design, Self-Assembly, Function*; Fages, F., Ed. 2005; Vol. 256, p 77. (b) Sugiyasu, K.; Fujita, N.; Shinkai, S. *J. Syn. Org. Chem. Jpn.* **2005**, *63*, 359. (c) de Loos, M.; Feringa, B. L.; van Esch, J. H. *Eur. J. Org. Chem.* **2005**, 3615.
- (3) (a) Steiner, T. *Angew. Chem. Int. Ed.* **2002**, *41*, 48. (b) Fan, E.; Vicent, C.; Geib, S. J.; Hamilton, A. D. *Chem. Mater.* **1994**, *6*, 1113. (c) Gilli, G.; Gilli, P. *The Nature of the Hydrogen Bond: Outline of a Comprehensive Hydrogen Bond Theory*; Oxford University Press, 2009. (d) Jeffrey, G. A. *An Introduction to Hydrogen Bonding*; Oxford University Press, 1997. (e) Desiraju, G. R.; Steiner, T. *The Weak Hydrogen Bond: In Structural Chemistry and Biology*; Oxford University Press, 2001.
- (4) Beginn, U.; Sheiko, S.; Moller, M. *Macromol. Chem. Phys.* **2000**, *201*, 1008.
- (5) Ahmed, S. A.; Sallenave, X.; Fages, F.; Mieden-Gundert, G.; Muller, W. M.; Muller, U.; Vogtle, F.; Pozzo, J. L. *Langmuir* **2002**, *18*, 7096.
- (6) Sumiyoshi, T.; Nishimura, K.; Nakano, M.; Handa, T.; Miwa, Y.; Tomioka, K. *J. Am. Chem. Soc.* **2003**, *125*, 12137.



- (7) Koshima, H.; Matsusaka, W.; Yu, H. T. *J. Photochem. Photobiol., A -Chem.* **2003**, *156*, 83.
- (8) Fan, E. K.; Yang, J.; Geib, S. J.; Stoner, T. C.; Hopkins, M. D.; Hamilton, A. D. *J. Chem. Soc., Chem. Commun.* **1995**, 1251.
- (9) Lightfoot, M. P.; Mair, F. S.; Pritchard, R. G.; Warren, J. E. *Chem. Commun.* **1999**, 1945.
- (10) Ryu, S. Y.; Kim, S.; Seo, J.; Kim, Y. W.; Kwon, O. H.; Jang, D. J.; Park, S. Y. *Chem. Commun.* **2004**, 70.
- (11) (a) Fitie, C. F. C.; Roelofs, W. S. C.; Magusin, P.; Wubbenhorst, M.; Kemerink, M.; Sijbesma, R. P. *J. Phys. Chem. B* **2012**, *116*, 3928. (b) Shikata, T.; Kuruma, Y.; Sakamoto, A.; Hanabusa, K. *J. Phys. Chem. B* **2008**, *112*, 16393. (c) Sugita, A.; Suzuki, K.; Tasaka, S. *Jpn. J. Appl. Phys.* **2008**, *47*, 8043. (d) Sugita, A.; Suzuki, K.; Kubono, A.; Tasaka, S. *Jpn. J. Appl. Phys.* **2008**, *47*, 1355. (e) Sakamoto, A.; Ogata, D.; Shikata, T.; Urakawa, O.; Hanabusa, K. *Polymer* **2006**, *47*, 956. (f) Sugita, A.; Suzuki, K.; Tasaka, S. *Chem. Phys. Lett.* **2004**, *396*, 131.
- (12) Masuda, M.; Jonkheijm, P.; Sijbesma, R. P.; Meijer, E. W. *J. Am. Chem. Soc.* **2003**, *125*, 15935.
- (13) Shirakawa, M.; Fujita, N.; Shinkai, S. *J. Am. Chem. Soc.* **2003**, *125*, 9902.
- (14) Hanabusa, K.; Kawakami, A.; Kimura, M.; Shirai, H. *Chem. Lett.* **1997**, 191.
- (15) Bao, C. Y.; Lu, R.; Jin, M.; Xue, P. C.; Tan, C. H.; Xu, T. H.; Liu, G. F.; Zhao, Y. Y. *Chem. Eur. J* **2006**, *12*, 3287.

- (16) Cu, J. X.; Zheng, Y. J.; Shen, Z. H.; Wan, X. H. *Langmuir* **2010**, *26*, 15508.
- (17) de Loos, M.; Ligtenbarg, A. G. J.; van Esch, J.; Kooijman, H.; Spek, A. L.; Hage, R.; Kellogg, R. M.; Feringa, B. L. *Eur. J. Org. Chem.* **2000**, 3675.
- (18) (a) Zweep, N.; Hopkinson, A.; Meetsma, A.; Browne, W. R.; Feringa, B. L.; van Esch, J. H. *Langmuir* **2009**, *25*, 8802. (b) Pal, A.; Dey, J. *Soft Matter* **2011**, *7*, 10369. (c) de Loos, M.; Ligtenbarg, Alette G. J.; van Esch, J.; Kooijman, H.; Spek, Anthony L.; Hage, R.; Kellogg, Richard M.; Feringa, Ben L. *Eur. J. Org. Chem.* **2000**, *2000*, 3675. (d) Dasgupta, D.; Srinivasan, S.; Rochas, C.; Thierry, A.; Schroder, A.; Ajayaghosh, A.; Guenet, J. M. *Soft Matter* **2011**, *7*, 2797. (e) Cui, J.; Zheng, Y.; Shen, Z.; Wan, X. *Langmuir* **2010**, *26*, 15508.
- (19) (a) George, M.; Snyder, S. L.; Terech, P.; Glinka, C. J.; Weiss, R. G. *J. Am. Chem. Soc.* **2003**, *125*, 10275. (b) Ghosh, A.; Dey, J. *Langmuir* **2009**, *25*, 8466. (c) Bag, B. G.; Dinda, S. K.; Dey, P. P.; Mallia, V. A.; Weiss, R. G. *Langmuir* **2009**, *25*, 8663.
- (20) (a) Ranganathan, D.; Kurur, S.; Karle, I. L. *Biopolymers* **2000**, *54*, 249. (b) Bose, P. P.; Drew, M. G. B.; Das, A. K.; Banerjee, A. *Chem. Commun.* **2006**, 3196. (c) Rajput, L.; Chernyshev, V. V.; Biradha, K. *Chem. Commun.* **2010**, *46*, 6530.
- (21) Jiménez, C. A.; Belmar, J. B.; Ortíz, L.; Hidalgo, P.; Fabelo, O.; Pasán, J.; Ruiz-Pérez, C. *Cryst. Growth Des.* **2009**, *9*, 4987.



## CHAPTER THREE

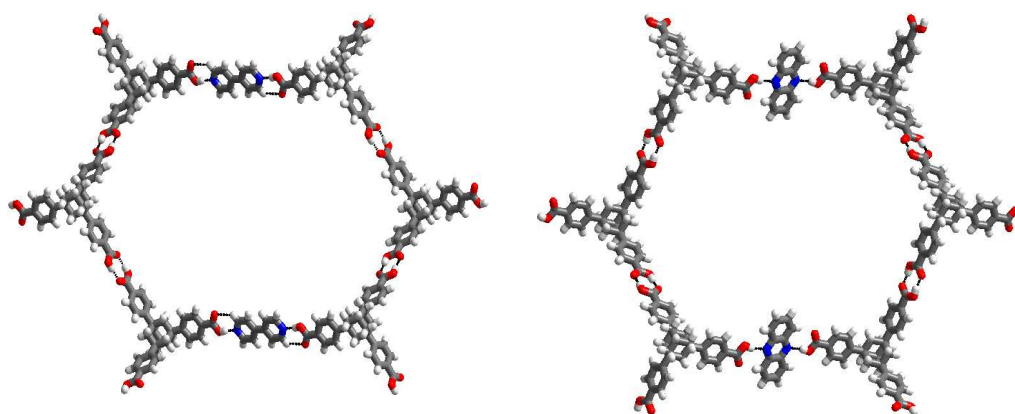
### Co-crystals of Trithiocyanuric acid with some *N*- donor compounds

### 3.1 Introduction

Co-crystal is basically a crystalline solid, containing at least two types of molecular entities other than solvent of crystallization or water, in a distinct stoichiometric ratio within the crystal lattice. However, in recent times, wide connotations of the co-crystals are described by various research groups to illustrate and emphasize the importance of the targeted co-crystals, which fall beyond the general approach. Nevertheless, design and synthesis of co-crystals direct at (i) understanding the recognition between molecules with complementary functionalities, thus, to get specific molecular patterns for particular applications.<sup>1</sup> (ii) varying the physical properties of a solid by incorporating another component into its crystal lattice.<sup>2</sup> (iii) designer co-crystal to arrive at molecular assembly with desired orientation.<sup>1a,1b,3</sup> These perspectives already were discussed with illustrating examples in Chapter 1.

The prime features play a significant role in the template directed synthesis of co-crystals are (i) the topology of the molecule, which plays a major role to obtain an assembly with desired arrangement, (ii) the molecular recognition sites to establish preferable intermolecular interactions. It is noteworthy to emphasize that the hydrogen bond is one of the most important intermolecular interactions, often encountered in the template directed organic assemblies.<sup>4</sup> In the process of finding effective molecular recognition sites, carboxylic acid / pyridyl based functional moieties are identified as most reliable units and numerous reports with different molecular systems are available in the literature.<sup>5</sup> This is because of the robust O-H $\cdots$ N/C-H $\cdots$ O hydrogen bonds that result between such functionalities. For example,

various carboxylic acid derivatives, of different molecular skeletons, which are topologically different due to the position of the substitution of  $-\text{COOH}$  groups, are being used with pyridyl based molecular templates with varied conformations, such as 4,4'-bipyridine (**bpy**), 1,2-bis(4-pyridyl)ethene (**bpyee**), 1,2-bis(4-pyridyl)ethane (**bpyea**), 1,3-bis(4-pyridyl)propane (**bpypa**), etc.<sup>5-6</sup> Thus, terephthalic acid with two  $-\text{COOH}$  groups in linear positions, interacts with **bpy** yielding linear tapes, while trimesic acid with three  $-\text{COOH}$  groups at trigonal position forms a cavity structure in two dimensional arrangement with **bpy**, as shown in Figure 1.5(c) in Chapter 1.

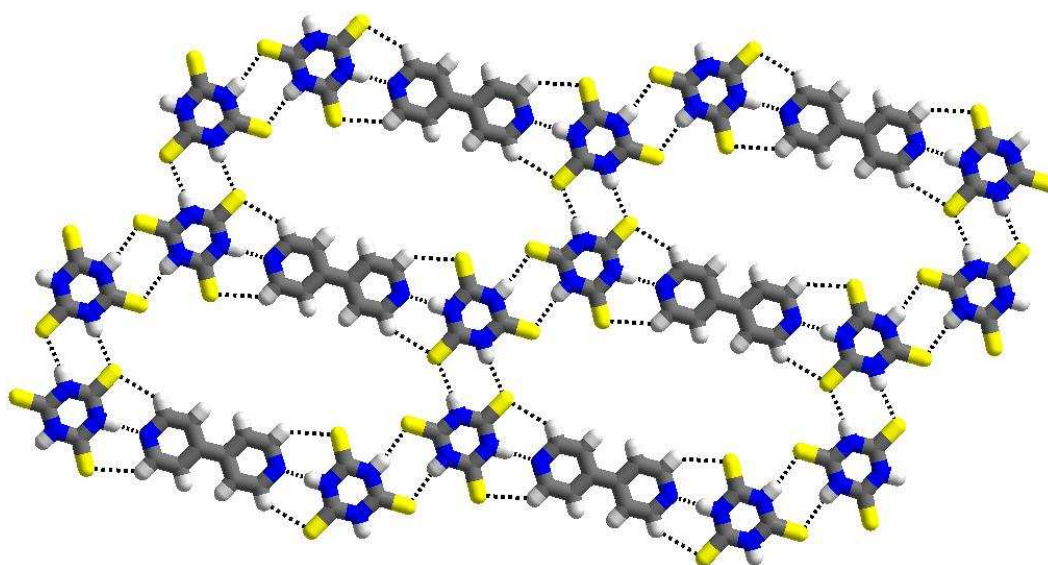


**Figure 3.1.** Voids observed in the self-assembled structures of adamantane tricarboxylic acid with a) bipyridine and b) phenazine.

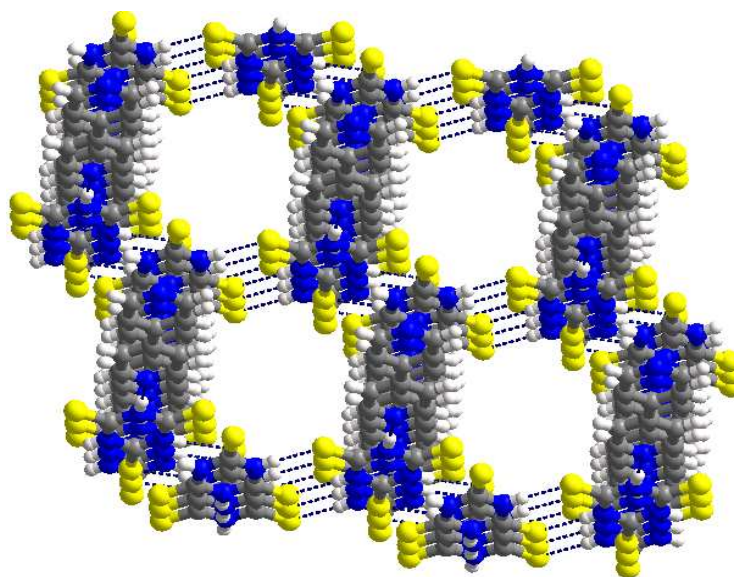
Among various network structures, such as ladders, sheets, cavity/voids structures, etc., assemblies with open-frame network structures possessing empty space are quite popular because such materials could be used in various applications. Towards the synthesis of such template directed open-frame structures, molecular complexes of adamantanetricarboxylic acid with **bpy** and phenazine serve as representative example,<sup>7</sup> in which cavities of huge dimension

are realized in two dimensional arrangement, within the crystal lattice (see Figure 3.1). However, to achieve the possible highest packing efficiency, sometimes, self filling of the cavities by the layers of molecules of same kind occurs, precluding the formation of voids, in three dimensional arrangement.

The template directed synthesis can also be achieved through a variety of acceptor-donor functionalities other than  $-\text{COOH}$  group. For example, trithiocyanuric acid (TCA), a cyclic imide derivative with  $D_{3h}$  symmetry, which possesses three each hydrogen bond donors and acceptors, was evaluated as a potential molecular template and found to be yielding void structures. A noteworthy example<sup>8</sup> being a complex of TCA and **bpy**, in which, the co-crystal formers are arranged in a sheet structure, yielding cavities (see Figure 3.2), which are stacked to yield a channel structure in three dimensional arrangement, as shown in Figure 3.3, incorporating various molecular entities as guests, such as benzene, toluene, xylenes, anthracene etc.



**Figure 3.2.** Arrangement of TCA and **bpy** with cavities in a sheet.

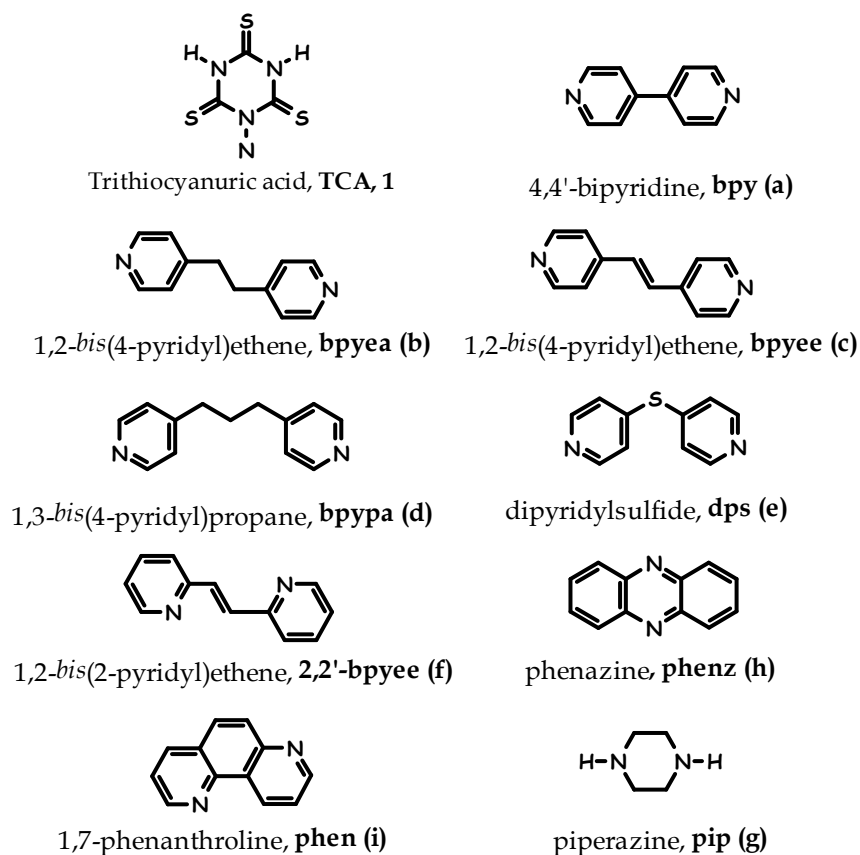


**Figure 3.3.** Channels observed in the crystals of molecular complex of TCA and **bpy**.

A noteworthy observation was that even after removal of the guest species from the channels, the apo-host is also stable, which is observed only in a few organic assemblies. However, surprisingly, not many examples of molecular complexes of TCA are known in the literature since the first study done in 1997 by Rao and co-workers.<sup>8</sup> A search done on Cambridge Structural Database, a well known repository for the information of crystal structure of organic and organometallic compounds/complexes retrieved only a few structures, which were indeed reported even before year 2005. Thus, to explore the potentiality of TCA in supramolecular synthesis as one of the exotic template, for the creation of tailor-made assemblies, molecular complexes of TCA with different types of aza-donor compounds, with varied topology, as shown in Chart 1, have been carried out.

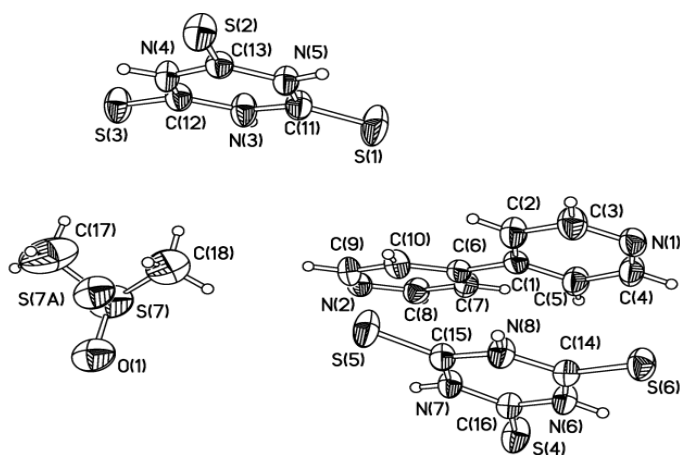


## Chart 1



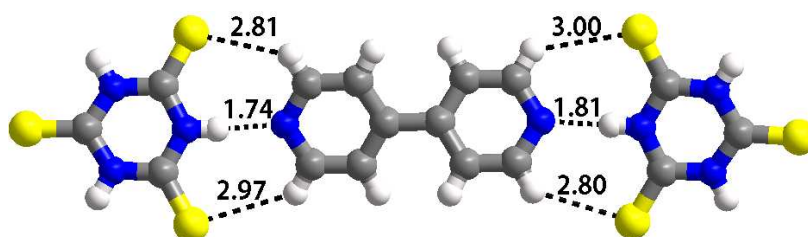
### 3.2 Structure of molecular complex of trithiocyanuric acid and 4,4'-bipyridine obtained from DMSO, 1a.

The known channel structure of TCA and **bpy** in the literature was prepared from a CH<sub>3</sub>OH solution of the appropriate guest species. To understand the possible structural variations in the resultant assembly, if the nature of the solvent is changed, for example, polarity, co-crystallization of TCA and **bpy** has been carried out in DMSO solution to study the effect of high polar solvents. Good quality crystals were obtained, over a period of 24 h, have been analysed by single crystal X-ray diffraction method.



**Figure 3.4.** ORTEP representation of the molecular components in complex, **1a**.

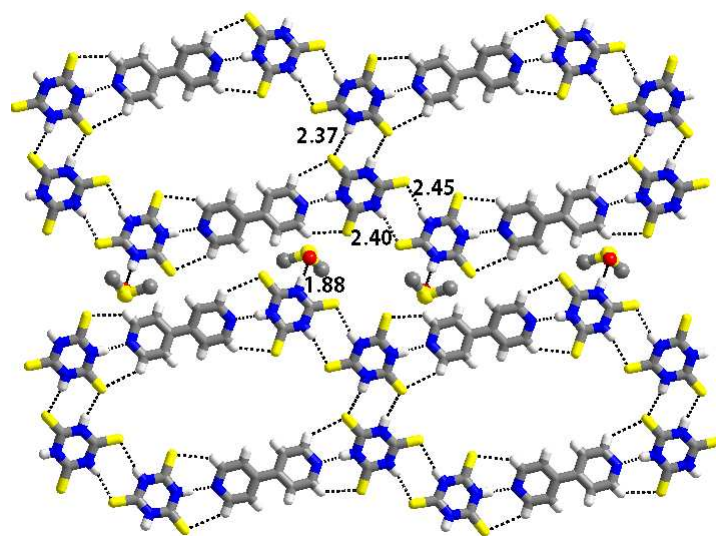
The structural analysis reveals a 2:1 molecular complex of TCA and **bpy**, respectively, along with a DMSO molecule in the asymmetric unit. ORTEP of the contents of asymmetric unit is shown in Figure 3.4. Salient crystallographic details are given in Table 3.1. Packing analysis reveals that each **bpy** molecule is connected to two TCA molecules, through a triple hydrogen bonding pattern, comprising of N-H $\cdots$ N and C-H $\cdots$ S hydrogen bonds, with the corresponding hydrogen bonded distances in each pattern being H $\cdots$ N, 1.74; H $\cdots$ S, 2.81, 2.97 and H $\cdots$ N, 1.81; H $\cdots$ S, 3.00, 2.80 Å. Such recognition is shown in Figure 3.5.



**Figure 3.5.** Molecular recognition between TCA and **bpy** involves the triple N-H $\cdots$ N/C-H $\cdots$ S hydrogen bonds.

Four of such adjacent ensembles are held together, in further self assembly, yielding an eight membered cyclic structure, establishing interaction through two

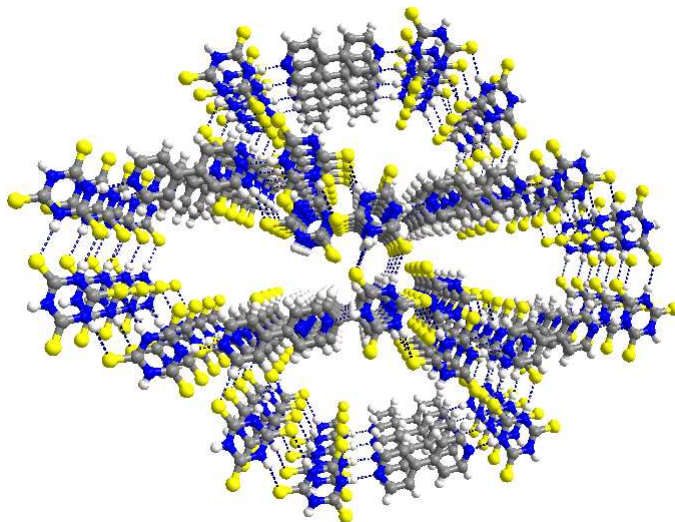
types of dimeric N-H $\cdots$ S hydrogen bonds formed between the TCA molecules. While one of the hydrogen bonding patterns is symmetrical with H $\cdots$ S distance of 2.37 Å, the other one being unsymmetrical with two different H $\cdots$ S distances, 2.40 and 2.45 Å. Such an association as shown in Figure 3.6, ultimately gives void space of dimension 15 × 17 Å<sup>2</sup>. Unlike in the similar assemblies reported in the literature, which were obtained from a CH<sub>3</sub>OH / CHCl<sub>3</sub> solution, in the assembly of **1a**, one dimensional open frame networks are realized, rather than a  $\beta$ -sheet. Further, DMSO molecules are embedded in between the rings in two dimensional packing, as pendants, by interacting with one of the TCA molecules through N-H $\cdots$ O hydrogen bond, with a distance of 1.88 Å.



**Figure 3.6.** Arrangement of molecules within a sheet, in complex **1a** and also interaction of DMSO molecules as pendants.

However, as we noted in many of the other assemblies, in complex **1a** also, the sheets are stacked in such a manner that the void space is aligned to project channels along a crystallographic axis, which are being filled by DMSO molecules.

The channel structure is represented in Figure 3.7, without DMSO molecules for better visualization.

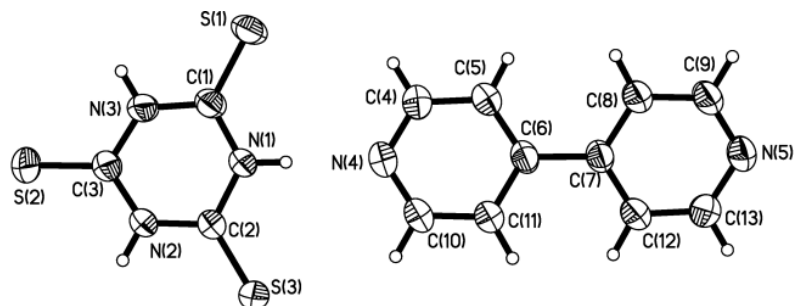


**Figure 3.7.** Channel structure observed in complex, **1a**.

### **3.3 Structure of molecular complex of trithiocyanuric acid and 4,4'-bipyridine obtained from DMSO/MeOH, **1a'****

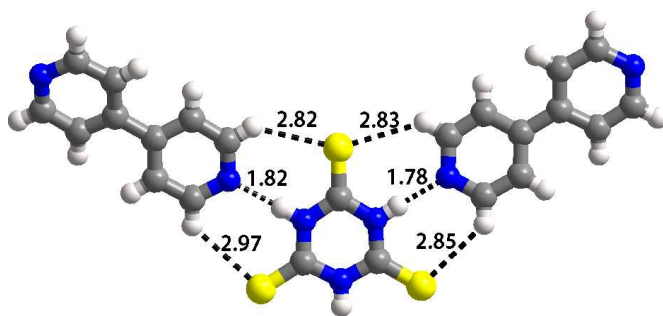
Comparing the similarity between the two assemblies formed by TCA and **bpy**, even upon crystallization from solvents of different polarities and also observation of incorporation of the solvents in the crystal lattice, it is proposed to study the preparation of co-crystals of TCA and **bpy** from a mixture of solvents, especially that were incorporated in the crystal lattices independently, to evaluate the nature of resultant assembly, that may arise. Thus, TCA and **bpy** upon co-crystallization from DMSO/MeOH solution gave good quality crystals, upon slow evaporation of the solution, over a period of 12 h. Analysis of the molecular complex by the single crystal X-ray diffraction method reveals that ratio of TCA

and **bpy** in the crystals is found to be 1:1. ORTEP of the contents of the asymmetric unit is shown in Figure 3.8.



**Figure 3.8.** 1:1 Molecular complex of TCA and **bpy**.

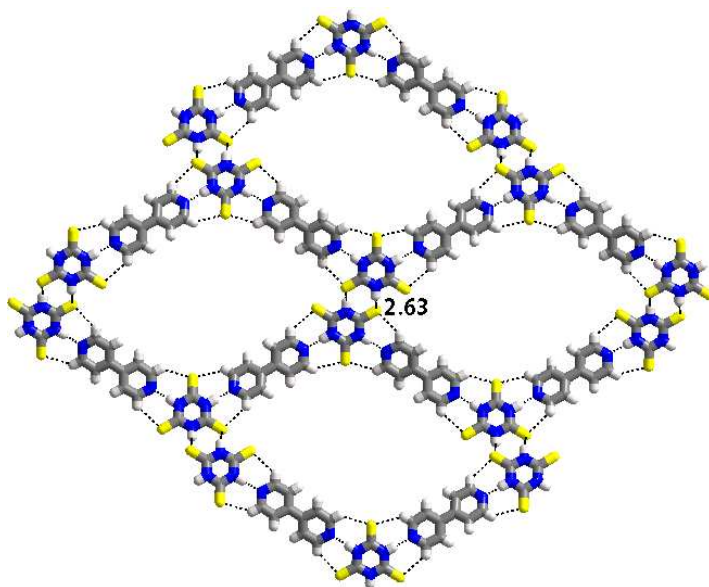
Surprisingly, no solvent of crystallization is observed in the crystal lattice unlike in the other structures described above. It is interesting to note that TCA and **bpy** are arranged alternatively, do interact by two different types of triple hydrogen bond patterns, comprising of  $\text{N-H}\cdots\text{N}$  and  $\text{C-H}\cdots\text{S}$  hydrogen bonds with the corresponding distances being  $\text{H}\cdots\text{N}$ , 1.82;  $\text{H}\cdots\text{S}$ , 2.82, and 2.97 Å while in the other pattern the corresponding distances are  $\text{H}\cdots\text{N}$ , 1.78;  $\text{H}\cdots\text{S}$ , 2.83 and 2.85 Å. A typical ensemble is shown in Figure 3.9.



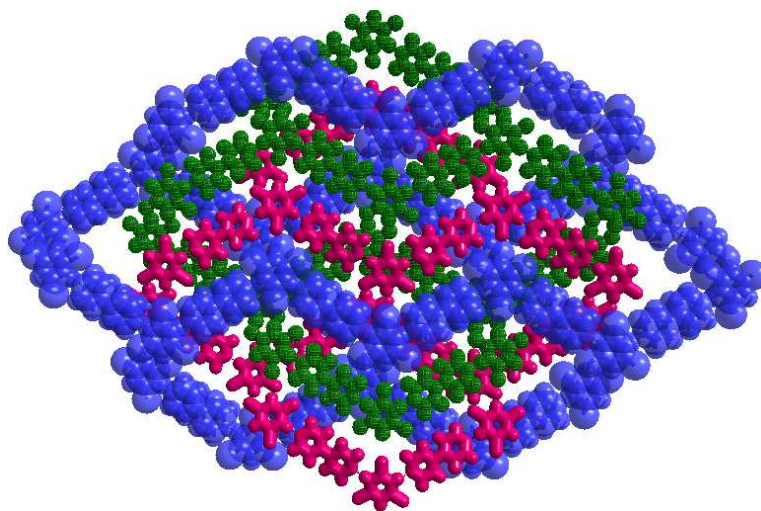
**Figure 3.9.** Triple hydrogen bonding pattern observed in **1a'**.

Thus, a crinkled tape is observed in one dimensional arrangement. Such adjacent tapes, however, are held together by a dimereic  $\text{N-H}\cdots\text{S}$  hydrogen bond

patterns formed by the TCA molecules. Such a network establishes two dimensional arrangement with cavities of  $19 \times 14 \text{ \AA}^2$  dimension.



**Figure 3.10.** Two dimensional arrangement of molecules in **1a'** with cavities



**Figure 3.11.** Molecular arrangement in crystal lattice of **1a'** with two fold interpenetration.

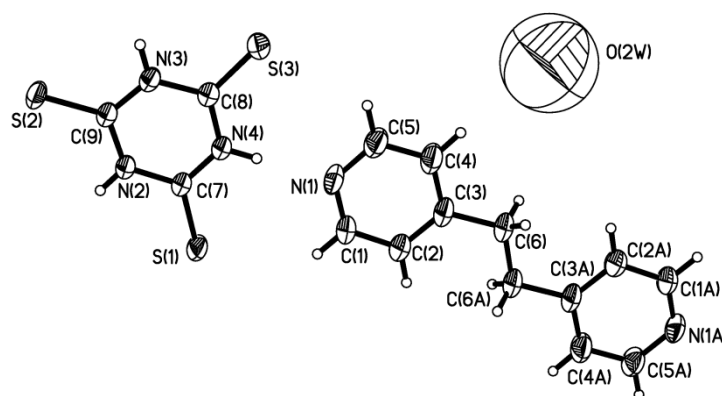
As described earlier, for example, in the self assembly of molecules of trimesic acid, if appropriate guest molecules are not available, the voids are

generally filled effectively by catenation or interpenetration process, by which the packing of molecules in three dimensional arrangement would attribute the desired stability to the lattice. Following the similar process, in the crystals of **1a'** also the sheets with voids are packed by 2-fold interpenetration. Such an assembly is shown in Figure 3.11.

Thus, crystals of **1a'** serve as a representative example to obtain anhydrous co-crystals of specific system by varying the polarity of the solvent of crystallization, especially whenever the solvents play a role in the stabilization of the assemblies. To further investigate such variations, other analogues of **bpy** have been considered to co-crystallize with TCA.

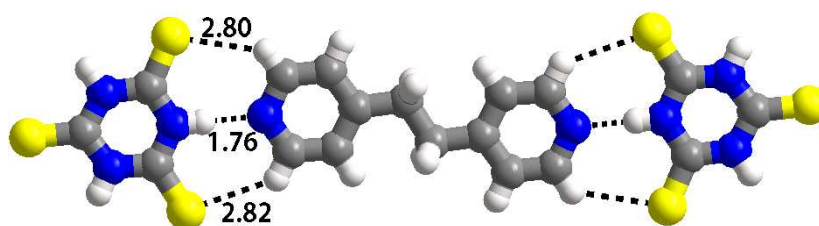
### 3.4 Structure of co-crystals of trithiocyanuric acid and 1,2-bis(4-pyridyl)ethane, **1b**

Good quality crystals of 1,2-bis-(4-pyridyl)ethane (**bpyea**) and TCA were obtained from a methanol solution, by slow evaporation process, over a period of 24 h.

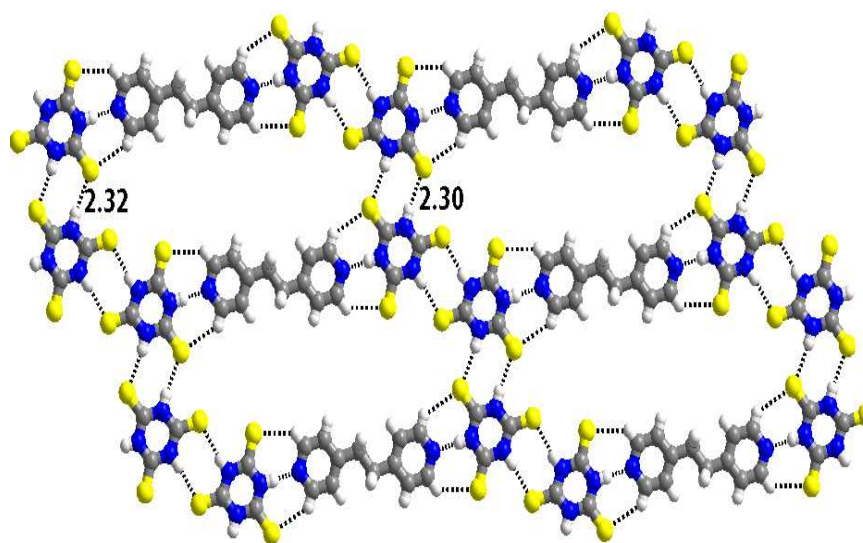


**Figure 3.12.** ORTEP of the molecular components in the crystal lattice of **1b**.

Single crystal X-ray diffraction analysis reveals TCA and **bpyea** molecules present in the asymmetric unit in a 2:1 ratio, along with a water molecule. An asymmetric unit in the form of ORTEP is shown in Figure 3.12. Pertinent crystallographic information is given in Table 3.1. TCA and aza-donor molecules are held together through triple hydrogen bond patterns, as described in **1a**, with each **bpyea** being connected to two TCA molecules by C-H $\cdots$ S / N-H $\cdots$ N / C-H $\cdots$ S hydrogen bonds. The ensemble is shown in Figure 3.13, annotating the hydrogen bond distances in dashed lines, H $\cdots$ N, 1.76, H $\cdots$ S, 2.80 and 2.82 Å. The complete characteristics of the hydrogen bonds are given in Table 3.2.



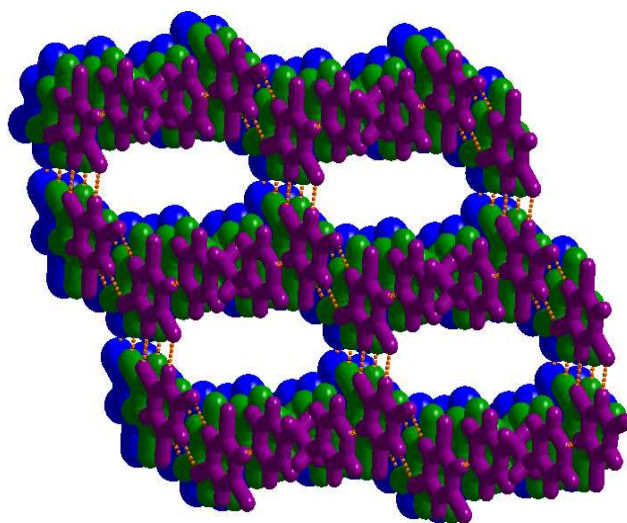
**Figure 3.13.** Recognition between TCA and **bpyea** through a triple hydrogen bonding patterns.



**Figure 3.14.** Arrangement of molecules in **1b**, in a sheet.



Further, following almost similar self assembly process as observed in **1a**, each four of the adjacent ensembles are held together establishing dimeric N-H $\cdots$ S hydrogen bonded patterns between the appropriate TCA molecules, with the corresponding H $\cdots$ S distances being 2.30 and 2.37 Å (Table 3.2). Thus, a layer structure is realized with cavities of dimension  $17 \times 6 \text{ \AA}^2$ , as shown in Figure 3.14.



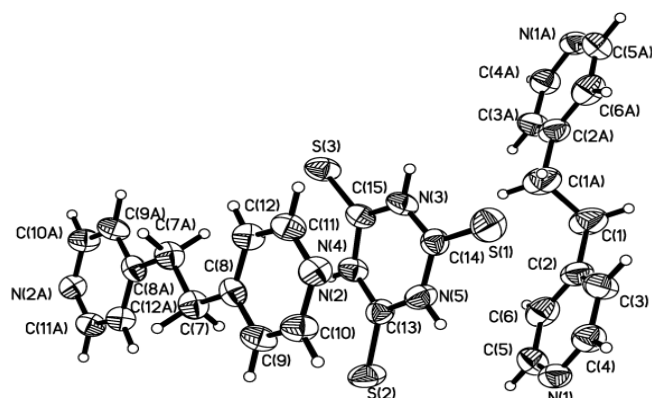
**Figure 3.15.** Packing of molecules in the crystal lattice of **1b**.

Such sheets are stacked aligning the voids, thereby, constitutes channels, which are being filled by water molecules. The channels without water molecules are shown in Figure 3.15. However, further attempts to obtain crystals from other solvents including high polar solvents were not successful, at ambient conditions.

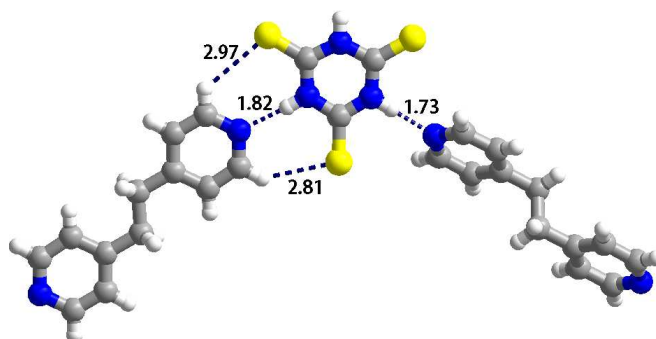
### **3.5 Structure of the molecular complex of trithiocyanuric acid and 1,2-bis-(4-pyridyl)ethane obtained under solvothermal conditions, **1b'**.**

When crystallization of TCA and **bpyea** was carried out at non-ambient conditions, solvothermal (at high temperature and pressure), gave good quality single crystals. While temperature of the system was maintained at 120°C, the

crystals were obtained over a period of 2 days under autogenous pressure. The structural analysis reveals that TCA and **bp<sub>y</sub>ea** are in a 1:1 ratio in the crystals of **1b'**, without any solvent of crystallization in the crystal lattice, thus, yielding an anhydrous analogue of **1b**. Contents of the asymmetric unit are shown in Figure 3.16, in the form of ORTEP. Crystallographic information is listed in Table 3.1.



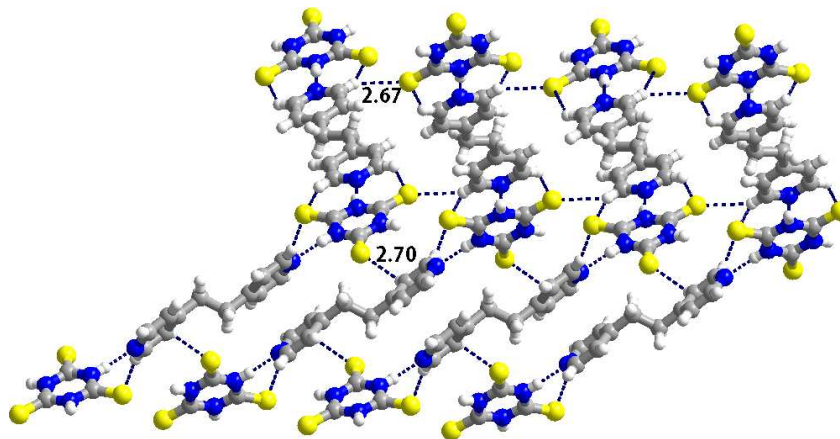
**Figure 3.16.** Asymmetric unit of complex **1b'**.



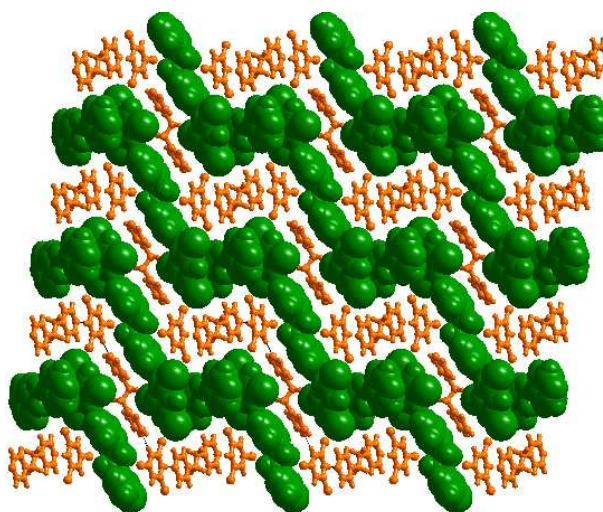
**Figure 3.17.** Molecular recognition between TCA and **bp<sub>y</sub>ea** through triple and single hydrogen bonding patterns.

Analysis of molecular interactions further highlights that each TCA molecule interact with two **bp<sub>y</sub>ea** molecules; while one of it establishes a triple hydrogen bonding, comprising of N-H...N (H...N, 1.82 Å) and C-H...S (H...S, 2.97 and 2.81 Å) hydrogen bonds, the other **bp<sub>y</sub>ea** is simply connected to TCA by a

single N-H $\cdots$ N hydrogen bond with the H $\cdots$ N distance of 1.73 Å. Complete characteristics of hydrogen bonds are listed in Table 3.2.



**Figure 3.18.** Two dimensional arrangement observed in **1b'** where the adjacent tapes are held together by C-H $\cdots$ S hydrogen bonds.



**Figure 3.19.** Layer structure obtained for complex **1b'** in three dimension.

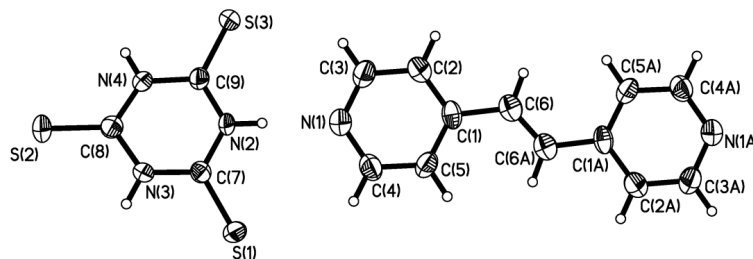
Such ensembles are propagated in two dimensional arrangement with the adjacent crinkled tapes are being held together by a series of C-H $\cdots$ S hydrogen bonds. However, in the crystal lattice, such layers are stacked as shown in Figure 3.19. Although, the structure of **1b'** is in anhydrous form of **1b**, the packing is quite

different with respect to **1b**, unlike the similarity observed between **1a** and **1a'**, about formation of voids.

Since TCA forms different assemblies with **bpy** and **bpyea** by simply following different crystallization conditions and varying polarity of the solvent of crystallization, experiments have been continued with other aza donor analogues. In this respect, however, except with 1,7-phenanthroline, the remaining assemblies could not be obtained in more than one form. However, the structural features of these assemblies are quite exotic in the nature with distinct variations as well as yielding exotic supramolecular architectures.

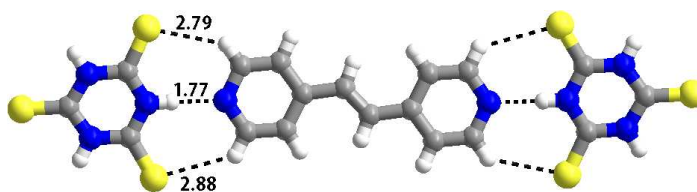
### 3.6 Packing analysis in the molecular complex of trithiocyanuric acid and 1,2-bis-(4-pyridyl)ethene, **1c**

Good quality single crystal of TCA with 1,2-bis(4-pyridyl)ethene (**bpyee**) is obtained from a solution of DMSO/CH<sub>3</sub>OH. However, attempts to obtain single crystals independently either from methanol or DMSO were futile. Molecular species present in the crystal lattice are in a 2:1 ratio of TCA and **bpyee**. Pertinent crystal details are given in Table 3.1. Contents of the asymmetric unit are shown in Figure 3.20.

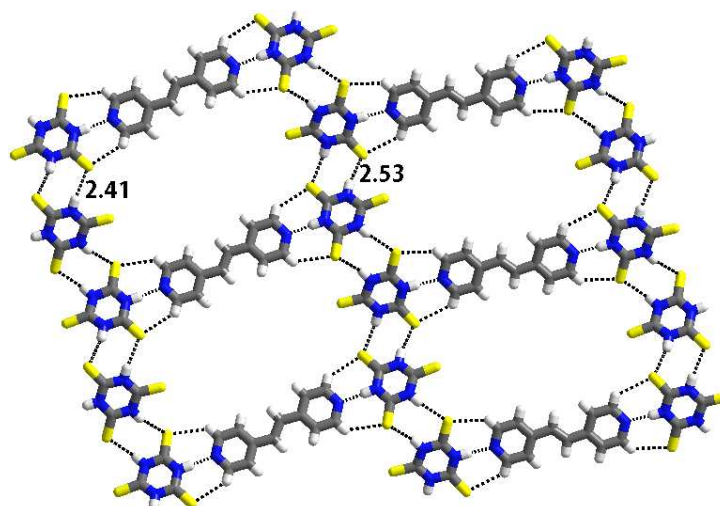


**Figure 3.20.** ORTEP drawing of molecular complex, **1c**.

It is noteworthy to mention that no solvent of crystallization is observed in the asymmetric unit, as observed in **1a'** in which also the solvent of crystallization was DMSO/CH<sub>3</sub>OH. But the composition is quite different with respect to the ratio of the co-crystal formers. While in **1a'**, it was 1:1 ratio of TCA and aza-donor, in **1c**, the same was found to be 2:1. The structural analysis further reveals that each **bpyee** molecule interacts with two TCA molecules through a triple hydrogen bonding pattern comprising of N-H $\cdots$ N / C-H $\cdots$ S, as discussed in the above structures **1a** and **1b**, with the corresponding distances being H $\cdots$ N, 1.77; H $\cdots$ S, 2.79 and 2.88 Å. The recognition pattern is shown in Figure 3.21.



**Figure 3.21.** Hydrogen bonding pattern observed between TCA and **bpyee** in **1c**.

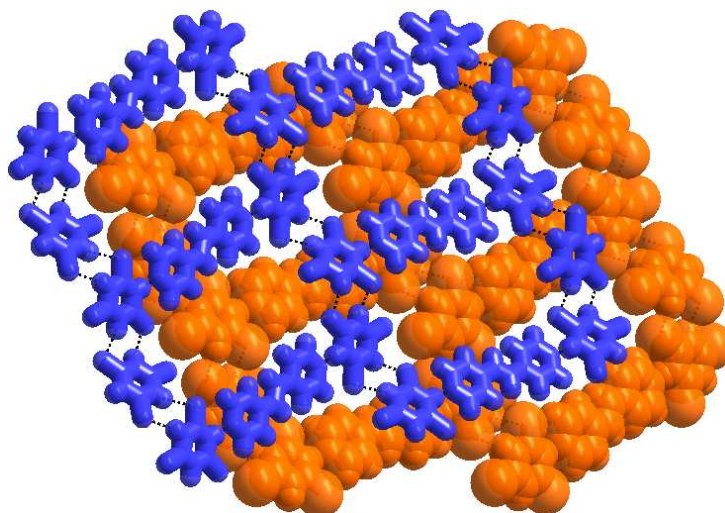


**Figure 3.22.** Cavity structure observed for complex **1c**, within a layer.

Further packing of the ensembles also follow the pattern as observed in the structures of **1a** and **1b**, with adjacent three membered supermolecules are held

together by N-H...S hydrogen bonds formed between the TCA molecules. Thus, cavities of  $14 \times 8 \text{ \AA}^2$  are observed within two dimensional packing (see Figure 3.22).

However, packing of these layers in the crystal lattice is distinctly different than so far observed in **1a**, **1a'**, **1b** and **1b'** as well as in the related structures reported in the literature. In the crystals of **1c**, interestingly the layers are stacked by skewing of the adjacent layers, just masking the voids within each layer by the electron density of the moieties from the top and bottom layers. Thus, a graphite layer type structure is established. The arrangement is shown in Figure 3.23.

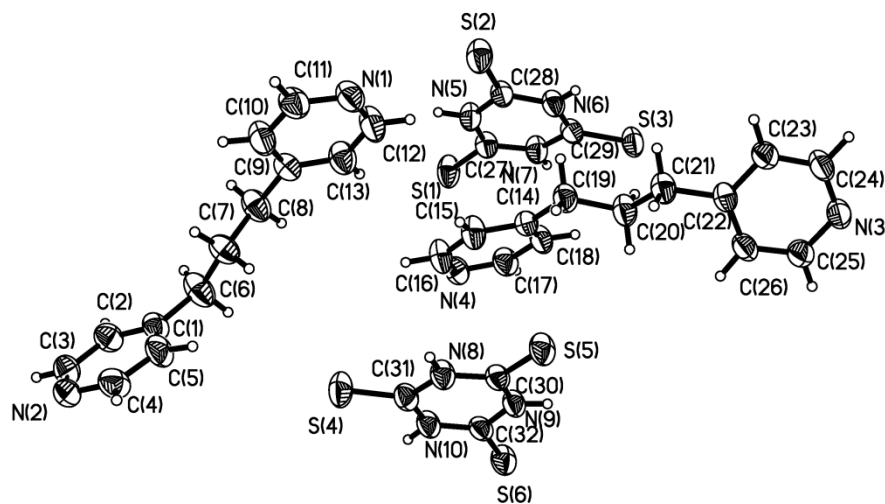


**Figure 3.23.** Three dimensional arrangement of molecules in **1c** showing self filled layer structure.

### **3.7 Structure of the molecular complex of trithiocyanuric acid with 1,3-bis(4-pyridyl)propane, 1d.**

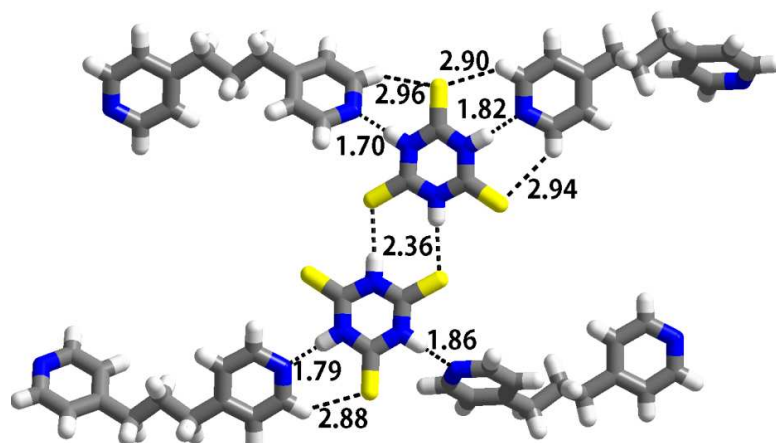
In further continuation, co-crystallization of TCA with higher analogues of aza-donors discussed in the earlier sections by increasing the methylene groups between the pyridyl moieties, has been carried out. TCA and 1,3-bis(4-

pyridyl)propane (**bpypa**), a flexible aza-donor gave single crystals with a molecular complex consisting of 1:1 ratio of the constituents, upon slow evaporation of the methanol solution at ambient laboratory conditions. The crystal structure was determined by X-ray diffraction technique.



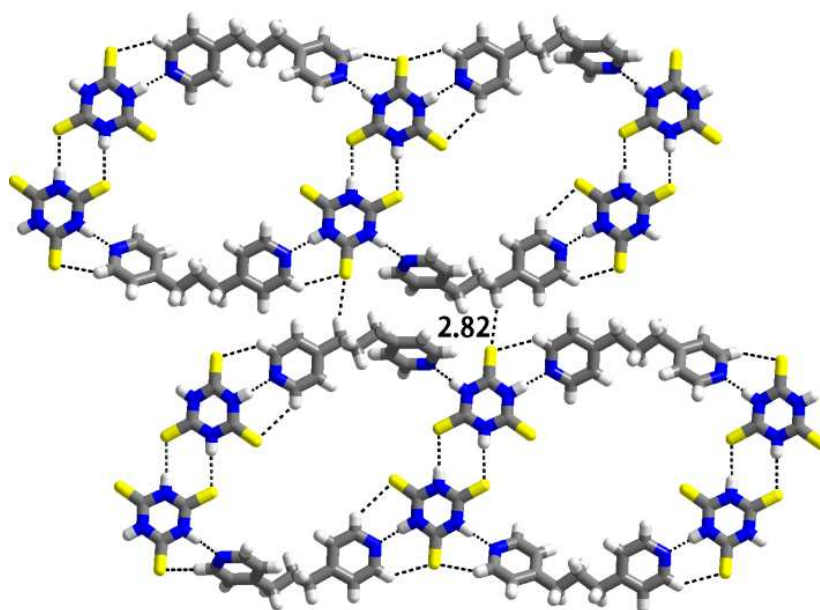
**Figure 3.24.** Representation of the asymmetric unit of molecular complex, **1d**.

The asymmetric unit contains two symmetry independent molecules of each TCA and **bpypa**, as shown in Figure 3.24, in the form of ORTEP. Recognition between the molecules is quite intriguing. While a pair of symmetry related TCA and **bpypa** interact with each other by a triple hydrogen bond interaction through C-H $\cdots$ S / N-H $\cdots$ N / C-H $\cdots$ S hydrogen bonds, as observed in the other related structures, with the H $\cdots$ N and H $\cdots$ S distances of 1.82, 2.90 and 2.94 Å, the other pair of symmetry related constituents establishes interaction by a dimeric hydrogen bonding patterns with N-H $\cdots$ N (H $\cdots$ N, 1.79 Å) and C-H $\cdots$ S (H $\cdots$ S, 2.88 Å) hydrogen bonds. Such adjacent moieties are ultimately connected to each other by N-H $\cdots$ S hydrogen bonds, with the corresponding H $\cdots$ S distance of 2.36 Å. The ensemble, thus, formed is shown in Figure 3.25.



**Figure 3.25.** Hydrogen bonding pattern observed between the molecules in a primary ensemble in **1d**.

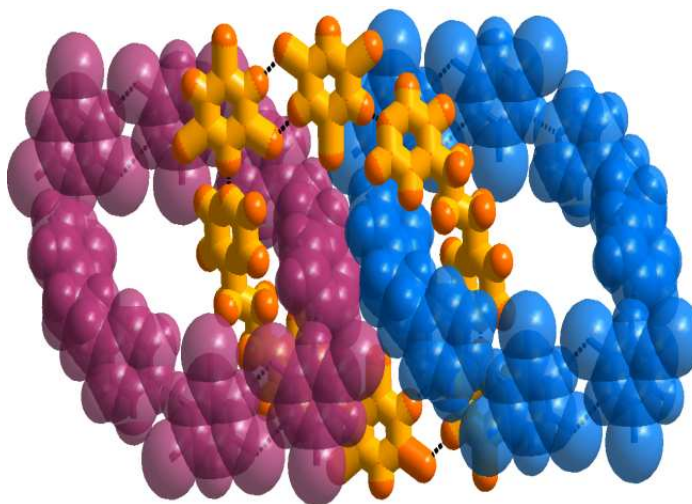
The adjacent ensembles further interact with each other in such a manner that, the **bypa** which participate in triple hydrogen bonding pattern establish a single N-H $\cdots$ N (H $\cdots$ N, 1.86 Å) with the TCA molecules of the adjacent ensembles.



**Figure 3.26.** One dimensional cavity structure of **1d** extended to two dimension through C-H $\cdots$ S hydrogen bonds.



But, the **bpypa** that forms a dimeric hydrogen bonding pattern, interact with the adjacent units through similar dimeric hydrogen bonding patterns but with different strength as evident by the corresponding hydrogen bond distances, H $\cdots$ N, 1.79 Å and H $\cdots$ S, 2.96 Å. Such an association form hexagonal rings held together in one dimension with each hexagon possessing void space of  $12 \times 9 \text{ \AA}^2$ . However, within a layer, the hexagons are connected to each other by C-H $\cdots$ S hydrogen bonds (see Figure 3.26). As noted in the structure of **1a'**, in the structure of **1d** also, the void space is being filled effectively in the crystal lattice by 2-fold interpenetration of the adjacent layers. The arrangement is represented in Figure 3.27.

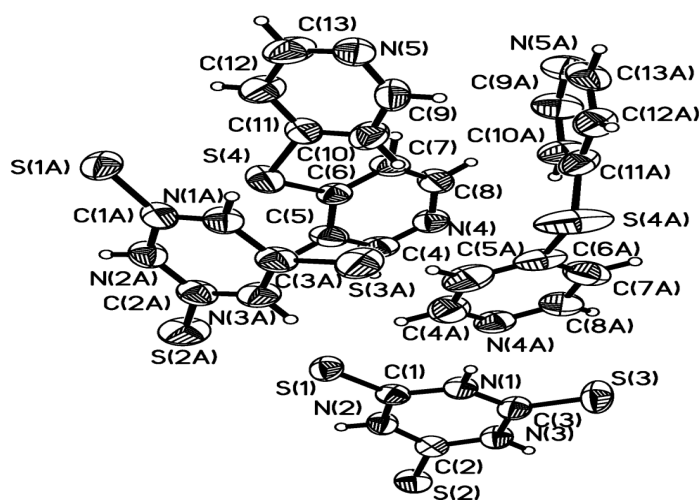


**Figure 3.27.** Three dimensional molecular arrangement of **1d** through interpenetration.

Comparing the structures, **1b**, **1c** and **1d**, it appears that flexible aza-donor apparently show tendency to form interpenetrated structures with TCA while rigid molecules adopt simple stacked arrangements. To explore the anomaly and establish further structural correlations, co-crystals of TCA with dipyridylsulfide has been carried out.

### 3.8 Molecular complex of TCA and dipyridylsulfide, **1e**.

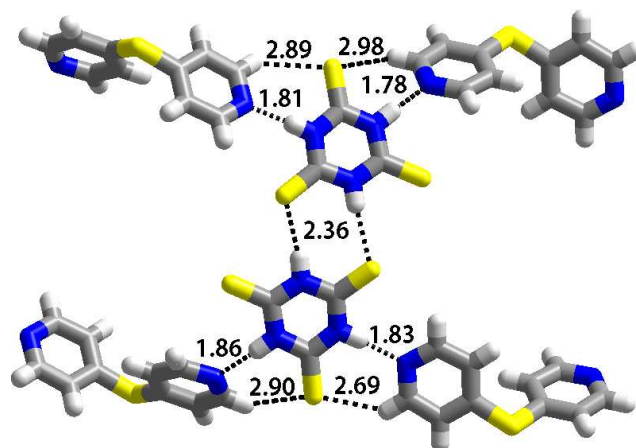
TCA and dipyridylsulfide (**dps**), a sulphur mediated aza-donor, yielded a molecular complex from methanol in a 1:1 ratio. Structure determination by single crystal X-ray diffraction reveals that asymmetric unit has two symmetry independent molecules as observed in **1d**. The contents of asymmetric unit in **1e** are shown in Figure 3.28 in the form of ORTEP.



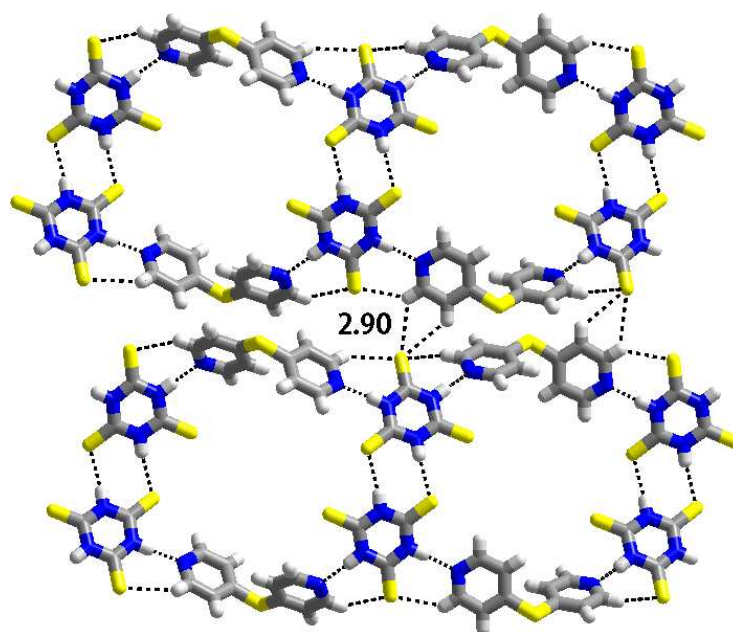
**Figure 3.28.** ORTEP of molecular components in the crystals of **1e**.

Also further structure analysis reveals that packing of molecules in **1e** has a close resemblance with **1d**, except for the topology of hydrogen bond patterns. In the structure **1e**, both the pairs of symmetry independent molecules shows the same hydrogen bonding patterns, except for the strength of the bonds. Thus, TCA and aza donors interact through dimers of N-H $\cdots$ N and C-H $\cdots$ S hydrogen bonds. One of the patterns shows the H $\cdots$ N and H $\cdots$ S distances of 1.78 and 2.98 Å respectively, whereas the other pair of symmetry related molecules have the corresponding distances as 1.86 and 2.90 Å. Such pairs are held together by dimeric N-H $\cdots$ S

hydrogen bonds with H...S distance of 2.36 Å. Arrangement of molecules in the typical ensemble is represented in Figure 3.29.



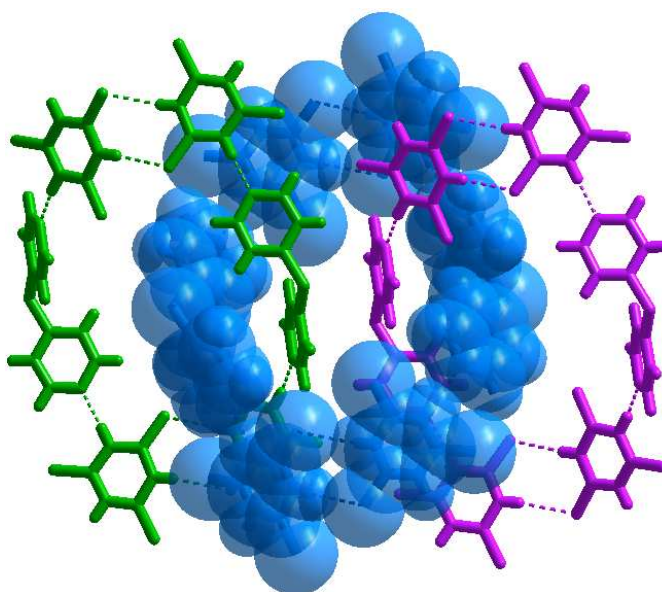
**Figure 3.29.** Molecular recognition observed in molecular complex, **1e**.



**Figure 3.30.** Two dimensional molecular arrangement of TCA and dipyridylsulfide with cavities in each hexagon.

These ensembles are held together constituting hexameric rings in one dimensional arrangement with cavities of dimension  $9 \times 8 \text{ \AA}^2$ . Further the hexagons

are connected to each other by series of C-H $\cdots$ S hydrogen bonds with distance of 2.90 Å in two dimensional propagation. The self assembly of the ensembles is shown in Figure 3.30. In addition, as observed in **1d**, in crystal lattice of **1e** also, the layers pack through 2-fold interpenetration. Such an arrangement is shown in Figure 3.31.



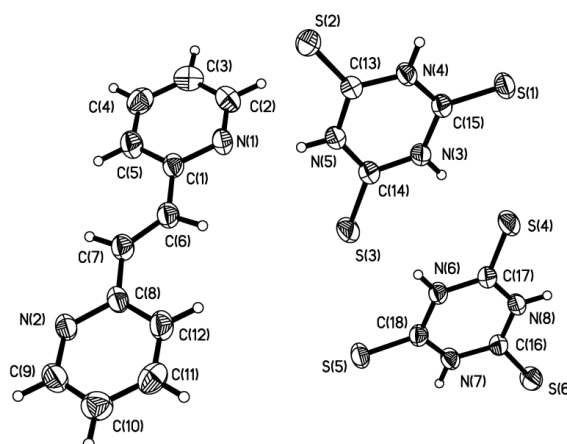
**Figure 3.31.** Interpenetrated assembly of **1e** in three dimension.

Noticing the similarity between **1d** and **1e**, investigation of variations with rigid ligands is carried out. For this purpose, maintaining close relation to the structures already obtained with such ligands, attempts were directed towards replacing 1,2-*bis*(4-pyridyl)ethene in the structure of **1c** with its analogue, simply differentiated by *N*-position, 1,2-*bis*(2-pyridyl)ethene.

### 3.9 Structure of trithiocyanuric acid with 1,2-*bis*-(2-pyridyl)ethene, **1f**.

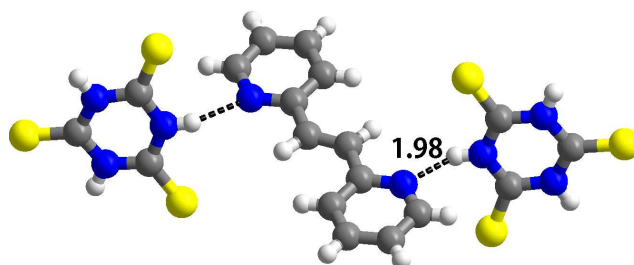
Molecular complex of TCA with 1,2-*bis*(2-pyridyl)ethene (**2,2'-bpyee**) was prepared from its methanol solution of the molecular components by slow

evaporation process. Good quality single crystals of **1f**, thus, obtained are analysed by single crystal X-ray diffraction method. The structure determination reveals that the asymmetric unit contains a 2:1 ratio of the molecular components, TCA and **2,2'-bpyee**, respectively. Contents of the asymmetric unit are shown in Figure 3.32 as an ORTEP.



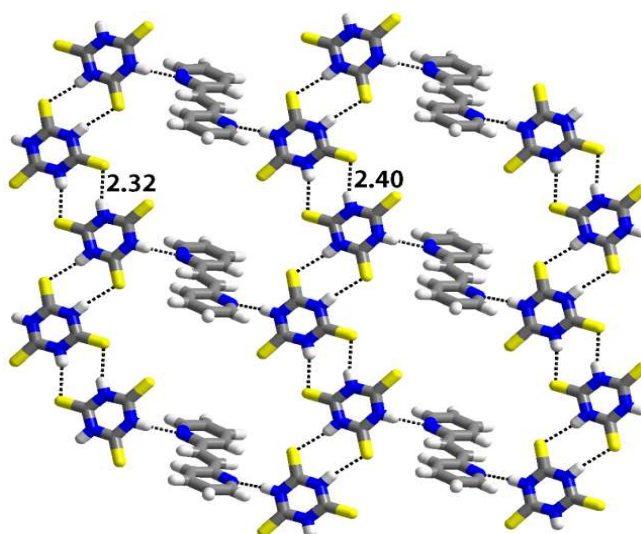
**Figure 3.32.** ORTEP representation of molecular complex, **1f**.

In the crystal structure, each **2,2'-bpyee** molecule establishes interaction with two TCA molecules through a single N-H $\cdots$ N (H $\cdots$ N, 1.98) hydrogen bond. Unlike in **1a**, **1b** and **1c**, no C-H $\cdots$ S hydrogen bonds were observed in the ensemble, as the **2,2'-bpyee** molecule is twisted by 68° from the mean plane of TCA molecules. The recognition pattern is shown in Figure 3.33.

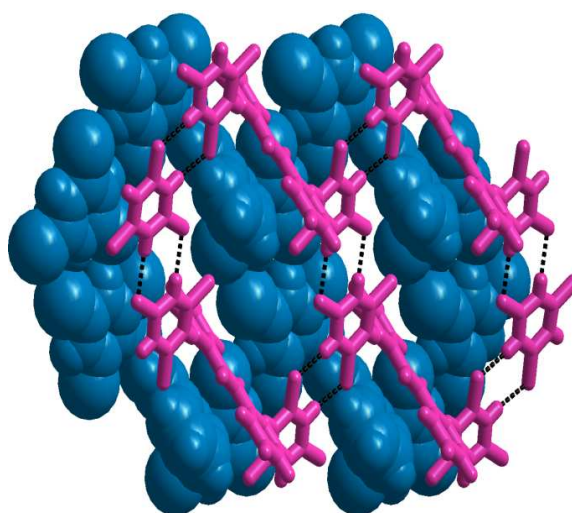


**Figure 3.33.** Molecular recognition between **2,2'-bpyee** and TCA in **1f**.

Such three member supermolecules are further held together within two dimensional arrangement through dimeric hydrogen bonding pattern, comprising of N-H $\cdots$ S hydrogen bonds, with H $\cdots$ S distances of 2.32 and 2.40 Å, formed by TCA molecules. Such an association is represented in Figure 3.34, with voids of 15 × 6 Å<sup>2</sup>.



**Figure 3.34.** Two dimensional structure of **1f** show the sheet structure with cavity.

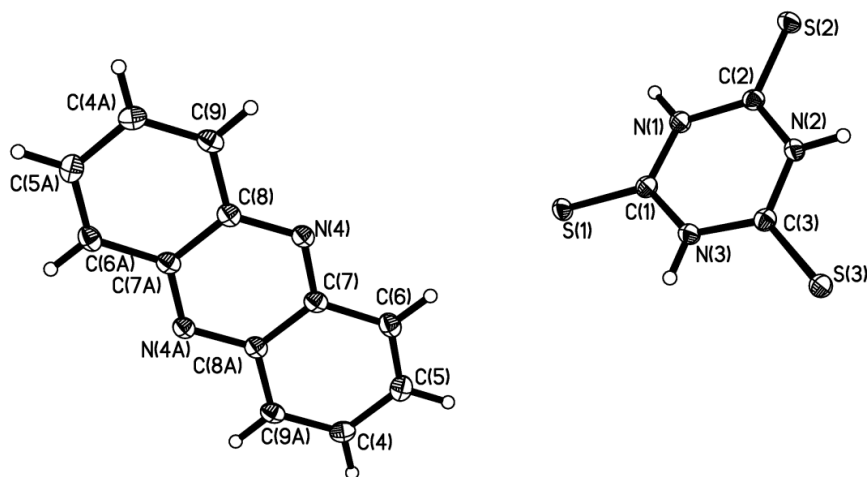


**Figure 3.35.** Three dimensional molecular arrangement of **1f** involves self filled layer structure.

Although crystallization was done from CH<sub>3</sub>OH solution, no solvent of crystallization is found in the crystal lattice to fill the voids; however, the sheets stacked in the crystal lattice with alternate layers are being skewed, masking the voids in a sheet by the electron density from the adjacent layers. This arrangement is indeed as similar to the feature observed in the crystal structure of **1c**, wherein also no solvent of crystallization was available. The skewed arrangement of layers is shown in Figure 3.35.

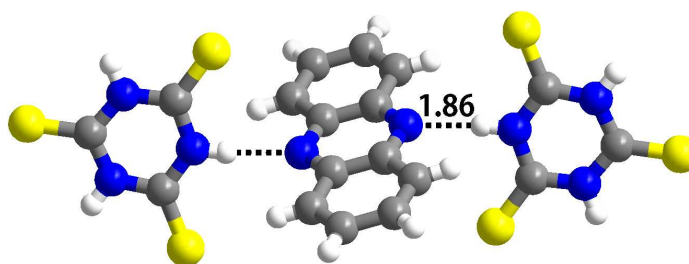
### 3.10 Structure of the molecular complex of trithiocyanuric acid with phenazine, **1g**.

Encouraged by the observed similarity between the assemblies **1c** and **1f** with TCA and rigid aza donor molecules, co-crystallization of TCA and other aza-donors with rigid geometry have been carried out. Co-crystallization of TCA with phenazine (**phenz**) in methanol is carried out by slow evaporation process, which yielded good quality single crystals, over a period of 48 h.



**Figure 3.36.** ORTEP of asymmetric unit in the crystal structure of **1g**.

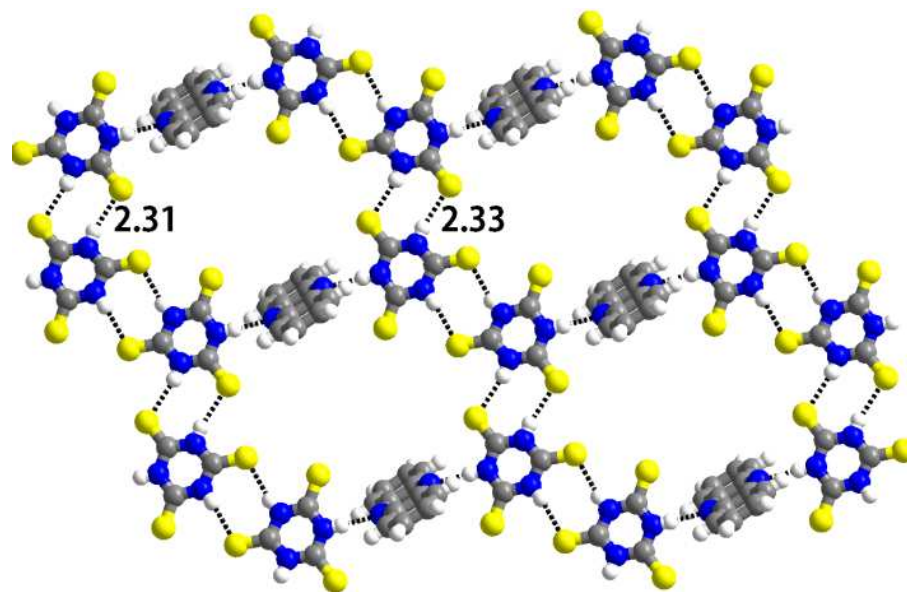
A 2:1 ratio of TCA and phenazine is found in the asymmetric unit, as shown in Figure 3.36, in the form of ORTEP, as revealed by structure determination by single crystal X-ray diffraction method. As noted in the crystal structure of **1f**, two TCA molecules are connected to each aza-donor, **phenz**, through N-H $\cdots$ N hydrogen bonds with H $\cdots$ N distances of 1.86 Å. The association is shown in Figure 3.37. In the structure of **1g** also, the aza-donor molecules are twisted by 62° from the mean plane of TCA, thus, precluding formation of any C-H $\cdots$ S hydrogen bonds along with N-H $\cdots$ N hydrogen bonds to yield dimeric or triple hydrogen bonding patterns that were observed in the other related structures, as described in the earlier sections.



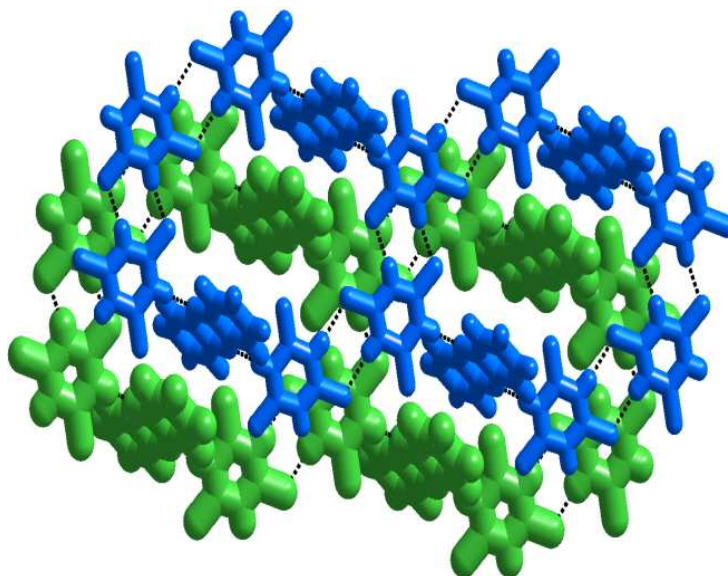
**Figure 3.37.** Molecular recognition observed between TCA and phenazine in **1g**.

Also, following the similar self-assembly process as noted in **1f**, the ensembles are aggregated through dimeric hydrogen bond patterns consisting of N-H $\cdots$ S hydrogen bonds, formed between TCA molecules, with H $\cdots$ S distances of 2.31 and 2.33 Å, leading to the formation of voids of  $11 \times 8 \text{ \AA}^2$  in each layer. Further, stacking of the layers along a crystallographic axis with skewing of adjacent layers such that the voids in a specific sheet are effectively filled by the electron density from the **phenz** molecules above and below sheets. The arrangement is shown in Figure 3.39.





**Figure 3.38.** Two dimensional cavity structure represents the TCA chains are connected by phenazine molecules.



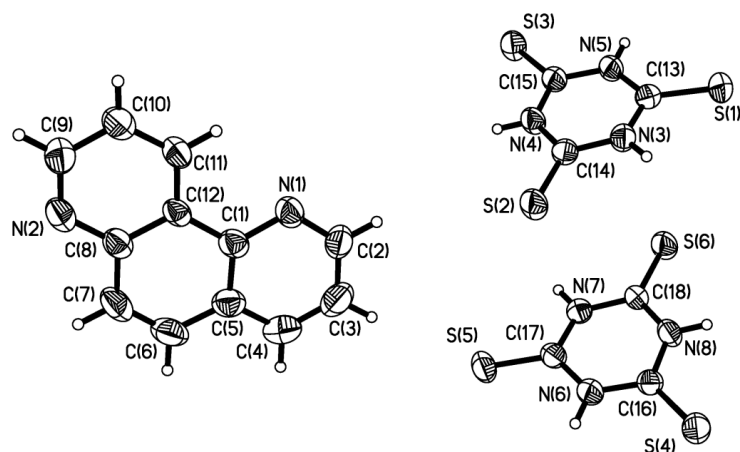
**Figure 3.39.** Three dimensional molecular arrangement of **1g**.

Thus, analysis of **1c**, **1f** and **1g** clearly establish that rigid molecules maintain formation of sheet structures with voids and subsequent stacking by skewing of layers rather than interpenetration. In further exploration to augment the

observations, co-crystallization of TCA with 1,7-phenanthroline was carried out. Interestingly, different types of co-crystals are found upon varying the solvent of crystallization. Apart from it, in both the assemblies sheets are realized and following the trend observed with other rigid ligands, no interpenetration was noted.

### 3.11 Structure of the molecular complex of trithiocyanuric acid with 1,7-phenanthroline, **1h**.

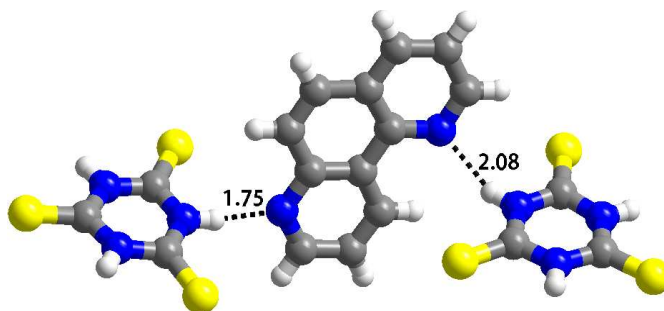
A molecular complex of TCA with 1,7-phenanthroline (**phen**) is prepared by crystallizing the components in DMSO/CH<sub>3</sub>OH. Crystals obtained by slow evaporation of the solution over a period of 36 h were analysed by single crystal X-ray diffraction analysis and it reveals formation of a 2:1 complex of TCA and **phen**. ORTEP of the contents of asymmetric unit is shown in Figure 3.40. Crystallographic data is given in Table 3.1.



**Figure 3.40.** Asymmetric unit of molecular complex, **1h**.

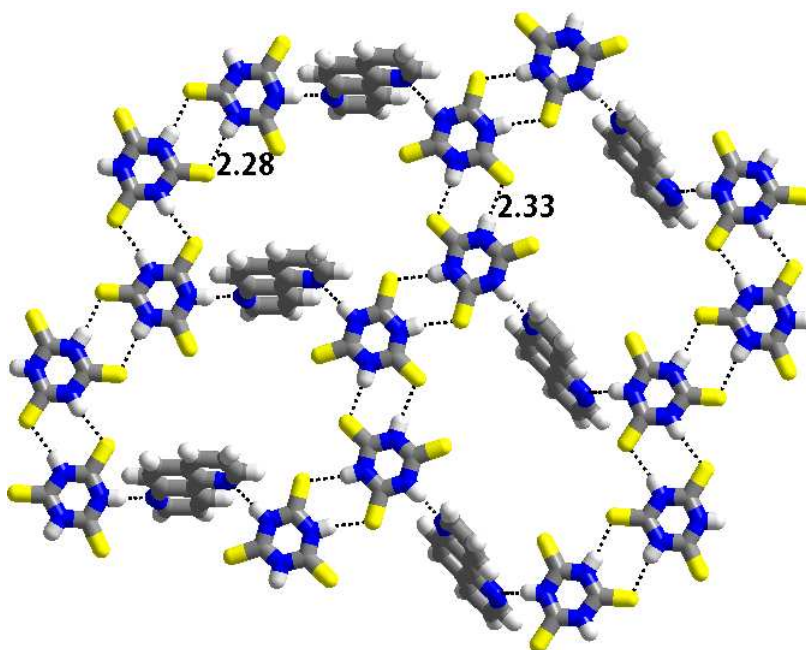
As no solvent of crystallization molecules are observed in the crystal lattice, the packing is expected to be following similar to other structures like **1c**, **1f** and **1g**

as discussed above. In fact, each **phen** molecules is connected to two TCA molecules by N-H $\cdots$ N hydrogen bonds with H $\cdots$ N distances of 1.75 and 2.08 Å (see Figure 3.41).



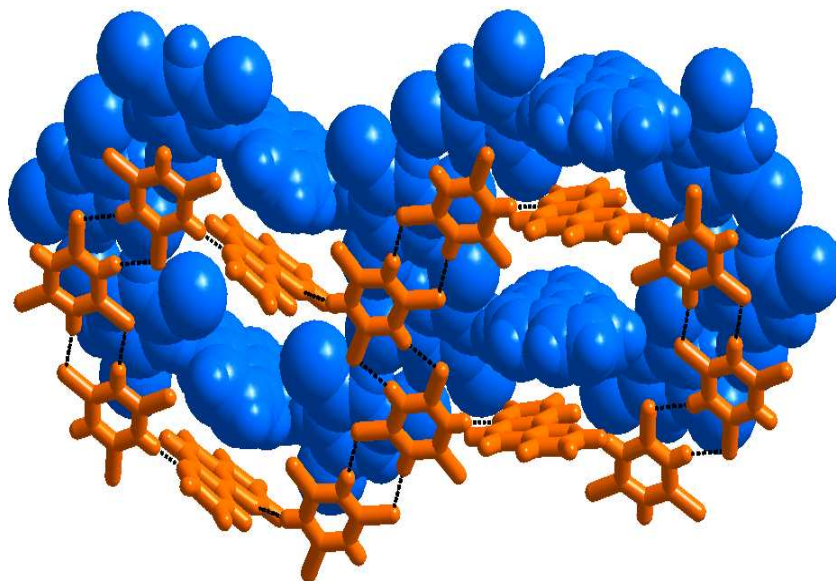
**Figure 3.41.** Molecular recognition between TCA and **phen** in **1h**.

Such ensembles are further self assembled such that each of four units are held together by N-H $\cdots$ S hydrogen bonds with H $\cdots$ S, 2.28 and 2.33 Å formed between TCA molecules. The arrangement lead to the formation of a sheet with voids of dimension  $12 \times 10 \text{ \AA}^2$ , as shown in Figure 3.42.



**Figure 3.42.** Cavities observed in a typical layer in molecular complex, **1h**.

Continuing the same feature noted in the other assemblies with rigid azadonor molecules, the sheets are stacked skewing with each other masking the voids in a sheet by the molecules from the top and bottom layers. The arrangement is shown in Figure 3.43.



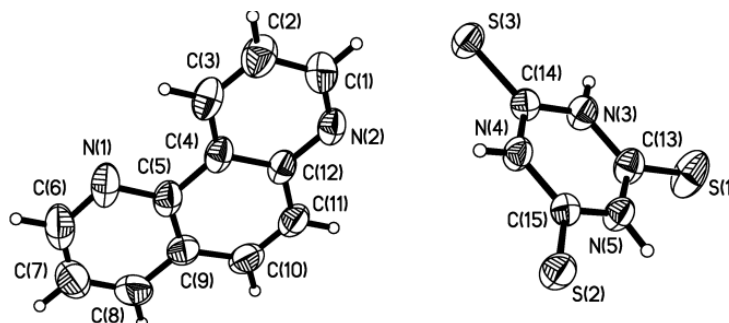
**Figure 3.43.** Self filled layers staking observed in complex, **1h**.

In the continued efforts to obtain varied assemblies by changing solvent of crystallization although such attempts were not successful in other examples except with **bpy** and **bpyea**, interestingly, **phen** gave a different assembly with TCA upon crystallization from DMSO alone.

### **3.12 Structure of the molecular complex of trithiocyanuric acid with 1,7-phenanthroline obtained from DMSO, 1h'.**

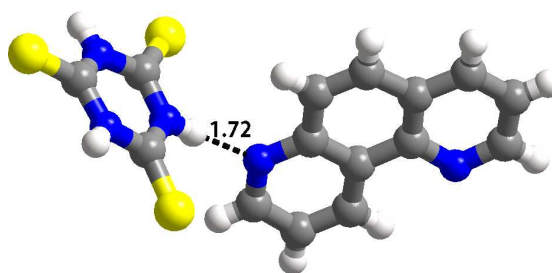
Analysis of the crystals by single crystal X-ray diffraction method reveals that a molecular complex in a 1:1 ratio of TCA and **phen** is formed, which is

different composition from that of **1h**, wherein the composition was 2:1. ORTEP of the contents is shown in Figure 3.44.



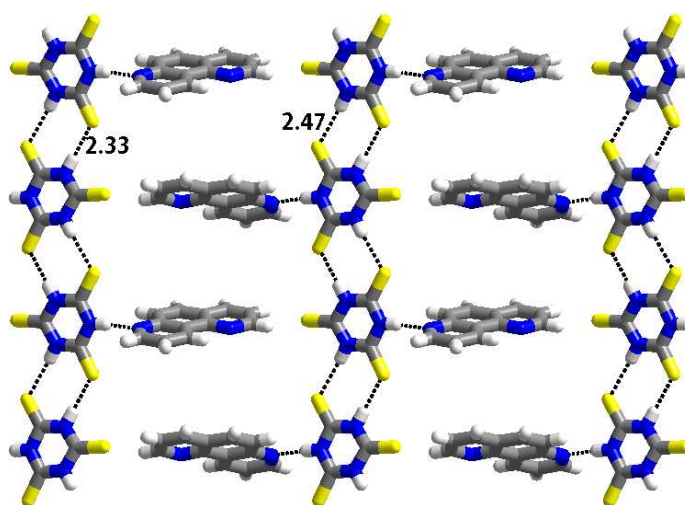
**Figure 3.44.** Representation of the asymmetric unit in a 1:1 ratio of TCA and **phen**.

At the same time, in contrast to the related structure wherein crystallization was carried out from DMSO (**1a**), DMSO molecules are not incorporated into the crystal lattice of **1h'**. Further the structural analysis shows that the aza-donor and TCA molecules are held together by a single N-H $\cdots$ N (H $\cdots$ N, 1.72) hydrogen bond, as shown in Figure 3.45.



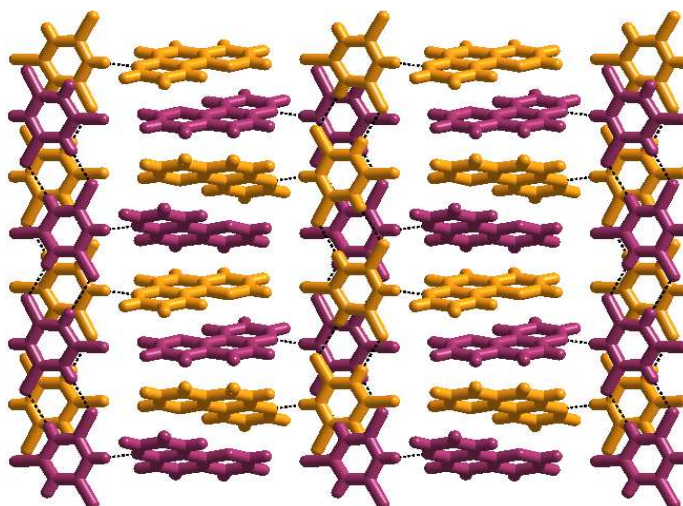
**Figure 3.45.** Molecular recognition between TCA and **phen** in **1h'**.

Such supermolecules are further held together by establishing dimeric N-H $\cdots$ S hydrogen bonds, with H $\cdots$ S distances of 2.33 and 2.47 Å, formed between TCA molecules constituting tapes of TCA molecules with **phen** molecules lie as pendants (see Figure 3.46).



**Figure 3.46.** Two dimensional arrangement of molecules of TCA and phen in **1h'**.

While within two dimensional arrangement, the tapes are arranged next to each other in an interdigitated manner, with the pendant **phen** moieties lie in between the tapes. Such network packs in the crystal structure, with the adjacent tapes along stacking direction sliding such that the **phen** moieties from the adjacent layers effectively fill in the void space in the latter layer. The arrangement is shown in Figure 3.47.

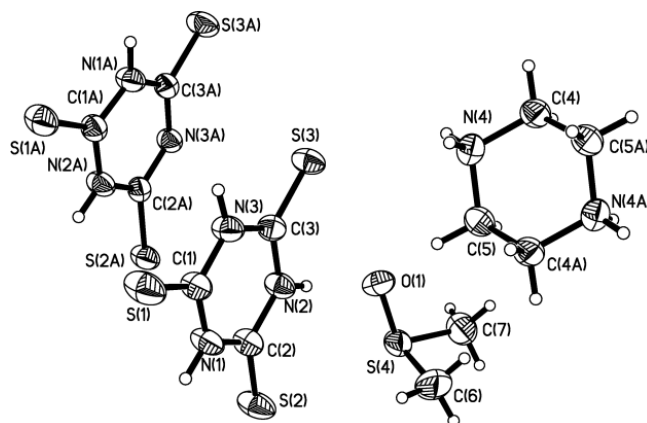


**Figure 3.47.** Representation of the stacked layer structure of **1h'**.

Taken into account the variable features observed with rigid and flexible aza-donors, to understand the nature of assembly that may be formed by TCA with aza compounds in which aza-group acts as hydrogen bond donor, co-crystallization of TCA with piperazine has been carried out.

### 3.13 Structure of adduct of trithiocyanuric acid with piperazine, **1i**.

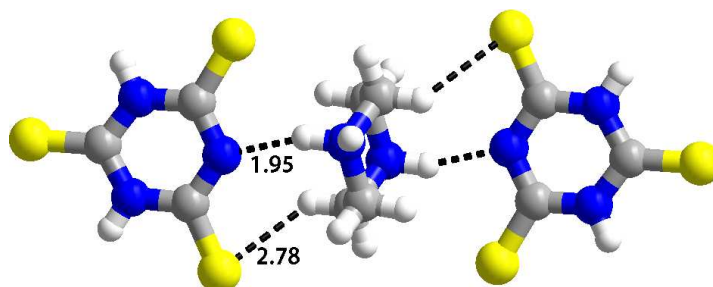
Co-crystallization of TCA and piperazine (**pip**) from a DMSO solution gave single crystals of good quality, suitable for structure determination by X-ray diffraction methods. The analysis reveals that the asymmetric unit in **1i**, is as shown in Figure 3.38, in the form of ORTEP, TCA and **pip** crystallize along with molecules of DMSO. Further, in the crystals of **1i**, the protons from both TCA molecules transferred to piperazine, perhaps due to the large  $\Delta pK_a$  between the constituents.



**Figure 3.48.** Asymmetric unit of the molecular complex, **1i**.

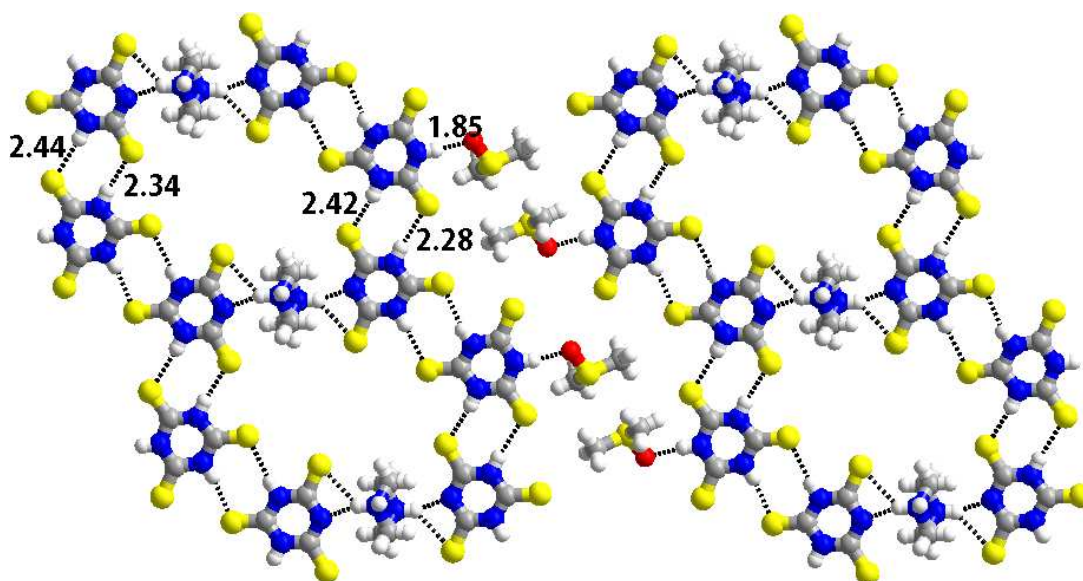
Since, **1i** has a closely related asymmetric unit as that of **1a**, the packing is also expected to be similar and indeed it was the case as discussed below. Each piperazine molecule is glued to the TCA molecules through  $N^+ \cdots H \cdots N^-$  and  $C-H \cdots S$

hydrogen bonds with the corresponding  $\text{H}\cdots\text{N}^-$  and  $\text{H}\cdots\text{S}$  distances being 1.95 and 1.78 Å. The association is shown in Figure 3.49.



**Figure 3.49.** Molecular recognition between TCA and piperazine molecules in **1i**, through a pairwise  $\text{N}^+-\text{H}\cdots\text{N}^-/\text{C}-\text{H}\cdots\text{S}$  hydrogen bonds.

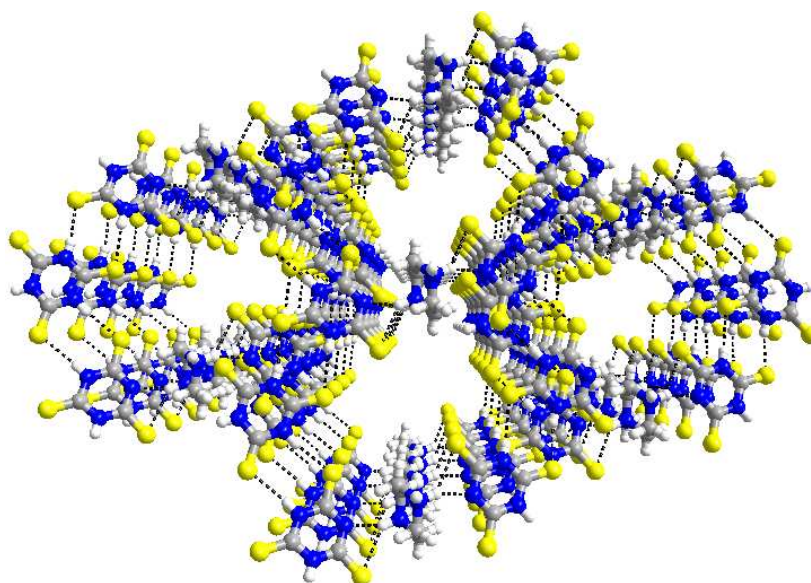
Further such tri-molecular units are held together by TCA molecules, to which DMSO molecules are already glued as pendants through  $\text{N}-\text{H}\cdots\text{O}$  ( $\text{H}\cdots\text{O}$ , 1.85 Å), through dimeric hydrogen bonding patterns comprising of  $\text{N}-\text{H}\cdots\text{S}$  hydrogen bonds.



**Figure 3.50.** Two dimensional molecular arrangement observed in **1i** where the DMSO molecules connected to the one dimensional cavity structure as a pendant.



Such association as found in **1a**, gave one dimensional hexagons with voids of dimension  $9 \times 6 \text{ \AA}^2$ , as shown in Figure 3.50, which, are in turn, packed in the crystal lattice by stacking such that voids being aligned along a crystallographic axis so that channels are realized and are filled by DMSO molecules (see Figure 3.51).



**Figure 3.51.** Channel structure obtained for **1i**.

### 3.14. Conclusions

1. Co-crystals of TCA with topologically varied aza-donors are prepared and characterized by X-ray diffraction methods.
2. The Structural analysis reveals different types of hydrogen bonding patterns from single to triple hydrogen bonds between TCA and aza donors observed.
3. All the molecular adducts shows cavity structures, at least in two dimension except **1b'** and **1h'**.

4. While aza-donors with flexible conformation yielded interpenetrated structures as observed in **1d** and **1e**, rigid aza-donor yields skewed stacked layer structures
5. Based on solvent polarity different molecular adducts are realized with different solvents for the molecular adducts of TCA with **bpy**, **bpyea** and **phen**.

### 3.15 Experimental Section

#### 3.15.1 Synthesis of Co-crystals of 1a-1i

All chemicals used in this study were obtained from Sigma Aldrich and used as such without any further purification. The solvents employed for the co-crystallization purpose were of spectroscopy grade of highest available purity. Co-crystals, **1b**, **1d**, **1e**, **1f** and **1g** are prepared by slow evaporation of the methanol solution of trithiocyanuric acid (TCA) with respective aza-donors in a 1:1 ratio. While co-crystals **1a**, **1c** and **1h** are prepared by the slow evaporation of the DMSO/MeOH solution, of TCA with respective aza-donors in a 1:1 ratio, **1a'**, **1h'** and **1i** are prepared from DMSO alone. Co-crystal, **1b'** is prepared under solvothermal condition at 120°C, methanol as a solvent in 1:1 of ratio reactants of TCA and **bpyea**.

#### 3.15.2 X-ray Structure Determination

Good quality single crystals of **1a-1i** were carefully selected using Leica microscope and glued to a glass fibre using an adhesive (cyanoacrylate). In all the cases, the crystals were smeared in the adhesive solution to prevent decomposition of crystals. The intensity data were collected on a Bruker single-crystal X-ray

diffractometer, equipped with an APEX detector. Subsequently, the data were processed using the Bruker suite of programs (SAINT), and the convergence was found to be satisfactory with good  $R_{\text{ini}}$  parameters. The details of the data collection and crystallographic information are given in Table 3.1. Absorption corrections were applied using SADABS package. The structure determination by direct methods and refinements by least-squares methods on  $F^2$  were performed using the SHELXTL-PLUS package. The processes were smooth without any complications. All non-hydrogen atoms were refined anisotropically, while hydrogen atoms are treated isotropically. All the intermolecular interactions were computed using PLATON. All packing diagrams are generated using Diamond software.

**Table 3.1.** Crystallographic information for the co-crystals **1a**, **1a'**, **1b**, **1b'**, **1c-1g**, **1h**, **1h'** and **1i**

	<b>1a</b>	<b>1a'</b>	<b>1b</b>	<b>1b'</b>	<b>1c</b>	<b>1d</b>
formula	2(C <sub>3</sub> H <sub>3</sub> N <sub>3</sub> S <sub>3</sub> ) :(C <sub>10</sub> H <sub>8</sub> N <sub>2</sub> ): (C <sub>2</sub> H <sub>6</sub> SO)	(C <sub>3</sub> H <sub>3</sub> N <sub>3</sub> S <sub>3</sub> ) :(C <sub>10</sub> H <sub>8</sub> N <sub>2</sub> )	2(C <sub>3</sub> H <sub>3</sub> N <sub>3</sub> S <sub>3</sub> ) :(C <sub>12</sub> H <sub>12</sub> N <sub>2</sub> )	(C <sub>3</sub> H <sub>3</sub> N <sub>3</sub> S <sub>3</sub> ): (C <sub>12</sub> H <sub>12</sub> N <sub>2</sub> )	2((C <sub>3</sub> H <sub>3</sub> N <sub>3</sub> S <sub>3</sub> ) :(C <sub>12</sub> H <sub>10</sub> N <sub>2</sub> ))	(C <sub>3</sub> H <sub>3</sub> N <sub>3</sub> S <sub>3</sub> ) :(C <sub>12</sub> H <sub>14</sub> N <sub>2</sub> )
<i>F</i> <sub>w</sub>	588.84	333.45	538.76	361.50	536.75	375.53
crystal shape	blocks	Needles	blocks	blocks	blocks	blocks
crystal color	yellow	Yellow	yellow	yellow	yellow	yellow
crystal system	Triclinic	Monoclinic	triclinic	monoclinic	monoclinic	triclinic
space group	<i>P</i> $\bar{1}$	<i>P</i> 2 <sub>1</sub> / <i>c</i>	<i>P</i> $\bar{1}$	<i>P</i> 2 <sub>1</sub> / <i>c</i>	<i>P</i> 2 <sub>1</sub> / <i>c</i>	<i>P</i> $\bar{1}$
<i>a</i> (Å)	7.311(1)	8.879(1)	7.084(1)	17.584(3)	8.948(2)	8.624(1)
<i>b</i> (Å)	12.674(1)	8.407(1)	10.356(1)	6.682(1)	12.236(3)	12.494(2)
<i>c</i> (Å)	13.968(1)	20.279(1)	11.362(1)	14.452(2)	11.631(2)	17.163(3)
$\alpha$ (deg)	92.78(1)	90	66.83(1)	90	90.00	80.52(1)
$\beta$ (deg)	91.73(1)	91.51(1)	85.04(1)	99.18(1)	116.10(1)	85.62(1)
$\gamma$ (deg)	91.83(1)	90	78.22(1)	90	90.00	78.42(1)
<i>V</i> (Å <sup>3</sup> )	1291.4(2)	1513.2(3)	750.1(1)	1676.3(4)	1143.6(4)	1785.1(5)
<i>Z</i>	2	4	1	4	2	4
<i>D</i> <sub>calc</sub> (g cm <sup>-3</sup> )	1.414	1.464	1.193	1.432	1.559	1.397
<i>T</i> (K)	298(2)	298(2)	298(2)	298(2)	298(2)	298(2)
<i>Mo</i> <sub>ka</sub>	0.71073	0.71073	0.71073	0.71073	0.71073	0.71073
$\mu$ (mm <sup>-1</sup> )	0.640	0.489	0.476	0.448	0.624	0.423
2 $\theta$ range (deg)	57.42	61.0	61.06	50.54	50.50	50.56
<i>F</i> (000)	608	688	278	752	552	784
total reflns	23360	15190	4562	11806	7115	13145
no. unique reflns [ <i>R</i> (int)]	(5124) 0.0274	(3167) 0.0274	3606(0.0812)	2484 (0.0716)	1496 (0.0616)	5115 (0.0434)
no. reflns used	6600	4582	16375	3032	2071	6429
no. Parameters	317	190	145	208	145	433
<i>GOF</i> on <i>F</i> <sup>2</sup>	1.048	1.031	2.208	1.264	1.043	1.037
<i>R</i> 1[ <i>I</i> >2 $\sigma$ ( <i>I</i> )]	0.0369	0.0421	0.0812	0.0716	0.0616	0.0434
<i>wR</i> 2	0.1179	0.1193	0.2919	0.1361	0.1177	0.1179

**Table 3.1.** Crystallographic information for the co-crystals **1a**, **1a'**, **1b**, **1b'**, **1c-1g**, **1h**, **1h'** and **1i**

	<b>1e</b>	<b>1f</b>	<b>1g</b>	<b>1h</b>	<b>1h'</b>	<b>1i</b>
formula	(C <sub>3</sub> H <sub>3</sub> N <sub>3</sub> S <sub>3</sub> ) :(C <sub>10</sub> H <sub>8</sub> N <sub>2</sub> S)	2(C <sub>3</sub> H <sub>3</sub> N <sub>3</sub> S <sub>3</sub> ) :(C <sub>12</sub> H <sub>10</sub> N <sub>2</sub> )	2(C <sub>3</sub> H <sub>3</sub> N <sub>3</sub> S <sub>3</sub> ) :(C <sub>12</sub> H <sub>8</sub> N <sub>2</sub> )	2(C <sub>3</sub> H <sub>3</sub> N <sub>3</sub> S <sub>3</sub> ) :(C <sub>12</sub> H <sub>8</sub> N <sub>2</sub> )	(C <sub>3</sub> H <sub>3</sub> N <sub>3</sub> S <sub>3</sub> ): (C <sub>12</sub> H <sub>8</sub> N <sub>2</sub> )	2(C <sub>3</sub> H <sub>3</sub> N <sub>3</sub> S <sub>3</sub> ): (C <sub>4</sub> H <sub>12</sub> N <sub>2</sub> ): 2(C <sub>2</sub> H <sub>6</sub> SO)
<i>F</i> <sub>w</sub>	365.51	536.75	534.79	534.73	357.47	951.45
crystal shape	blocks	blocks	Blocks	Needles	blocks	Blocks
crystal color	yellow	yellow	Yellow	Yellow	yellow	Yellow
crystal system	triclinic	triclinic	Triclinic	Monoclinic	monoclinic	Triclinic
space group	<i>P</i> $\bar{1}$	<i>P</i> $\bar{1}$	<i>P</i> $\bar{1}$	<i>P</i> 21	<i>P</i> 2 <sub>1</sub> / <i>c</i>	<i>P</i> $\bar{1}$
<i>a</i> (Å)	9.689(2)	4.426(1)	6.506(2)	4.369(1)	15.610(1)	7.385(1)
<i>b</i> (Å)	13.001(2)	10.978(2)	6.753(2)	29.078(6)	13.199(1)	11.474(2)
<i>c</i> (Å)	14.545(3)	12.259(2)	13.888(4)	9.186(2)	7.945(1)	13.353(2)
$\alpha$ (deg)	109.55(1)	101.22(1)	81.82(1)	90.00	90	111.54(1)
$\beta$ (deg)	105.73(1)	95.34(1)	81.43(1)	102.27(1)	102.78(1)	97.50(1)
$\gamma$ (deg)	95.32(1)	95.89(1)	63.92(1)	90.00	90	102.16(1)
<i>V</i> (Å <sup>3</sup> )	1627.6(5)	577.3(2)	539.9(3)	1140.3(4)	1596.4(3)	1001.6(3)
<i>Z</i>	4	1	1	2	4	1
<i>D</i> <sub>calc</sub> (g cm <sup>-3</sup> )	1.492	1.544	1.645	1.557	1.487	1.5777
<i>T</i> (K)	298(2)	298(2)	298(2)	298(2)	298(2)	298(2)
Mo $\kappa\alpha$	0.71073	0.71073	0.71073	0.71073	0.71073	0.71073
$\mu$ (mm <sup>-1</sup> )	0.586	0.618	0.660	0.625	0.469	0.803
2 $\theta$ range (deg)	50.56	50.52	50.58	50.50	54.96	50.54
<i>F</i> (000)	752	276	274	548	736	492
total reflns	5891	5598	4594	5858	14022	3612
no. unique reflns [ <i>R</i> (int)]	5211(0.0666)	1913 (0.0392)	1918 (0.0351)	3956 (0.0395)	(2880) 0.0252	3113 (0.0338)
no. reflns used	15781	2096	1949	4023	3651	9646
no. Parameters	418	145	146	289	208	234
<i>GOF</i> on <i>F</i> <sup>2</sup>	1.218	1.051	1.132	1.162	1.018	1.048
<i>R</i> 1[ <i>I</i> >2 $\sigma$ ( <i>I</i> )]	0.0666	0.0392	0.0351	0.0395	0.0354	0.0338
<i>wR</i> 2	0.1458	0.1049	0.0916	0.0997	0.0939	0.0877

**Table 3.2.** Characterization of hydrogen bond distances (Å) and angles (°) observed in the structures **1a**, **1a'**, **1b**, **1b'**, **1c-1g**, **1h**, **1h'** and **1i** <sup>§</sup>

H-bond	1a	1a'	1b	1b'	1c	1d
C-H...S	2.80 3.63 128	2.82 3.65 135	2.80 3.63 133	2.70 3.75 165	2.79 3.63 136	2.90 3.75 161
	2.81 3.57 129	2.83 3.65 134	2.82 3.63 135	2.67 3.55 137	2.88 3.66 131	2.94 3.75 135
	2.97 3.73 130	2.85 3.64 132		2.81 3.67 138		2.96 3.71 127
	3.00 3.74 128	2.97 3.73 130		2.97 3.71 128		2.88 3.62 128
						2.82 3.75 161
N-H...S	2.45 3.43 165	2.63 3.31 125				
	2.40 3.32 152		2.32 3.32 170		2.53 3.38 144	2.36 3.34 167
	2.37 3.34 161		2.30 3.30 172		2.41 3.38 164	
N-H...N						1.70 2.71 176
	1.88 2.79 149					1.82 2.83 175
			1.76 2.76 179		1.77 2.78 179	1.86 2.76 150
						1.79 2.79 176

§ In each row the three numbers for every structure represent H...A and D...A distances and <D-H...A

Contd....

**Table 3.2.** Characterization of hydrogen bond distances (Å) and angles (°) §

H-bond	1e	1f	1g	1h	1h'	1i
C-H...S	2.89 3.62 127	2.66 3.70 159	2.73 3.70 150	2.78 3.53 126		2.78 3.50 124
	2.98 3.73 129	2.73 3.69 147	2.72 3.50 129	2.62 3.59 148		2.70 3.58 139
	2.90 3.71 133					
	2.69 3.53 136					
N-H...S			2.33 3.33 170		2.33 3.30 160	2.42 3.41 168
	2.36 3.36 170	2.32 3.31 171	2.31 3.30 167	2.33 3.34 173	2.47 3.48 175	2.44 3.44 171
		2.40 3.38 164		2.28 3.27 171		2.34 3.31 162
						2.73 3.49 132
N-H...N	1.86 2.86 168	1.98 2.83 140	1.86 2.86 169	1.75 2.75 170	1.72 2.72 169	
	1.78 2.77 169			2.08 2.98 148		
	1.83 2.83 174					
	1.81 2.82 175					
N <sup>+</sup> -H...O						2.03 2.89 142
						1.85 2.83 165
N <sup>+</sup> -H...N <sup>-</sup>						1.95 2.91 159

§ In each row the three numbers for every structure represent H...A and D...A distances and <D-H...A

### 3.16 References

- (1) (a) Braga, D.; Grepioni, F.; Orpen, A. G.; Division, N. A. T. O. S. A. *Crystal engineering: from molecules and crystals to materials*; Kluwer Academic Publishers, 1999. (b) Kole, G. K.; Tan, G. K.; Vittal, J. J. *Crystengcomm* **2011**, *13*, 3138. (c) Sekiya, R.; Kuroda, R. *Chem. Commun.* **2011**, *47*, 10097. (d) Wong, M. S.; Pan, F.; Gramlich, V.; Bosshard, C.; Gunter, P. *Adv. Mater.* **1997**, *9*, 554. (e) Ravindra, H. J.; Chandrashekar, K.; Harrison, W. T. A.; Dharmaprakash, S. M. *Appl. Phys. B-Lasers O.* **2009**, *94*, 503. (f) Burgi, H. B.; Hulliger, J.; Langley, P. J. *Curr. Opin. Solid St. M.* **1998**, *3*, 425. (g) Horiuchi, S.; Hasegawa, T.; Tokura, Y. *J. Phys. Soc. Jpn.* **2006**, *75*. (h) Panthofer, M.; Jansen, M. *Chemphyschem* **2002**, *3*, 507. (i) Kwon, S. J.; Kwon, O. P.; Jazbinsek, M.; Gramlich, V.; Gunter, P. *Chem. Commun.* **2006**, 3729. (j) Friscic, T.; Jones, W. *Faraday Discuss.* **2007**, *136*, 167.
- (2) (a) Vishweshwar, P.; McMahon, J. A.; Bis, J. A.; Zaworotko, M. J. *J. Pharm. Sci.* **2006**, *95*, 499. (b) Shan, N.; Zaworotko, M. J. *Drug Discov. Today* **2008**, *13*, 440. (c) Aakeroy, C. B.; Forbes, S.; Desper, J. *J. Am. Chem. Soc.* **2009**, *131*, 17048. (d) Yadav, A. V.; Shete, A. S.; Dabke, A. P.; Kulkarni, P. V.; Sakhare, S. S. *Indian J. Pharm. Sci.* **2009**, *71*, 359. (e) Schultheiss, N.; Newman, A. *Cryst. Growth Des.* **2009**, *9*, 2950. (f) Qiao, N.; Li, M. Z.; Schlindwein, W.; Malek, N.; Davies, A.; Trappitt, G. *Int. J. Pharm.* **2011**, *419*, 1. (g) Chen, J. M.; Wu, C. B.; Lu, T. B. *Chem. J. Chinese U.* **2011**, *32*, 1996.
- (3) (a) Braga, D.; Grepioni, F. *Making Crystals by Design: Methods, Techniques and Applications*; John Wiley & Sons, 2007. (b) Mingos, D. M. P.



- Supramolecular Assembly Via Hydrogen Bonds*; Springer, 2004. (c) Cavallo, G.; Biella, S.; Lu, J. A.; Metrangolo, P.; Pilati, T.; Resnati, G.; Terraneo, G. *J. Fluorine Chem.* **2010**, *131*, 1165.
- (4) (a) Gilli, G.; Gilli, P. *The Nature of the Hydrogen Bond: Outline of a Comprehensive Hydrogen Bond Theory*; Oxford University Press, 2009. (b) Jeffrey, G. A. *An Introduction to Hydrogen Bonding*; Oxford University Press, 1997. (c) Desiraju, G. R.; Steiner, T. *The Weak Hydrogen Bond: In Structural Chemistry and Biology*; Oxford University Press, 2001.
- (5) (a) Varughese, S.; Pedireddi, V. R. *Chem. Eur. J.* **2006**, *12*, 1597. (b) Arora, K. K.; Pedireddi, V. R. *J. Org. Chem.* **2003**, *68*, 9177. (c) Bhogala, B. R.; Nangia, A. *New J. Chem.* **2008**, *32*, 800. (d) Men, Y. B.; Sun, J. L.; Huang, Z. T.; Zheng, Q. Y. *Crystengcomm* **2009**, *11*, 2277. (e) Varughese, S.; Pedireddi, V. R. *Tetrahedron Lett.* **2005**, *46*, 2411. (f) Shattock, T. R.; Arora, K. K.; Vishweshwar, P.; Zaworotko, M. J. *Cryst. Growth Des.* **2008**, *8*, 4533.
- (6) (a) Bhogala, B. R.; Basavoju, S.; Nangia, A. *Crystengcomm* **2005**, *7*, 551. (b) Kapadia, P. P.; Ditzler, L. R.; Baltrusaitis, J.; Swenson, D. C.; Tivanski, A. V.; Pigge, F. C. *J. Am. Chem. Soc.* **2011**, *133*, 8490. (c) Shattock, T. R.; Vishweshwar, P.; Wang, Z. Q.; Zaworotko, M. J. *Cryst. Growth Des.* **2005**, *5*, 2046. (d) Ebenezer, S.; Muthiah, P. T. *J. Mol. Struct.* **2011**, *990*, 281. (e) Bowes, K. F.; Ferguson, G.; Lough, A. J.; Glidewell, C. *Acta Crystallogr., Sec. B: Strut. Sci.* **2003**, *59*, 100. (f) Paz, F. A. A.; Klinowski, J. *Crystengcomm* **2003**, *5*, 238. (g) Bhunia, M. K.; Das, S. K.; Bhaumik, A. *Chem. Phys. Lett.* **2010**, *498*, 145. (h) Shan, N.; Jones, W. *Tetrahedron Lett.* **2003**, *44*, 3687. (i) Papaefstathiou, G. S.; Kipp, A. J.; MacGillivray, L. R.

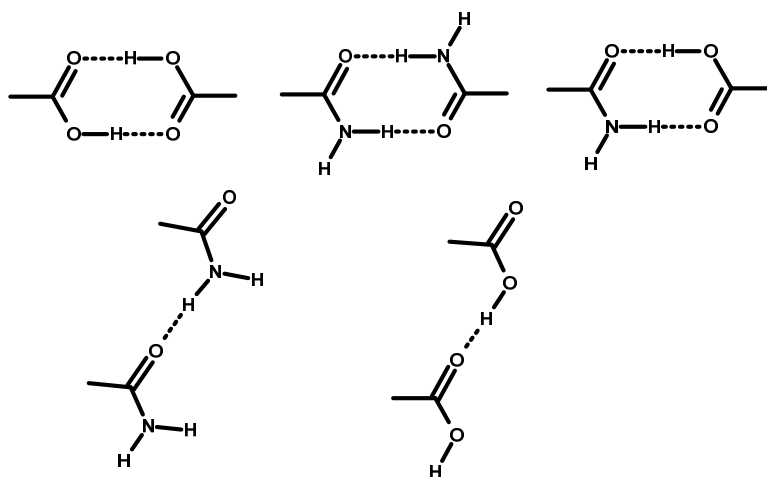
- Chem. Commun.* **2001**, 2462. (j) Yang, Y. X.; Li, Q. *J. Chem. Crystallogr.* **2011**, *41*, 929. (k) Shan, N.; Bond, A. D.; Jones, W. *Cryst. Eng.* **2002**, *5*, 9.
- (7) Men, Y. B.; Sun, J.; Huang, Z. T.; Zheng, Q. Y. *Angew. Chem. Int. Ed.* **2009**, *48*, 2873.
- (8) (a) Ranganathan, A.; Pedireddi, V. R.; Chatterjee, S.; Rao, C. N. R. *J. Mater. Chem.* **1999**, *9*, 2407. (b) Pedireddi, V. R.; Chatterjee, S.; Ranganathan, A.; Rao, C. N. R. *J. Am. Chem. Soc.* **1997**, *119*, 10867.

## CHAPTER FOUR

### Rational Analysis of Supramolecular Assemblies of Cyanuric acid

## 4.1 Introduction

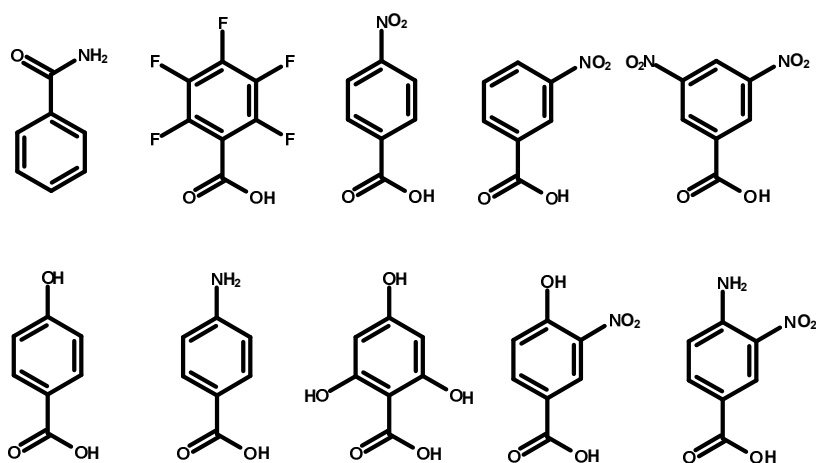
Molecular recognition between acceptors and donors is the fundamental step in the design and synthesis of multi-components mediated crystals, often referred as co-crystals. Identification of potential functional groups with such properties, is thus, utmost crucial as nature of the ultimate structural assembly depends upon the ability to yield the designed intermolecular interactions<sup>1</sup> as well as the position of the functional groups. Since the intermolecular interactions formed by functional groups are generally in the form of distinct patterns,<sup>2</sup> as discussed in Chapter 1 and also as highlighted in Figure 4.1, tuning of intermolecular interactions by varying functional groups may yield the desired materials with tailor made properties. Among the known versatile functional groups, -COOH



**Figure 4.1.** Recognition patterns observed between acid-acid, amide-amide and acid-amide functionalities.

group is well utilized as it would form robust dimeric patterns comprising of strong O-H $\cdots$ O hydrogen bonds, by self recognition, as well as catemeric hydrogen bonding patterns as represented in Figure 4.1. In addition –COOH group also forms a variety of hydrogen bonded patterns with other complimentary functional groups such as aza donors, yielding *heteromeric* patterns.<sup>3</sup>

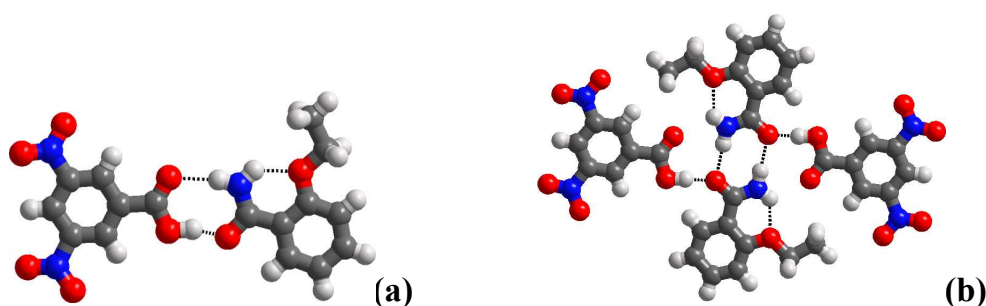
Apart from –COOH groups, the amide group which also mimics the dimeric and catemeric patterns of the carboxylic acid is another exotic functional moiety well utilized in supramolecular chemistry,<sup>4</sup> though not to the extent that –COOH group was explored. Interestingly, it is known from the literature that the amide group forms robust intermolecular interactions with –COOH group, in the form of *heteromeric* hydrogen bonding patterns than with any other functional groups. Some representative examples involving such molecular recognition between some carboxylic acid and primary amides are discussed below.



**Figure 4.2.** Structures of some derivatives of benzoic acid used in the co-crystallization experiments with benzamide.

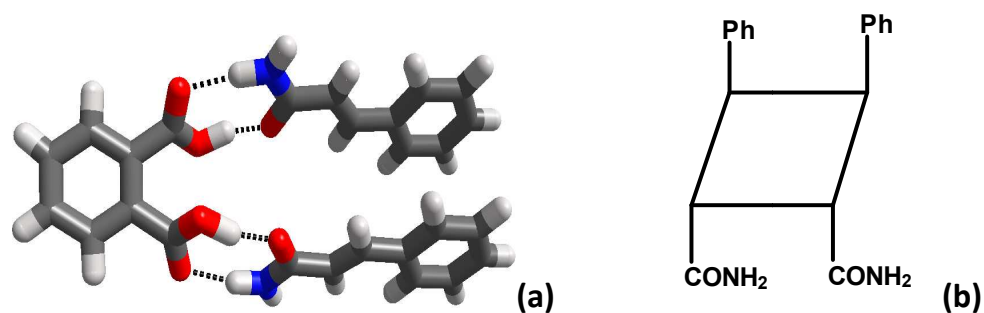
A simple primary amide, benzamide, forms co-crystals with various carboxylic acids, for example, with succinic acid as reported by Lieserowitz.<sup>5</sup> However, it fails to yield co-crystals with unsubstituted benzoic acid while a few examples are known with substituted benzoic acids<sup>4e</sup> possessing electron withdrawing groups, as shown in Figure 4.2. Further, the observations were supported by Hammett constant, based on energy calculations on acid-amide dimer and packing energy, done by Seaton and co-workers.

The molecular recognition between acid and amide is not only intriguing as observed in the above example, but also the possible *homomeric* and *heteromeric* patterns (acid-acid, acid-amide and amide-amide) in the co-crystals even may help to obtain new polymorphic materials, with different physical properties. For example, ethenzamide<sup>6</sup> (see Figure 4.3) is an anti-inflammatory drug, which is a benzamide derivative, that forms dimorphic co-crystals with 3,5-dinitrobenzoic acid. The stable form I possesses acid-amide interaction (Figure 4.3a), while the unstable form II possesses amide-amide interaction (Figure 4.3b).



**Figure 4.3.** Molecular interactions in the co-crystals of ethenzamide and 3,5-dinitrobenzoic acid a) acid-amide interaction observed in form I. b) amide-amide interaction in form II.

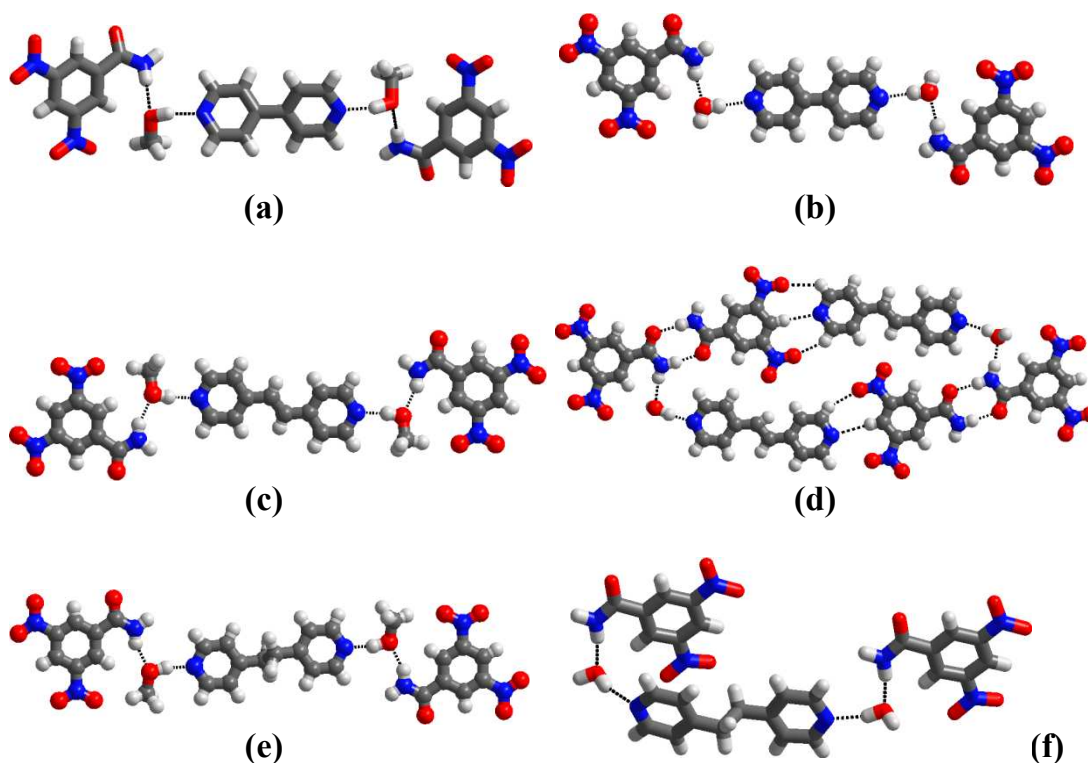
In addition, the acid-amide interaction is also utilized as a template to achieve [2+2] cycloaddition reactions as reported by Ito and co-workers. For example, cinnamide<sup>7</sup> forms co-crystals with phthalic acid and recognize each other, as shown in Figure 4.4a. However, confirmation of the adjacent cinnamide molecules is not in favour of [2+2] cycloaddition. Upon irradiation of the co-crystal, in spite of the unfavourable confirmation, it forms a cycloaddition product in a head to head fashion. The authors explained the formation of  $\beta$ -truxinamide product attributing to the paddle like conformational change observed in the cinnamide molecule in the excited state after irradiation. Such dynamic supramolecular exchange is confirmed through *in situ* single crystal X-ray diffraction experiment.<sup>8</sup>



**Figure 4.4.** a) Molecular recognition observed between phthalic acid and cinnamide. b) Structure of  $\beta$ -truxinamide.

Apart from the recognition of primary amides with acid molecules, molecular recognition studies of amide moiety with other functional groups are also not well known in the literature until recently the explorations done in our research group.<sup>3j,4i,9</sup> It was noted that amide/N-donor co-crystals show different recognition features as compared to co-crystals of acid/N-donor compounds. Thus,

upon co-crystallization of 3,5-dinitrobenzamide with *N*-donor compounds, in almost all the complexes the amide and *N*-donor functionality were glued together through solvent of crystallization, either water or methanol molecules, as shown in Figure 4.5, as the case may be, instead of establishing a direct interaction that can bind the amide and *N*-donor site.

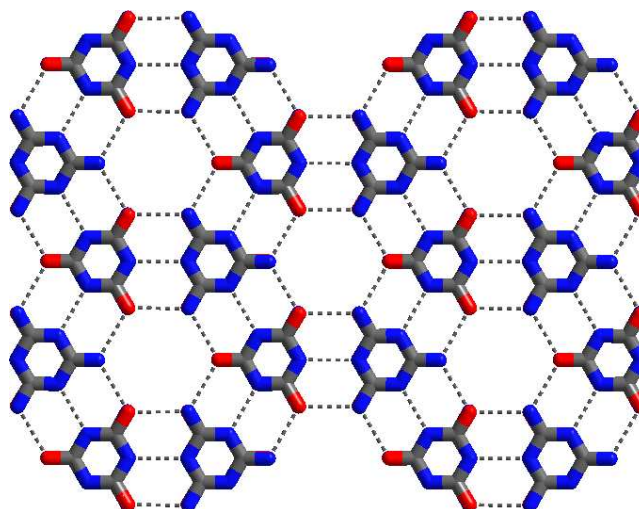


**Figure 4.5.** Molecular recognition observed between 3,5-dinitrobenzamide and different aza-donor compounds through water and methanol.

Similarly co-crystal studies for secondary amides are also limited, but imides are well studied as these moieties have appropriate hydrogen bond acceptor/donor functionalities for the formation of a variety of hydrogen bond patterns, for example triple hydrogen bonding. The best example till date for the robust molecular assembly through the triple hydrogen bond is the molecular

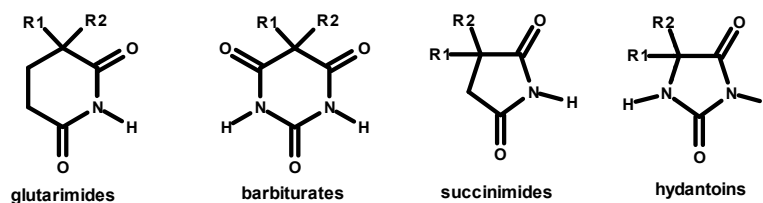


adduct of cyanuric acid-melamine,<sup>10</sup> which forms a rosette structure utilizing 18-hydrogen bonds, as shown in Figure 4.6.



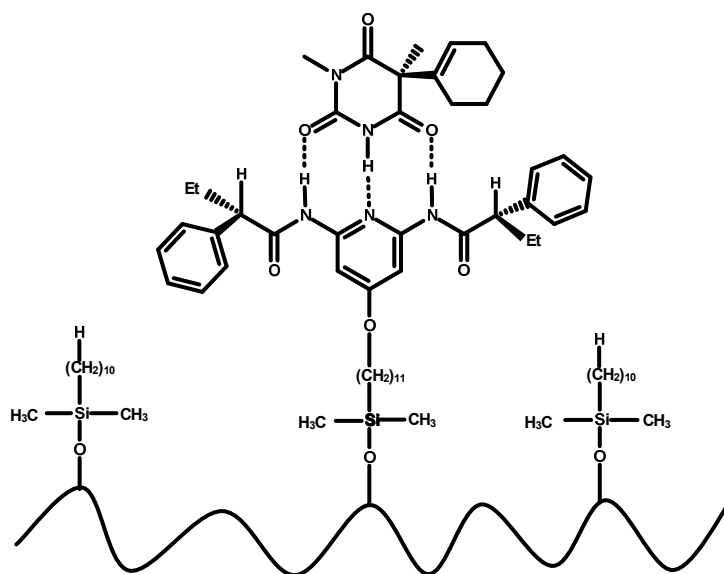
**Figure 4.6.** Rosette structure observed in cyanuric acid-melamine adduct.

Also, it is known from the literature that molecular recognition even been well utilized to achieve chiral separation. In this process, a class of compounds, barbiturates,



**Figure 4.7.** Structures of some drugs containing imide functionality.

succinimides, glutaramides, hydantoins, as shown in Figure 4.7, which are also known to be drugs, as well as consisting of imide moiety, have been resolved by molecular recognition process, especially utilizing the triple hydrogen bonding patterns similar to the topology noted in cyanuric acid-melamine adduct.

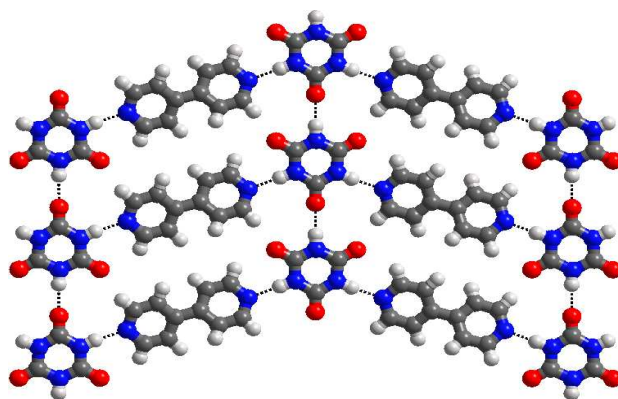


**Figure 4.8.** Structure of the complex formed between the barbiturates and the complimentary molecule which is attached to the stationary phase.

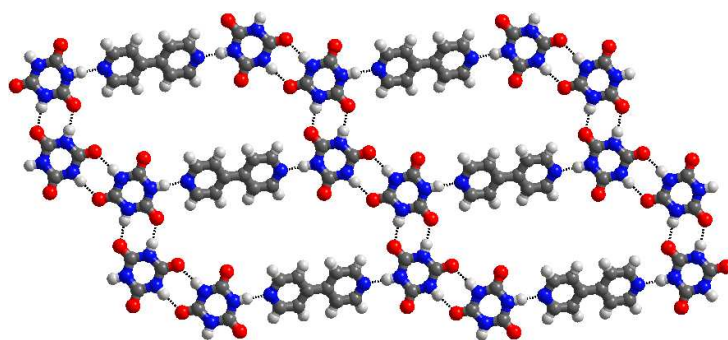
In a typical example, Feibush<sup>11</sup> and co-workers reported chiral separation of 1-(1-cyclohexen-1-yl)-1,5-dimethyl-2,4,6-(1*H*,3*H*,5*H*)pyrimidinetrione that possess imide group by mobilizing on to the solid phase system having *N,N'*-[4-(10-undecenyloxy)-2,6-pyridinediyl]bis(*S*)-2-phenylbutanamide] moiety, which could form desired hydrogen bonding pattern with the imides, as shown in Figure 4.8. In fact, to achieve better recognition between the complimentary moieties without much interference with the stationary phase moieties, the substituents are separated by long chain alkyl groups. This process is proven to be an excellent method for the imides shown in Figure 4.7, except for succinimides. Further, numerous reports from the research group of Whitesides<sup>12</sup> highlight the efficiency of triple hydrogen bonding patterns, for the synthesis of exotic and tailor-made supramolecular assemblies.

In imides, further studies of co-crystals with aza-donor compounds which form varied supramolecular assemblies are well documented in the literature.<sup>13</sup> In this series, cyanuric acid has been explored towards molecular recognition studies as it is symmetric molecule with both hydrogen bond donor and acceptor moieties present in alternative positions. To illustrate the significance and highlight the excellence of structural assemblies, co-crystals of cyanuric acid (CA) with 4,4'-bipyridine have been described below.

Co-crystallization of CA with 4,4'-bipyridine (**bpy**), gives two different types of assemblies upon crystallization from different solvents.<sup>13b</sup> Crystals obtained from water gives a sheet structure, as shown in Figure 4.9, with adjacent CA molecules being held together by single N-H $\cdots$ O hydrogen bonds, yielding chains, which are being connected by **bpy** molecules, establishing N-H $\cdots$ N hydrogen bonds. In the crystals obtained from methanol, the structure is very much similar to the one one obtained with water, except that the adjacent CA molecules do interact by cyclic N-H $\cdots$ O hydrogen bonding patterns, as shown in Figure 4.10.

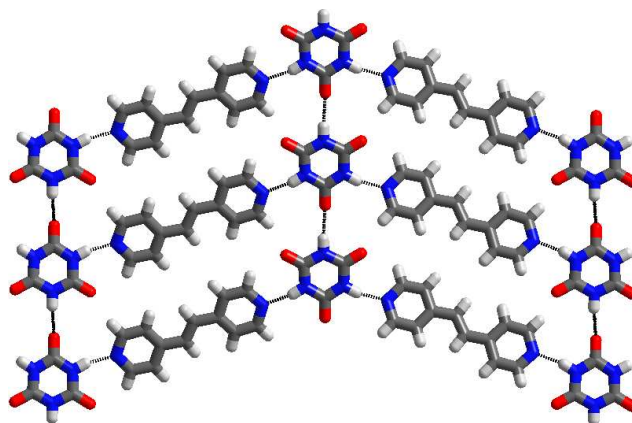


**Figure 4.9.** Sheet structure observed for the co-crystals of CA and **bpy**. CA forms tapes through single N-H $\cdots$ O hydrogen bonds.



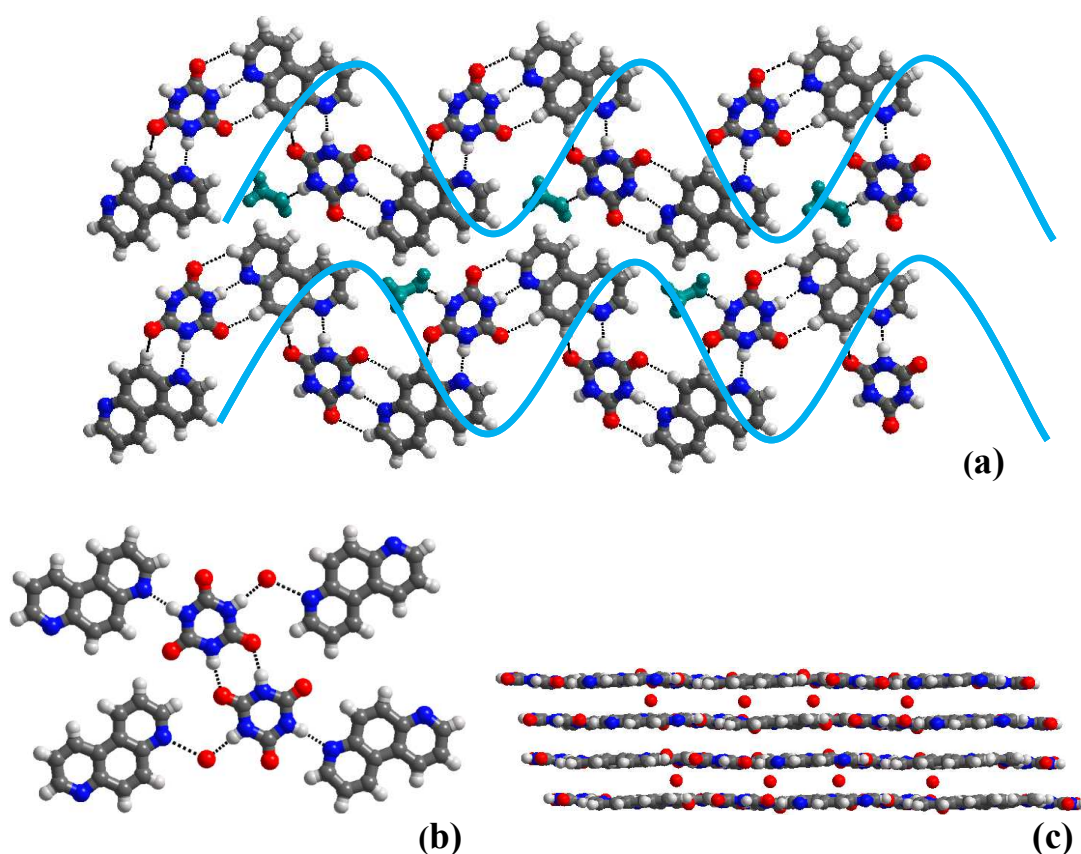
**Figure 4.10.** Sheet structure obtained for the co-crystal of CA and **bpy** with cavities in two dimension, the CA molecules forms tapes through dimeric N-H $\cdots$ O hydrogen bonds.

Similarly, co-crystals of CA with 1,2-*bis*-(4-pyridyl)ethane (**bpyee**), an homologous analogue of **bpy**, is reported by Neil Champness *et al.*, were obtained as dimorphic crystals with plates and needle morphology, by diffusion of **bpyee** in acetonitrile into the solution of CA in methanol. The structural analysis infers that, in both the cases, sheet structure only prevails, as shown in Figure 4.11. However, notable change observed is in the asymmetric unit of one of the forms has only one molecule while other contains two symmetry independent molecules of each CA and **bpyee**<sup>13g</sup>.



**Figure 4.11.** Sheet structure observed for both forms of CA and **bpyee** co-crystals.

Further, in the series of co-crystals of CA with aza-donor compounds which are structurally rigid, for instance 1,7-phenanthroline (**phen**), also found to be yielding two different structural arrangements upon crystallization from water or methanol.<sup>13a</sup> Interestingly, the differences are mainly due to the incorporation of the solvent of crystallization in their crystal lattices.



**Figure 4.12.** a) Ribbon structure obtained in the co-crystal of CA with **phen** from methanol. b) Molecular recognition in the co-crystal of CA and **phen** obtained from methanol. c) Water chain connects the layers of in the co-crystal of CA and **phen**.

Structural variations between the two assemblies are shown in Figure 4.12. While the crystals obtained from methanol has a ribbon structure, with methanol molecules being inserted between the ribbons within two dimensional network, in

the crystals obtained from water, solvent of crystallization is embedded between the panar sheets formed by CA and **phen** (see Figure 4.12 (b) and (c)).

An interesting point to note from the representative co-crystals of CA and aza-donor described above, that CA molecule form different types of interactions in different co-crystals, depending upon the aza molecules, in the form of chains or tapes of cyanuric acid. Such anomaly in the topological arrangement of CA molecules may be attributed to the topology of the aza-donor as well as the conditions of crystallization. However, as the number of examples in this series are limited, a study of large number of supramolecular assemblies of CA may be enunciated to draw more effective conclusions about variable features of hydrogen bonding patters formed by CA molecules and also in the process, to obtain exotic novel supramolecular assemblies. For this purpose, some organic ligands at least possessing one hydrogen bond donor or acceptor moiety, as listed in Chart 1, have been chosen for the preparation of supramolecular assemblies with CA molecules. The structural features of these co-crystals are described below.

### Chart 1

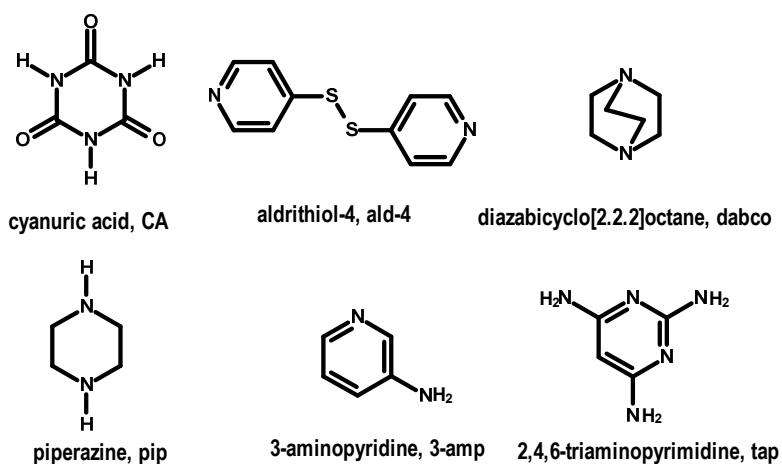


Chart 2

Reactants (ratio)	Solvent	Product (ratio)
CA + <b>ald-4</b> (1:1)	Methanol	<b>1a</b> (1:1)
CA + <b>dabco</b> (1:1)	Methanol	<b>1b</b> (2:1)
CA + <b>pip</b> (1:1)	Methanol	<b>1c</b> (2:1)
CA + <b>3-amp</b> (1:1)	Methanol	<b>1d</b> (2:1)
CA + <b>tap</b> (1:1)	Methanol	<b>1e</b> (1:1)

#### 4.2 Structural analysis of co-crystals of cyanuric acid and aldrithiol-4, **1a**.

Co-crystallization of CA with aldrithiol-4 (**ald-4**), which is a thio analogue of 1,2-*bis*(4-pyridyl)ethane, with the replacement of C-C bond by S-S, gave good quality single crystals in methanol. The crystals were analysed by single crystal X-ray diffraction method. The analysis reveals formation of a 1:1 complex of CA and **ald-4**, as shown in Figure 4.13. Pertinent crystallographic information is listed in Table 4.1.

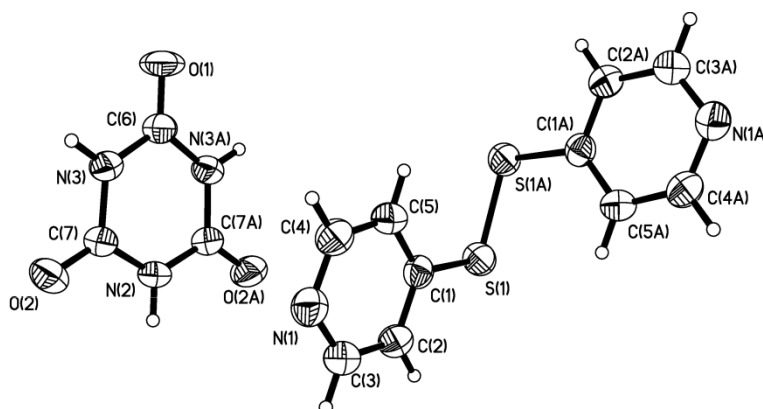
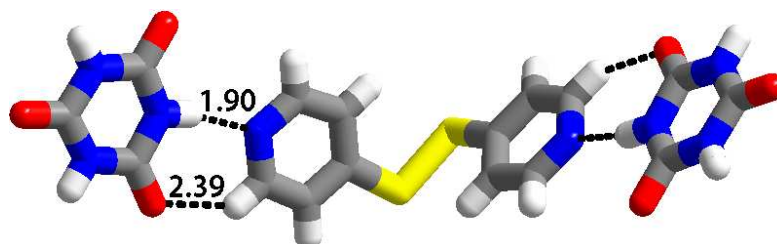


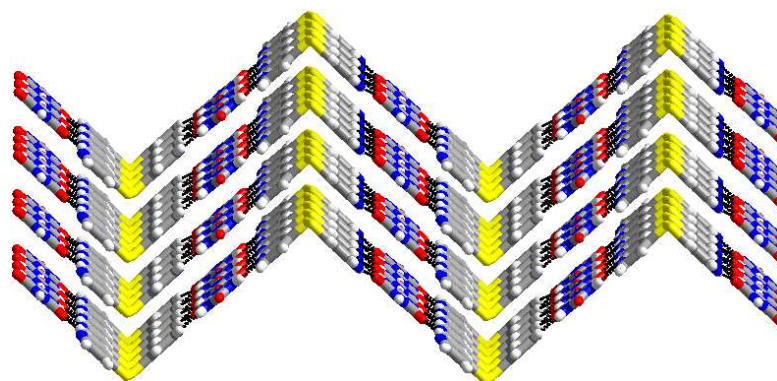
Figure 4.13. ORTEP of the molecular components of **1a**.

Further, the molecules of CA and **ald-4** were observed to be held together through N-H $\cdots$ N / C-H $\cdots$ O (H $\cdots$ N, 1.90 / H $\cdots$ O, 2.39 Å) pairwise hydrogen bonds as shown in Figure 4.14. Complete characteristics of hydrogen bonds are given in Table 4.2.



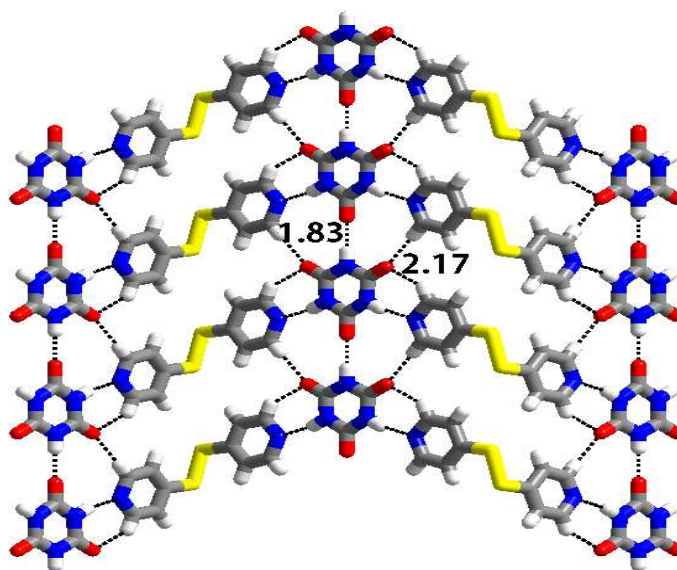
**Figure 4.14.** Molecular recognition between CA and **ald-4** in **1a**.

Such ensembles ultimately pack in the crystal lattice in the form of stacked sheets, as depicted in Figure 4.15. However, arrangement of molecules in a typical sheet, as shown in Figure 4.16, is quite intriguing. Further, the adjacent CA molecules in the sheets are held together by single N-H $\cdots$ O (H $\cdots$ O, 1.83 Å, Table 4.2) hydrogen bonds, thus, constituting chains. The chains are being separated by the molecules of **ald-4** in the same manner as observed in the reported assemblies of CA with other aza donors **bpy** and **bpyee**.



**Figure 4.15.** Three dimensional arrangement of molecular shows the stacked beta sheets.

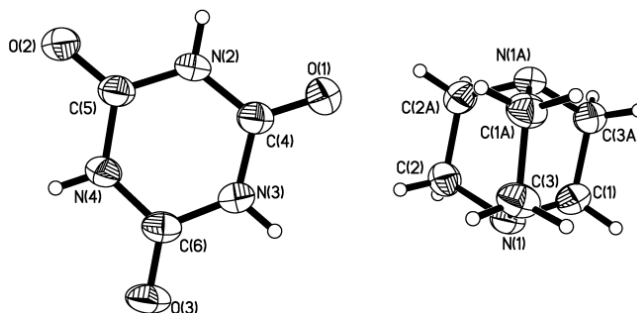




**Figure 4.16.** Two dimensional molecular arrangement observed in **1a**.

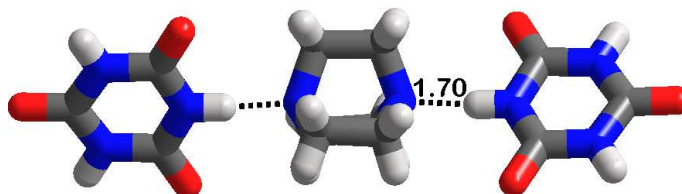
#### 4.3 Co-crystals of cyanuric acid with diazabicyclo[2.2.2]octane, **1b**.

In continuation, co-crystallization of CA and diazabicyclo[2.2.2]octane (**dabco**), an aliphatic bicyclic N-donor, possessing the topology of aromatic aza-donor, gave good quality single crystals from methanol. Analysis of crystals through single crystal X-ray diffraction method reveals a 2:1 molecular complex. The complex is labelled as **1b** for the ease of discussion. ORTEP of the contents of asymmetric unit observed in **1b** is shown in Figure 4.17. Details of crystal data and refinement parameters are given in Table 4.1.



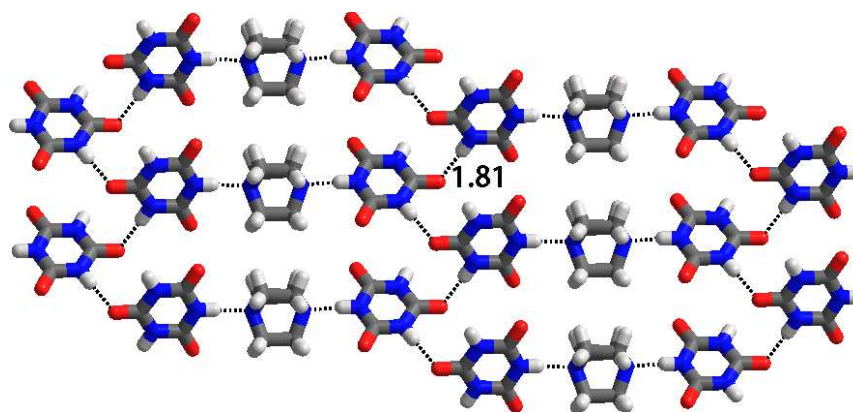
**Figure 4.17.** ORTEP of contents in the asymmetric unit of **1b**.

The molecular recognition between **dabco** and CA molecules is established through N-H $\cdots$ N (H $\cdots$ N, 1.70 Å) hydrogen bonds as observed in many other similar assemblies. The recognition pattern is shown in Figure 4.18.

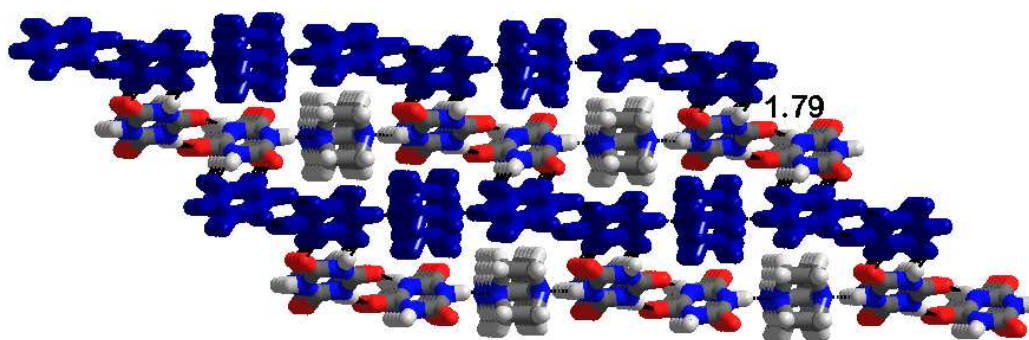


**Figure 4.18.** Molecular recognition between **dabco** and CA through an N-H $\cdots$ N hydrogen bond.

In the crystals of **1b** also, CA molecules form chains by joining the adjacent molecules through N-H $\cdots$ O (H $\cdots$ O, 1.81Å, Table 4.2) hydrogen bonds. The arrangement is shown in Figure 4.19. However, it is noteworthy to mention that the chains are not linear as observed in **1a** and also in the other similar assemblies. Between such corrugated chains, the **dabco** molecules are situated through the formation of N-H $\cdots$ N hydrogen bonds, as illustrated and highlighted in Figure 4.19. Such sheets are stacked in three dimensional arrangement, as shown in Figure 4.20



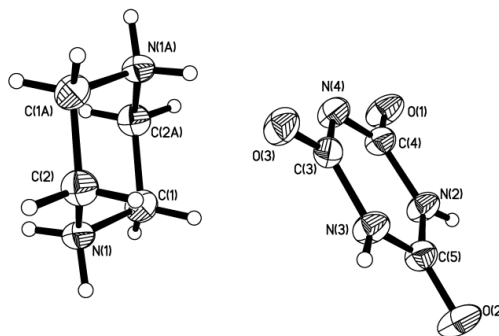
**Figure 4.19.** Sheet structure observed in **1b**, wherein the CA molecules form tapes through N-H $\cdots$ O catemeric hydrogen bonds.



**Figure 4.20.** Stacked layers in the structure of **1b**, with the layers being connected by dimeric N-H...O hydrogen bonds formed between the CA molecules.

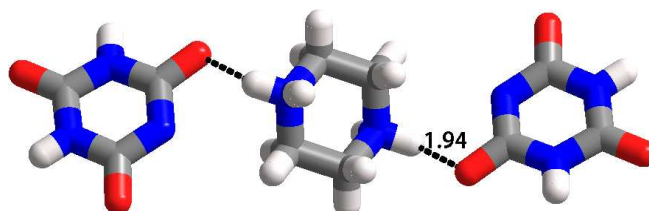
#### 4.4 Self assembly of molecules in co-crystals of cyanuric acid with piperazine, **1c**.

Cyanuric acid and piperazine (**pip**), which is topologically very much similar to **dabco**, were dissolved in methanol and allowed for crystallization by slow evaporation process. Good quality single crystals were obtained over a period of 24 h. The crystals were analysed by single crystal X-ray diffraction analysis. The analysis reveals the formation of a 2:1 molecular complex, as shown in Figure 4.21. Requisite crystallographic details are listed in Table 4.1. It is evident from Figure 4.21 that proton transfer from CA to **pip** is observed, perhaps due to the high  $\Delta pK_a$  (2.9), between CA and **pip**.

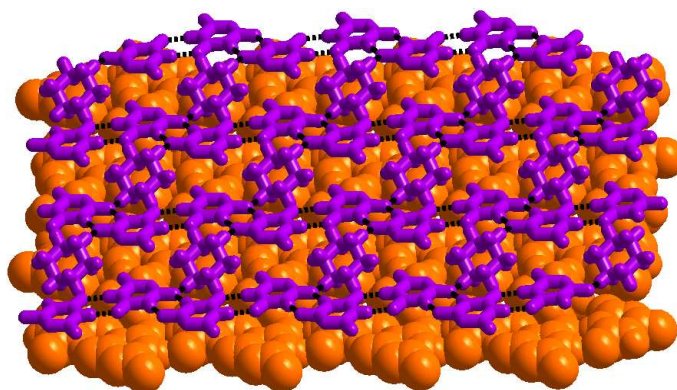


**Figure 4.21.** ORTEP drawing representing the molecular components of **1c**.

As a consequence of it, recognition between piperazine and CA occurred through  $N^+ \cdots H \cdots O$  ( $H \cdots O$ , 1.94 Å, Table 4.2) hydrogen bonds. The recognition pattern is shown in Figure 4.22.

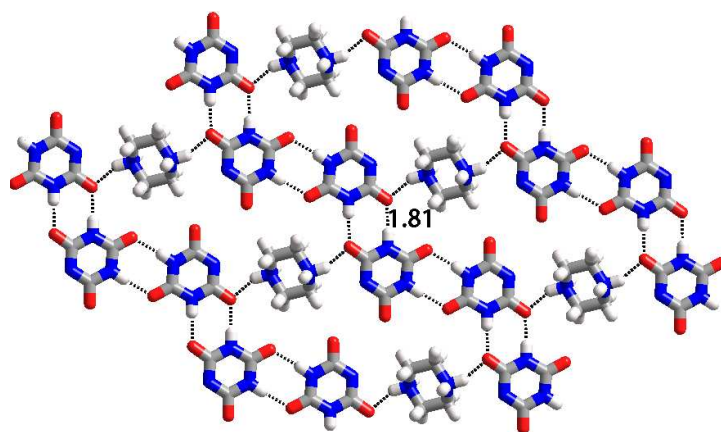


**Figure 4.22.** Molecular recognition between CA and piperazine through  $N^+ \cdots H \cdots O$  hydrogen bond.



**Figure 4.23.** Packing of layers in the crystals of **1c**.

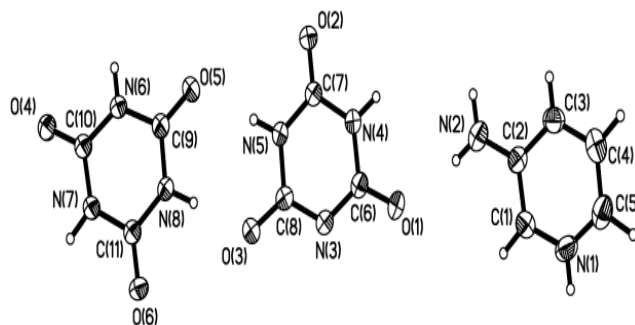
Such ensembles pack in the crystals to yield stacked layers structure as shown in Figure 4.23. Analysis of arrangement of molecules within a sheet, however, reveals that adjacent CA molecules are held together by cyclic hydrogen bonding pattern, comprising of  $N \cdots H \cdots O$  hydrogen bonds with  $H \cdots O$  distance of 1.81 Å, and constitute molecular tapes. Such tapes are held together through molecules of **pip**. The arrangement is shown in Figure 4.24. It is quite intriguing to note that the observed arrangement in the sheet structure is as found in similar and related assemblies formed by aza donors, while crystallizing from methanol solvent.



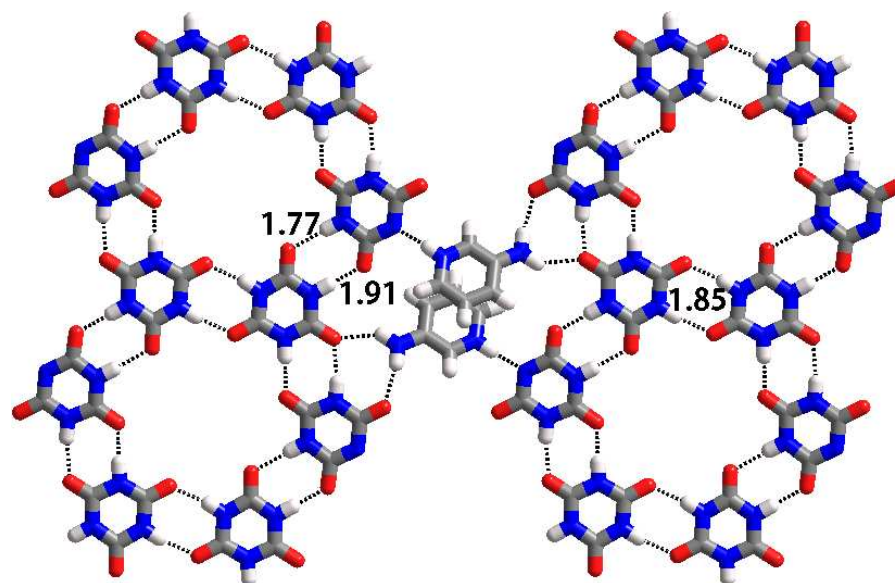
**Figure 4.24.** Arrangement of molecules in a typical sheet of **1c**.

#### 4.5 Molecular complex of cyanuric acid with 3-aminopyridine, **1d**.

Further to understand the rational behaviour of CA in the co-crystals based on the information obtained in **1a-1c**, preparation of a molecular complex of cyanuric acid with 3-aminopyridine (**3-amp**), which possesses both hydrogen bond donor ( $\text{-NH}_2$  group) as well as acceptor (pyridyl nitrogen), is carried out through a slow evaporation method, from water. Good quality single crystals were obtained in about 24 h and structure determination was carried out by single crystal X-ray diffraction technique. The structural analysis infers that CA and **3-amp** present in a 2:1 ratio. Information of structure solution and refinement is given in Table 4.1. An ORTEP of the asymmetric unit is shown in Figure 4.25.



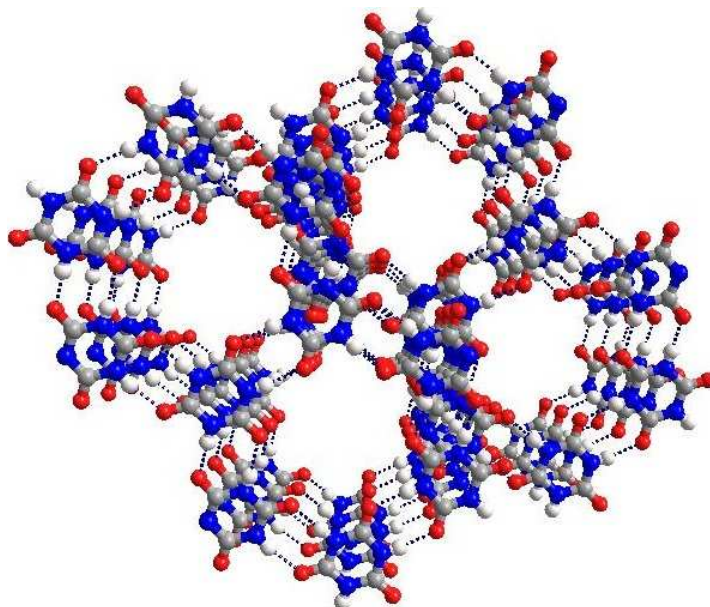
**Figure 4.25.** ORTEP of the contents in a 2:1 ratio of CA and **3-amp** in **1d**.



**Figure 4.26.** Hexagonal structure of CA connected by 3-amp in two dimension.

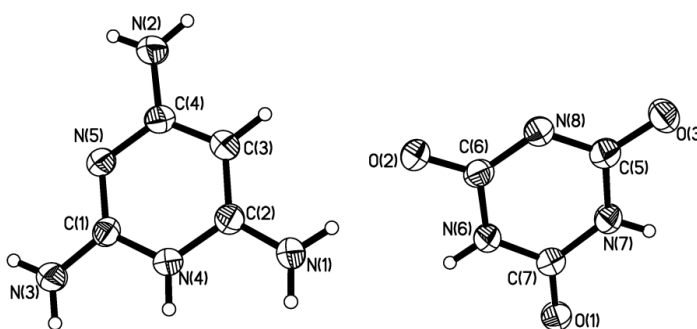
As observed in the co-crystals of CA with piperazine, **1c**, in the co-crystal of **1d** also proton transfer is observed. Thus, one of the CA molecules transfers its N-H proton to the pyridyl nitrogen of **3-amp**. Packing analysis reveals that adjacent CA molecules recognize themselves to form a hexagonal cyclic structure, as shown in Figure 4.27, and such hexagonal cyclic units are further extended in one direction. Within a hexagon, each deprotonated and neutral CA molecules are held together by two different types of cyclic N-H $\cdots$ O hydrogen bonds with H $\cdots$ O distances of 1.77 and 1.85 Å in each cyclic pattern. Complete characteristics of the hydrogen bonds are given in Table 4.2. It is quite astonishing to note that among the co-crystals of CA, either known in the literature or in the present study, hexagonal arrangement of CA molecules, as observed in **1d**, is hitherto unknown, although such ensemble was noted in trithiocyanuric acid, a thio analogue of CA. Such hexagons are further held together by **3-amp** molecules, as illustrated in Figure 4.26. Further, the ensembles are packed in the crystal lattice, in such a

manner that hexagons are stacked along a crystallographic axis creating channels, being filled by **3-amp** molecules. Channels structure is shown in Figure 4.27, omitting **3-amp** molecules for the purpose of clear visualization of channels.



**Figure 4.27.** Three dimensional structure of **1d**, projecting the channel.

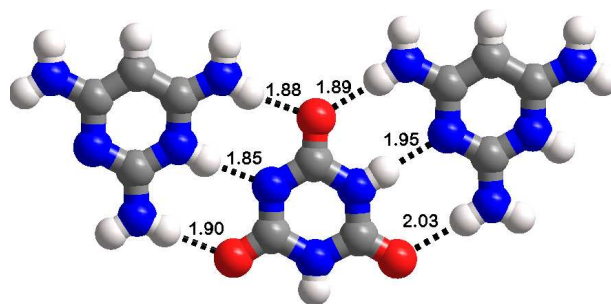
#### 4.6 Packing analysis in the co-crystals of cyanuric acid with 2,4,6-triaminopyrimidine, **1e**.



**Figure 4.28.** ORTEP of 1:1 Molecular complex of CA and **tap**.

In further exploration to evaluate the nature of CA in the presence of other complimentary molecules, co-crystallization of CA with 2,4,6-triaminopyrimidine

(**tap**) that contains more number of both hydrogen bond donors as well as acceptors than **3-amp** has been carried out, under solvothermal condition at 120°C with methanol as a solvent. Good quality single crystals isolated by viewing through a microscope, are analysed by single crystal X-ray diffraction method. The analysis reveals formation of a complex CA and **tap**, in a 1:1 ratio. In Table 4.1 statistics of crystallographic data are given. Composition of the contents is shown as ORTEP, as depicted in Figure 4.28. Further, as observed in **1c** and **1d**, proton transfer from CA to **tap** is observed.

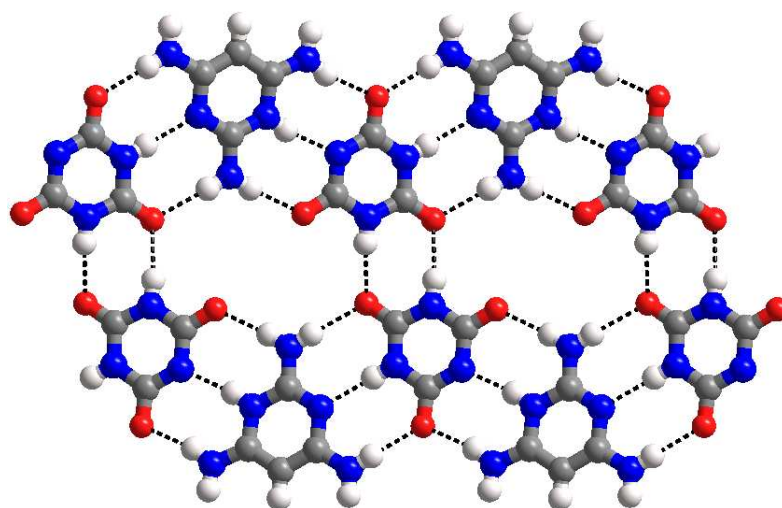


**Figure 4.29.** Molecular recognition observed between CA and **tap**.

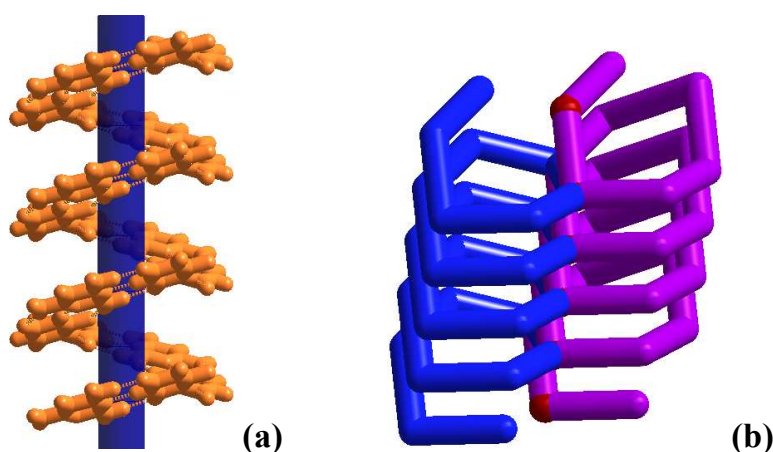
Molecular recognition between CA and the molecules of **tap** is shown in Figure 4.29. Interestingly, each CA molecule is connected to two **tap** molecules through triple hydrogen bonding pattern. While one of the patterns comprises of N-H $\cdots$ O / N-H $\cdots$ N / N-H $\cdots$ O with H $\cdots$ O distances 1.89 and 2.03 Å and H $\cdots$ N, 1.95 Å, the second pattern is through N-H $\cdots$ O / N<sup>+</sup>-H $\cdots$ N<sup>-</sup> / N-H $\cdots$ O with H $\cdots$ O distances 1.88 and 1.90 Å and H $\cdots$ N<sup>-</sup>, 1.85 Å. Such trimeric ensembles are held together by a typical cyclic N-H $\cdots$ O hydrogen bonds formed between the adjacent CA molecules yielding hexagonal networks, as shown in Figure 4.30. However, it is worth mentioning that the hexagonal networks are not planar, instead adopt a helical



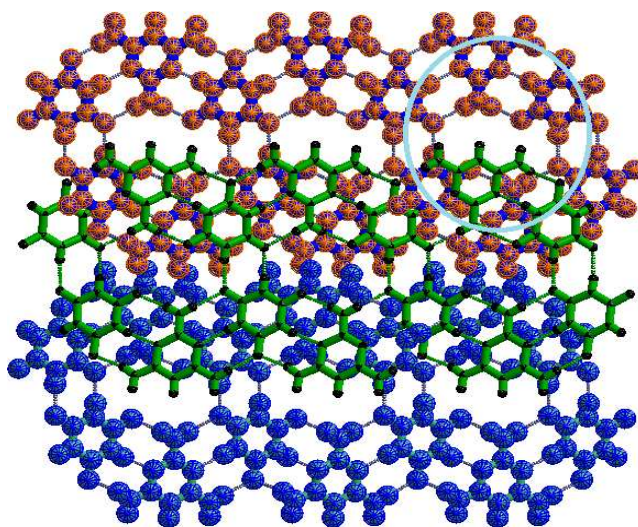
pattern, as shown for each hexagon and also for the hexagons held together in one dimension. This kind of helical structure were found especially in the assemblies of pyrimidines as reported recently for the complex of trimethoprim and 2-aminoterephthalic acid<sup>14</sup>. However, in three dimensional arrangement, the hexagons are packed with the pitch of helix (interaction between the CA molecules) lying along the stacking direction. The perspective three dimensional packing is shown in Figure 4.32.



**Figure 4.30.** Hexagonal network observed in **1e**.



**Figure 4.31.** Helical pattern observed in a) single hexagon b) extended hexagon.



**Figure 4.32.** Three dimensional arrangement in the crystal structure of **1e**.

#### 4.6 Conclusions

1. Co-crystals of cyanuric acid are prepared with co-formers possessing varied number of hydrogen bonding donors and / or acceptors.
2. The co-crystals are analysed through single crystal X-ray diffraction method to reveal the nature of CA assemblies within the co-crystals prepared.
3. Tapes, dimers, cyclic hexamer molecular patterns of CA are observed in the co-crystals reported herein.

**Table 4.1.** Crystallographic information for the co-crystals, **1a-1e**.

	<b>1a</b>	<b>1b</b>	<b>1c</b>	<b>1d</b>	<b>1e</b>
formula	(C <sub>3</sub> H <sub>3</sub> N <sub>3</sub> O <sub>3</sub> ) (C <sub>8</sub> H <sub>10</sub> N <sub>2</sub> S <sub>2</sub> )	2(C <sub>3</sub> H <sub>3</sub> N <sub>3</sub> O <sub>3</sub> ) :(C <sub>6</sub> H <sub>12</sub> N <sub>2</sub> )	2(C <sub>3</sub> H <sub>3</sub> N <sub>3</sub> O <sub>3</sub> ) :(C <sub>4</sub> H <sub>10</sub> N <sub>2</sub> )	2(C <sub>3</sub> H <sub>3</sub> N <sub>3</sub> O <sub>3</sub> ) :(C <sub>5</sub> H <sub>6</sub> N <sub>2</sub> )	(C <sub>3</sub> H <sub>3</sub> N <sub>3</sub> O <sub>3</sub> ) :(C <sub>4</sub> H <sub>7</sub> N <sub>5</sub> )
<i>F<sub>w</sub></i>	174.69	370.34	344.31	352.29	254.23
crystal shape	blocks	blocks	blocks	blocks	platelets
crystal color	colourless	colourless	colourless	colourless	colourless
crystal system	orthorhombic	monoclinic	triclinic	triclinic	monoclinic
space group	<i>C</i> 222 <sub>1</sub>	<i>C</i> 2/ <i>c</i>	<i>P</i> $\bar{1}$	<i>P</i> $\bar{1}$	<i>C</i> 2/ <i>c</i>
<i>a</i> (Å)	6.780(1)	20.322(3)	5.754(1)	6.703(2)	18.381(2)
<i>b</i> (Å)	8.503	6.066(1)	6.520(1)	10.354(4)	7.038(1)
<i>c</i> (Å)	25.753(5)	12.874(2)	10.333(2)	11.806(4)	15.557(2)
$\alpha$ (°)	90	90	75.42(1)	69.73(1)	90
$\beta$ (°)	90	95.45(1)	84.41(1)	74.03(1)	91.96(1)
$\gamma$ (°)	90	90	65.42(1)	77.66(1)	90
<i>V</i> (Å <sup>3</sup> )	1484.7(4)	1579.8(4)	341.16(10)	732.6(4)	2011.4(4)
<i>Z</i>	4	4	1	2	8
<i>D</i> <sub>calc</sub> (g cm <sup>-3</sup> )	1.563	1.557	1.676	1.597	1.679
<i>T</i> (K)	298(2)	298(2)	298(2)	298(2)	298(2)
Mo <i>k</i> $\alpha$	0.71073	0.71073	0.71073	0.71073	0.71073
$\mu$ (mm <sup>-1</sup> )	0.381	0.127	0.140	0.133	0.136
2 $\theta$ range (deg)	50.58	50.50	50.52	50.50	50.50
<i>F</i> (000)	720	776	180	364	1056
total reflns	3827	3784	3331	7062	4885
no. unique reflns [ <i>R</i> (int)]	1325(0.0327)	1291 (0.0429)	1232 (0.0426)	2626 (0.0470)	1506 (0.0502)
no. reflns used	1358	1430	1129	2254	1822
no. parameters	107	119	109	270	163
GOF on <i>F</i> <sup>2</sup>	1.109	1.085	1.108	1.074	1.088
<i>R</i> <sub>1</sub> [ <i>I</i> >2 $\sigma$ ( <i>I</i> )]	0.0327	0.0429	0.0382	0.0457	0.0502
<i>wR</i> <sub>2</sub>	0.0766	0.1239	0.1055	0.1303	0.1490

**Table 4.2.** Characterization of hydrogen bond distances (Å) and angles (°) observed in the structures **1a-1e**.<sup>§</sup>

H-bonds	1a	1b	1c	1d	1e
C-H <sup>⋯</sup> O	2.50 3.23 133	2.59 3.45 148	2.42 3.22 129	2.31 3.30 152	1.88 2.86 165
	2.32 3.23 168		2.46 3.41 145		1.90 2.86 160
					1.89 2.90 176
			1.94 2.79 139	1.96 2.95 168	2.03 3.04 175
			1.81 2.81 177	1.85 2.85 171	1.90 2.91 173
			1.85 2.86 176	1.93 2.92 167	1.95 2.93 163
N-H <sup>⋯</sup> O	1.83 2.84 180	1.81 2.81 170	1.89 2.82 152	1.80 2.80 173	
		1.79 2.80 175		1.91 2.91 176	
				1.77 2.77 177	1.92 2.93 179
				2.16 2.98 137	1.85 2.84 168
					1.88 2.86 165
N-H <sup>⋯</sup> N	1.90 2.89 167	1.70 2.70 171	2.20 2.98 150	1.76 2.75 169	1.90 2.86 160
					1.89 2.90 176

<sup>§</sup> In each row the three numbers for every structure represent H<sup>⋯</sup>A and D<sup>⋯</sup>A distances and <D-H<sup>⋯</sup>A.

## 4.7 Experimental Section

### 4.7.1 Synthesis of Co-crystals **1a-1e**

All chemicals used in this study were obtained from Sigma Aldrich and used as such without any further purification. The solvents employed for the co-crystallization purpose were of spectroscopy grade of highest available purity. Co-crystals, **1a**, **1b** and **1c** were prepared by slow evaporation of the methanol solution of cyanuric acid (CA) with the corresponding aza-donors in a 1:1 ratio. Co-crystals of **1d** is prepared by slow evaporation of the water solution of CA and **3-amp** in a 1:1 ratio. However, co-crystals of **1e** were prepared under solvothermal condition at 120°C by dissolving CA and **tap** in a 1:1 ratio in methanol.

### 4.7.2 X-ray Structure Determination

Good quality single crystals of **1a-1e** are carefully selected using Leica microscope and glued to a glass fibre using an adhesive (cyanoacrylate). In all the cases, the crystals were smeared in the adhesive solution to prevent decomposition of crystals. The intensity data were collected on a Bruker single-crystal X-ray diffractometer, equipped with an APEX detector. Subsequently, the data were processed using the Bruker suite of programs (SAINT), and the convergence was found to be satisfactory with good  $R_{\text{ini}}$  parameters. The details of the data collection and crystallographic information are given in Table 1. Absorption corrections were applied using SADABS package. The structure determination by direct methods and refinements by least-squares methods on  $F^2$  were performed using the SHELXTL-PLUS package. The processes were smooth without any complications. All non-hydrogen atoms were refined anisotropically, while hydrogen atoms are

treated isotropically. All the intermolecular interactions were computed using PLATON. All packing diagrams are generated using Diamond software.

#### 4.8. References

- (1) (a) Aakeroy, C. B. *Acta Crystallogr., Sect. B: Struct. Sci.* **1997**, *53*, 569. (b) Ivasenko, O.; Perepichka, D. F. *Chem. Soc. Rev.* **2011**, *40*, 191.
- (2) Melendez, R. E.; Hamilton, A. D. In *Design of Organic Solids*; Weber, E., Ed. 1998; Vol. 198, p 97.
- (3) (a) Vishweshwar, P.; Nangia, A.; Lynch, V. M. *J. Org. Chem.* **2002**, *67*, 556. (b) Bhogala, B. R.; Basavoju, S.; Nangia, A. *Crystengcomm* **2005**, *7*, 551. (c) Bhogala, B. R.; Nangia, A. *New J. Chem.* **2008**, *32*, 800. (d) Babu, N. J.; Nangia, A. *Cryst. Growth Des.* **2006**, *6*, 1995. (e) Kumar, V. S. S.; Kuduva, S. S.; Desiraju, G. R. *Acta Crystallogr., Sect. E: Struct. Rep. Online* **2002**, *58*, o865. (f) Pedireddi, V. R.; Varughese, S. *Inorg. Chem.* **2004**, *43*, 450. (g) Arora, K. K.; Pedireddi, V. R. *J. Org. Chem.* **2003**, *68*, 9177. (h) Varughese, S.; Pedireddi, V. R. *Chem. Eur. J.* **2006**, *12*, 1597. (i) Varughese, S.; Pedireddi, V. R. *Tetrahedron Lett.* **2005**, *46*, 2411. (j) Arora, K. K.; PrakashaReddy, J.; Pedireddi, V. R. *Tetrahedron* **2005**, *61*, 10 793. (k) Manjare, Y.; Pedireddi, V. R. *Cryst. Growth Des.* **2011**, *11*, 5079.
- (4) (a) Reddy, L. S.; Nangia, A.; Lynch, V. M. *Cryst. Growth Des.* **2004**, *4*, 89. (b) Aakeroy, C. B.; Desper, J.; Helfrich, B. A. *Crystengcomm* **2004**, *6*, 19. (c) Babu, N. J.; Reddy, L. S.; Nangia, A. *Mol. Pharmaceut.* **2007**, *4*, 417. (d) Goswami, S.; Jana, S.; Fun, H. K. *Crystengcomm* **2008**, *10*, 507. (e) Seaton, C. C.; Parkin, A. *Cryst. Growth Des.* **2011**, *11*, 1502. (f) Moragues-

- Bartolome, A. M.; Jones, W.; Cruz-Cabeza, A. J. *Crystengcomm* **2012**, *14*, 2552. (g) Seo, M.; Park, J.; Kim, S. Y. *Org. Biomol. Chem.* **2012**, *10*, 5332. (h) Arman, H. D.; Kaulgud, T.; Miller, T.; Poplaukhin, P.; Tiekink, E. R. T. *J. Chem. Crystallogr.* **2012**, *42*, 673. (i) PrakashaReddy, J.; Pedireddi, V. R. *Tetrahedron* **2004**, *60*, 8817. (j) Pedireddi, V. R.; PrakashaReddy, J.; Arora, K. K. *Tetrahedron Lett.* **2003**, *44*, 4857. (k) Reddy, L. S.; Bhatt, P. M.; Banerjee, R.; Nangia, A.; Kruger, G. J. *Chem. Asian J.* **2007**, *2*, 505. (l) Rajput, L.; Biradha, K. *Cryst. Growth Des.* **2009**, *9*, 40. (m) Rajput, L.; Santra, R.; Biradha, K. *Aust. J. Chem.* **2010**, *63*, 578.
- (5) (a) Leiserowitz, L. *Acta Crystallogr.; Sec. B: Struct. Sci.* **1976**, *32*, 775. (b) Huang, C. M.; Leiserow.L; Schmidt, G. M. J. *J. Chem. Soc., Perkin Trans. 2* **1973**, 503.
- (6) Aitipamula, S.; Chow, P. S.; Tan, R. B. H. *Cryst. Growth Des.* **2010**, *10*, 2229.
- (7) Ito, Y.; Hosomi, H.; Ohba, S. *Tetrahedron* **2000**, *56*, 6833.
- (8) Ohba, S.; Hosomi, H.; Ito, Y. *J. Am. Chem. Soc.* **2001**, *123*, 6349.
- (9) Pedireddi, V. R.; PrakashaReddy, J. *Tetrahedron Lett.* **2003**, *44*, 6679.
- (10) Ranganathan, A.; Pedireddi, V. R.; Rao, C. N. R. *J. Am. Chem. Soc.* **1999**, *121*, 1752.
- (11) Feibush, B.; Figueroa, A.; Charles, R.; Onan, K. D.; Feibush, P.; Karger, B. L. *J. Am. Chem. Soc.* **1986**, *108*, 3310.
- (12) (a) Zerkowski, J. A.; Seto, C. T.; Whitesides, G. M. *J. Am. Chem. Soc.* **1992**, *114*, 5473. (b) Seto, C. T.; Whitesides, G. M. *J. Am. Chem. Soc.* **1993**,

- 115, 905. (c) Seto, C. T.; Whitesides, G. M. *J. Am. Chem. Soc.* **1993**, *115*, 1330. (d) Seto, C. T.; Whitesides, G. M. *J. Am. Chem. Soc.* **1990**, *112*, 6409. (e) Mathias, J. P.; Simanek, E. E.; Seto, C. T.; Whitesides, G. M. *Macromol. Symp.* **1994**, *77*, 157. (f) Mathias, J. P.; Seto, C. T.; Whitesides, G. M. *Abstr. Papers Am. Chem. Soc.* **1993**, *205*, 196. (g) Zerkowski, J. A.; Macdonald, J. C.; Whitesides, G. M. *Chem. Mater.* **1994**, *6*, 1250. (h) Zerkowski, J. A.; Macdonald, J. C.; Seto, C. T.; Wierda, D. A.; Whitesides, G. M. *J. Am. Chem. Soc.* **1994**, *116*, 2382. (i) Whitesides, G. M.; Simanek, E. E.; Mathias, J. P.; Seto, C. T.; Chin, D. N.; Mammen, M.; Gordon, D. M. *Acc. Chem. Res.* **1995**, *28*, 37. (j) Simanek, E. E.; Mammen, M.; Gordon, D. M.; Chin, D.; Mathias, J. P.; Seto, C. T.; Whitesides, G. M. *Tetrahedron* **1995**, *51*, 607. (k) Mathias, J. P.; Simanek, E. E.; Zerkowski, J. A.; Seto, C. T.; Whitesides, G. M. *J. Am. Chem. Soc.* **1994**, *116*, 4316. (l) Mathias, J. P.; Simanek, E. E.; Whitesides, G. M. *J. Am. Chem. Soc.* **1994**, *116*, 4326. (m) Mammen, M.; Shakhnovich, E. I.; Deutch, J. M.; Whitesides, G. M. *J. Org. Chem.* **1998**, *63*, 3821. (n) Li, X. H.; Chin, D. N.; Whitesides, G. M. *J. Org. Chem.* **1996**, *61*, 1779. (o) Choi, I. S.; Li, X. H.; Simanek, E. E.; Akaba, R.; Whitesides, G. M. *Chem. Mater.* **1999**, *11*, 684. (p) Chin, D. N.; Gordon, D. M.; Whitesides, G. M. *J. Am. Chem. Soc.* **1994**, *116*, 12033.
- (13) (a) Marivel, S.; Suresh, E.; Pedireddi, V. R. *Tetrahedron Lett.* **2008**, *49*, 3666. (b) Ranganathan, A.; Pedireddi, V. R.; Sanjayan, G.; Ganesh, K. N.; Rao, C. N. R. *J. Mol. Struct.* **2000**, *522*, 87. (c) Jetti, R. K. R.; Thallapally, P. K.; Xue, F.; Mak, T. C. W.; Nangia, A. *Tetrahedron* **2000**, *56*, 6707. (d)



Nichol, G. S.; Clegg, W. *Cryst. Growth Des.* **2006**, *6*, 451. (e)  
Akhtaruzzaman, M.; Tomura, M.; Nishida, J.; Yamashita, Y. *J. Org. Chem.*  
**2004**, *69*, 2953. (f) Arora, K. K.; Talwelkar, M. S.; Pedireddi, V. R. *New J.*  
*Chem.* **2009**, *33*, 57. (g) Barnett, S. A.; Blake, A. J.; Champness, N. R.  
*Crystengcomm* **2003**, 134.

(14) Delori, A.; Jones, W. *Crystengcomm* **2011**, *13*, 6315.

## Publications

---

1. Understanding the molecular structures of fibres of the molecular gels of some *N,N',N''*-(triphenyl)-1,3,5-benzenetricarboxamide derivatives.  
V. Nagarajan and V. R. Pedireddi. (Manuscript under preparation)
2. Template Directed Synthesis of Cavity Structures of Co-crystals of Trithiocyanuric Acid with N-donor Compounds. V. Nagarajan and V. R. Pedireddi. (Manuscript under preparation)
3. Abnormal Assemblies of Cyanuric acid in the Co-crystals of Cyanuric Acid with N-donor Compounds. V. Nagarajan and V. R. Pedireddi. (Manuscript under preparation).
4. Synthesis of Co-crystals of Trithiocyanuric Acid with Some Aza-donors at Different Reaction Conditions. V. Nagarajan and V. R. Pedireddi. (Manuscript under preparation).

## Symposia/Poster Presentation

---

1. XX International Conference on the Chemistry of the Organic Solid State  
ICCOSS XX, Indian Institute of Science, Bangalore, India, 25-30<sup>th</sup> June,  
2011.
2. RSC West India Ph. D Students Symposium 2010, Goa University, Goa,  
India, 3<sup>rd</sup> & 4<sup>th</sup> September, 2010.
3. 38th National Seminar on Crystallography, Mysore, India, 11-13<sup>th</sup>  
February, 2009.
4. International Conference on Molecules and Materials: New Directions,  
Jawaharlal Nehru Centre for Advanced Scientific Research, Bangalore,  
India, 4-6<sup>th</sup> December, 2008.